Extra-Tropical Cyclones in a Warming Climate: Trends and Clustered Activity in the Northern Hemisphere

Dissertation with the aim of achieving a doctoral degree

at the Faculty of Mathematics, Informatics and Natural Sciences
Department of Earth Sciences
at Universität Hamburg

submitted by

Alexia Karwat
from Bielefeld

Hamburg, March 2023

Alexia Karwat
aus Bielefeld, Deutschland

Meteorologisches Institut
Grindelberg 5
20144 Hamburg

Tag der Disputation: 26. Mai 2023

Folgende Gutachter empfehlen die Annahme der Dissertation:
PD Dr. Richard Blender
Prof. Dr. Christian Franzke

Vorsitzender des Promotionsausschusses:
Prof. Dr. Hermann Held

Dekan der MIN-Fakultät:
Prof. Dr.-Ing. Norbert Ritter

Abstract

Extra-tropical cyclones are the primary natural hazard to affect the mid-latitudes. As individual and clustered cyclones are the most intense in winter, and may also be accompanied by wind gusts and heavy precipitation, they have the potential to cause severe damage across societies like Europe. To project the impact of cyclones on society, it is crucial to comprehend long-term trends of cyclone characteristics and the storms' capacity to cluster within short periods of time – especially in a world that is rapidly warming.

In this thesis, long-term trends of cyclone characteristics are investigated using the recently extended ERA5 reanalysis, focussing on the North Atlantic – European and the North Pacific regions. During 1950-2021, extra-tropical cyclones have significantly intensified in the entire Northern Hemisphere, while also traveling more poleward and for longer distances, but at a slower pace. Since 1979 wind gusts from North Atlantic and precipitation extremes from North Pacific cyclones have also significantly increased, which have led to large socio-economic losses.

Not only strong individual Northern Hemispheric winter storms have changed in terms of showing higher intensities in the last few decades, but sequences of cyclones, so-called cyclone clusters, are projected to increase in certain regions by 2060-2100 compared to the reference period 1980-2020. Using Large Ensemble simulations from the Community Earth System Model version 2 (CESM2-LE) of an upper-middle Shared Socioeconomic Pathway forcing scenario (SSP3-7.0), cyclone clustering over Europe increases for 3 and 4 cyclones within 7 days by up to 25% on average during 2060-2100 compared to 1980-2020. In contrast, cyclone clustering along the west coast of the US and Canada is projected to decrease significantly by up to 24.3% in the future. A similar decrease in cyclone clustering was detected in the Gulf of Alaska by up to 10.1% on average during 2060-2100.

These results demonstrate the importance of understanding long-term trends of cyclone features and clustered cyclone activity in a warmer winter climate. Quantifying the economic cost of individual as well as of clustered cyclones will become more important in the case of more volatile events in the future. Since the climate signal between 2060-2100 and 1980-2020 shows enhanced changes in the clustering of cyclones across Europe due to global warming, higher anthropogenic greenhouse gas emissions should be avoided to minimize all future socio-economic impacts.

Zusammenfassung

Außertropische Wirbelstürme stellen die primäre Naturgefahr für die mittleren Breiten dar. Da einzelne und gruppierte Stürme, die von Windböen und starken Niederschlägen begleitet werden können, im Winter am intensivsten sind haben sie das Potenzial in Gesellschaften wie Europa schwere Schäden anzurichten. Um die zukünftigen Auswirkungen von Zyklonen auf unsere Sozioökonomie vorherzusagen ist es entscheidend die langfristigen Trends der Zykloneigenschaften und die Fähigkeit der Stürme, sich innerhalb kurzer Zeit als Gruppe oder Zyklonfamilie zu häufen, zu verstehen – insbesondere in einer Welt, die sich schnell erwärmt.

In dieser Dissertation werden langfristige Trends von Zykloneigenschaften unter Verwendung der kürzlich erweiterten ERA5-Reanalyse mit Fokus auf den Nordatlantik – Europa und über dem Nordpazifik untersucht.

Zwischen 1950 und 2021 haben sich außertropische Wirbelstürme in der gesamten nördlichen Hemisphäre signifikant intensiviert, während sie sich gleichzeitig auch mehr polwärts und über längere Strecken bewegen, jedoch mit langsamer Geschwindigkeit. Seit 1979 haben auch Windböen aus Nordatlantik- und Niederschlagsextreme aus Nordpazifik-Zyklonen deutlich zugenommen, die in der Vergangenheit zu großen wirtschaftlichen Schäden geführt haben.

Nicht nur starke einzelne nordhemisphärische Winterstürme haben sich in den letzten Jahrzehnten dahingehend verändert, dass sie höhere Intensitäten zeigten, sondern es wird auch prognostiziert, dass Sequenzen von Zyklonen, sogenannte Zykloncluster, in bestimmten Regionen bis 2060-2100 im Vergleich zum Referenzzeitraum 1980-2020 zunehmen werden. Unter Verwendung von Large-Ensemble-Simulationen aus dem Community Earth System Model Version 2 des SSP3-7.0-Szenarios nimmt die Zyklon-Clusterbildung über Europa für 3 und 4 Zyklonen innerhalb von 7 Tagen im Zeitraum 2060-2100 im Vergleich zu 1980-2020 im Durchschnitt um bis zu 25% zu. Die Zyklonenhäufung entlang der Westküste der USA und Kanadas nimmt innerhalb von 7 Tagen hingegen signifikant um bis zu 24.3% ab. Ein ähnlicher Rückgang der Zyklon-Clusterbildung um bis zu 10.1% im Mittel wurde für den Zeitraum 2060-2100 im Golf von Alaska festgestellt.

Diese Ergebnisse zeigen wie wichtig es ist langfristige Trends von Zyklonmerkmalen und geclusterter Zyklonaktivität in wärmeren Winterklimata zu verstehen. Die Quantifizierung der Kosten, sowohl einzelner als auch gehäufter Wirbelstürme, wird bei volatileren Ereignissen in Zukunft an Bedeutung gewinnen. Da das Klimaänderungssignal zwischen 2060-2100 und 1980-2020 signifikante Veränderungen in der Häufung von Wirbelstürmen in ganz Europa aufgrund der globalen Erwärmung impliziert, sollten höhere anthropogene Treibhausgasemissionen vermieden werden um alle zukünftigen sozioökonomischen Auswirkungen zu minimieren.

Declaration of Authorship

Parts of this dissertation pre-published or intended for publication

The following papers have been included in this thesis. The components carried out by the candidate and the other authors are stated below.

Karwat, A., C. L. E. Franzke, and R. Blender (2022), "Long-Term Trends of Northern Hemispheric Winter Cyclones in the Extended ERA5 Reanalysis", *J. Geophys. Res. Atmos.*, vol. 127, no. 22, e2022JD036952, https://doi.org/10.1029/2022JD036952 – Chapter 3

Karwat, A., C. L. E. Franzke, J. G. Pinto, S.-S. Lee, and R. Blender (2023), "Northern Hemisphere Extra-Tropical Cyclone Clustering in ERA5 Reanalysis and the CESM2 Large Ensemble", *submitted*. – Chapter 4

The concept for the studies listed above was developed by all the authors. The analysis, creation of figures, and writing of the text was completed by A. Karwat. The remainder of the authors provided feedback and comments to produce the final manuscripts.

Acknowledgements

At first, I would like to thank my PhD supervisor PD Dr. Richard Blender for his great support and help over the years. I am grateful that after 2.5 years of the covid19 pandemic we finally got to enjoy an in-situ conference-like atmosphere during the final meeting of our climXtreme project in November last year.

I am also thankful to Prof. Dr. Christian Franzke for the intriguing conversations, his enthusiasm and patience whenever I had a question, and finding new ways to motivate me.

I would like to thank Prof. Dr. Jin-Song von Storch for supporting me throughout my PhD and being a great panel chair.

Thanks go out to everyone in the "Atmospheric Dynamics and Predictability" group, led by Prof. Dr. Nedjeljka Žagar, for the interesting chats and discussions over the years.

I would like to thank Frank Sielmann for the technical help and Dr. Hartmut Borth for his very recent advice in the final stage of my PhD.

Last year, I was very fortunate to spend 2.5 months at the ICCP directed by Prof. Dr. Axel Timmermann in Busan, South Korea, which was an incredible experience and a truly memorable time – in many different ways. I particularly want to thank Susmit, Zhen, Jyoti & Nitesh for their warm welcome and the fun times.

A special thank you goes to Prof. Dr. Joaquim G. Pinto for his great advice and sharing his expertise on our recent cyclone clustering paper.

I much appreciate the honest feedback by Dr. Leonard Borchert on an earlier draft.

In no particular order I would like to thank Nataliya, Marie, Céline, Catherine, Michael, Maria and Mel who inspire me more than they could possibly know.

Lars, No. 14 – thank you for being the best friend I could ask for (and not a cylon)!

Finally, I would like to thank my parents for always allowing me to follow my dreams. Without your support I would not be where I am right now.

Last but not least, I am also and especially grateful to my grandma, Ruth, who at 90, is still curious about what I do and what I am up to all the time. Thank you Omi for always supporting me. This thesis is for you.

Contents

List of Figures

List of Tables

List of Abbreviations

AEP	**A**nnual **E**xceedance **P**robability
AR6	**6**th **A**ssessment **R**eport
CAN	**C**anada
CESM-LE	**C**ommunity **E**arth **S**ystem **M**odel (version 1) - **L**arge **E**nsemble
CESM2-LE	**C**ommunity **E**arth **S**ystem **M**odel (version 2) - **L**arge **E**nsemble
CMIP3	**C**oupled **M**odel **I**ntercomparison **P**roject **3**
CMIP5	**C**oupled **M**odel **I**ntercomparison **P**roject **5**
CMIP6	**C**oupled **M**odel **I**ntercomparison **P**roject **6**
CO2	**C**arbon **D**ioxide
DJF	**D**ecember, **J**anuary, and **F**ebruary
ECMWF	**E**uropean **C**enter **M**edium-Range **W**eather **F**orecast
EKE	**E**ddy **K**inetic **E**nergy
ERA	**E**CMWF **R**e-**A**nalysis (e.g., ERA40, ERA-Interim, ERA5, ERA5-BE)
ERA5-BE	**E**CMWF **R**e-**A**nalysis **B**ack **E**xtension of ERA5
GCM	**G**lobal **C**limate **M**odel
IPCC	**I**ntergovernmental **P**anel on **C**limate **C**hange
mslp	**m**ean **s**ea **l**evel **p**ressure
NA	**N**orth **A**tlantic
NAO	**N**orth **A**tlantic **O**scillation (phase)
NOAA	**N**ational **O**ceanic and **A**tmospheric **A**dministration (e.g., NOAA reanalysis)
no.	**n**umber
NP	**N**orth **P**acific
OEP	**O**ccurrence **E**xceedance **P**robability
PDF	**P**robability **D**ensity **F**unction
PNA	**P**acific **N**orth **A**merican pattern
QQ	**Q**uantile **Q**uantile (Plot)
RCP	**R**epresentative **C**oncentration **P**athway (Scenario)
RQ	**R**esearch **Q**uestion
SSI	**S**torm **S**everity **I**ndex
SSP	**S**hared **S**ocioeconomic **P**athways
SST	**S**ea **S**urface **T**emperature
UK	**U**nited **K**ingdom (of Great Britain and Northern Ireland)
US	**U**nites **S**tates (of America)
z1000	1,000 hPa geopotential field

List of Symbols

ρ	check function
β	regression coefficient
τ	specified quantile (as used in Chapter 2)
ε	intersection with the y-axis
λ	rate parameter (as used in Chapter 2)
ψ	dispersion statistic
σ^2	variance of the number of cyclone occurrences
μ	mean of the number of cyclone occurrences
α	significance level
ρ	autocorrelation function
λ	test statistic (as used in Chapter 3)
τ	change-point position (as used in Chapter 3)
$\hat{\theta}$	maximum likelihood estimate
σ	standard deviation

Chapter 1

Introduction

1.1 Motivation

Extra-tropical cyclones (also often referred to, for example, as mid-latitude storms or low pressure systems) are an important part of the atmospheric circulation in the mid-latitudes due to their ability to transport large amounts of moisture and momentum. Over 70% of the total precipitation across Europe in winter is caused by extra-tropical cyclones (Hawcroft et al., 2012). Cyclones are also responsible for the day-to-day variability in the mid-latitudes and can be accompanied by strong wind gusts and heavy precipitation: leading to flooding, storm surges, and damage in many areas (Roberts et al., 2014). These extreme events pose severe risks for vulnerable environments and socio-economies, including the infrastructure therein (Gliksman et al., 2022). In the Northern Hemisphere, not only has there been more intense strong individual winter storms (Fink et al., 2009), but there has also been an emergence of sequences of cyclones, known as cyclone clusters, which have led to extensive socio-economic damage (Priestley et al., 2017; Mühr et al., 2022).

This thesis aims to address the gaps in the knowledge of long-term trends of Northern Hemispheric winter cyclones and related impacts such as wind gusts and heavy precipitation, and to show specifically how this climatological information may be used in a regional-to-local context to project future impact locations from extreme winter storms. Understanding how cyclones have changed over the last 71+ years will enhance the predictability of mid-latitude weather extremes induced by cyclones. In addition to historical changes, such as an intensification of cyclones due to natural variability and global warming, this thesis also aims to fully comprehend how a warmer winter climate will affect the activity and occurrence of Northern Hemisphere clustered cyclones at the end of the 21st century.

The remaining part of this chapter will evaluate the current state of knowledge on this topic. Section 1.2 is dedicated to the formation of extra-tropical cyclones. The Northern Hemisphere storm tracks are discussed in Section 1.3, focussing on the main methods for detection, their features and locations. The specific phenomenon of cyclone clustering is discussed in Section 1.4, with a focus on the definition, dynamics and main conclusions from climate models. An overview of the impacts from individual and clustered cyclones will be given in Section 1.5, while Section 1.6 reviews the different "Shared Socioeconomic Pathways" (SSPs). Current knowledge gaps between long-term trends of cyclone features and clustered cyclones from past observations and future projections are addressed in Section 1.7. Finally, the study's aims, structure, and research questions of this thesis are presented in Section 1.8.

1.2 Formation of Extra-Tropical Cyclones

How do extra-tropical cyclones form? The most common models to describe extra-tropical cyclone development are the Norwegian and the Shapiro-Keyser models (Bjerknes, 1922; Schultz et al., 2019; Dacre, 2020). In the classical Norwegian cyclone model, a stationary front forms between cold and warm air masses, creating a strong vertical wind shear within the troposphere. As a result of the perturbation between the two air masses, a surface low-pressure system develops where warm air is advected north and cold air is advected south by a cyclonic circulation system (in the Northern Hemisphere). Along this stationary front, the cyclone begins to grow and develops a warm and a cold front. This process is typically triggered by an upper-level trough. As the cyclone deepens, both fronts become more clearly defined and a warm sector emerges. When the cold front catches up to the warm front, the so-called occlusion process is initiated. The cyclone reaches its peak intensity at this point (Bjerknes, 1922). Soon after, the cyclone decays. In the Shapiro-Keyser model, the early phases of cyclone development are similar, however the cold front does not catch up to the warm front, but builds a T-bone structure instead of a warm sector during occlusion as in the classical model (Shapiro and Keyser, 1990).

1.3 Storm Tracks

1.3.1 Eulerian Approach

Storm tracks are regions of high synoptic timescale activity, for example, in the mid-latitudes, where the variability associated with low pressure centers is enhanced (Blackmon, 1976). Blackmon (1976) was the first to classify these mid-latitude active variability patterns using band-pass filtering of 500 hPa geopotential height data over a specific period of time (2.5-6 days). By removing the diurnal and greater-than-weekly variability of the atmospheric data, the temporal filtering revealed two regions of high storm variance in the Northern Hemisphere: one over the North Atlantic and the other over the North Pacific (Blackmon, 1976). Through calculating the standard deviation of the filtered data at each longitude and latitude, the climatological baroclinic wave activity was interpolated (Wallace et al., 1988). Storm tracks are an essential and particularly important part of our climate, since they transport eddy kinetic energy (EKE) poleward, minimizing the energy imbalance between the equator and the pole (Shaw et al., 2016).

Filtering out such regions is what is understood by the Eulerian (storm track) approach. Since its discovery in the 1970s, this approach has been used in several studies to characterize storm track activity and changes in storm locations (e.g., Hoskins and Hodges (2002), Wettstein and Wallace (2010), Harvey et al. (2014), Harvey et al. (2020), Montoya Duque et al. (2021), and Yang et al. (2021)). An example of the Eulerian storm track, high-pass filtered by the storms' EKE, is given in Fig. 1.1 (see coloured shaded areas within black contours, Shaw et al. (2016)).

However, the Eulerian approach does not provide any information about individual cyclone characteristics such as the storm frequency, its intensity or other more specific cyclone parameters (e.g., storm radius) that can be used to identify trends

or changes in impacts (Hoskins and Hodges, 2002; Zappa et al., 2013a; Zappa et al., 2013b; Walker et al., 2020).

1.3.2 Lagrangian-based Approach

The specific cyclone characteristics, for example, intensity, life time and size are known when storms are individually tracked using a Lagrangian-based approach. This is also more broadly referred to as objective feature tracking of cyclones (Hoskins and Hodges, 2002). In this manner, cyclone-related impacts, such as wind gusts and precipitation extremes, can even be linked to particular events (e.g., Caldas-Alvarez et al. (2022))[1]. This is because the Lagrangian-based approach allows for the tracking of these features at any location in space and time rather than just one region at any particular time as in the Eulerian approach (e.g., Flaounas et al. (2023)[2]. Furthermore, this is very useful for climatological analyses such as detecting long-term trends in cyclones (Karwat et al., 2022). An illustration of individual Lagrangian 'cyclone' tracks is shown in Fig. 1.1 (see blue lines, Shaw et al. (2016)).

Most Lagrangian-based cyclone tracking algorithms use mean sea-level pressure (e.g., Murray and Simmonds (1991), Pinto et al. (2005), and Wernli and Schwierz (2006)), relative vorticity (e.g., Sinclair (1994), Hodges (1995), Hodges (1996), and Hodges (1999)) or the 1000 hPa geopotential (height) (Blender et al., 1997; Blender and Schubert, 2000; Raible et al., 2018; Karwat et al., 2022). Thus, only Lagrangian trajectories provide the cyclone spatial and temporal information needed for a thorough investigation of storms and related impacts.

1.3.3 North Atlantic and Europe

The entire life cycle (or time) of an extra-tropical cyclone spans approximately at least 48 hours (Blender et al., 1997; Mailier et al., 2006). It is divided into the process of cyclogenesis, further development, and lysis, which are discussed in the following section. The physical processes through which cyclones form and develop are widely understood (see Section 1.2). In a broader sense, low pressure systems are produced by baroclinic instability due to Rossby waves. This part is commonly referred to as cyclogenesis. Cyclogenesis often occurs near the North American east coast and is triggered by strong temperature gradients: by the sea-surface temperature gradient of the Gulf Stream and the opposite temperatures emerging off the North American continent (Priestley et al., 2020).

The North Atlantic storm track has a typical southwest-northeast tilt (see areas within thick black contour lines on right side of Fig. 1.1, Shaw et al. (2016)). The western part of the storm track - the region along the east-coast states of the US and Canada - is typically associated with strong baroclinicity, which dominates in these regions during the winter season. This is most favourable for cyclogenesis (Mailier et al., 2006). Hence, storms are the most intense during this season. To develop more rapidly, strong upper-level divergence and vertical ascent at the right entrance and left exit of the jet streaks are needed (Pinto et al., 2014). Propagating due east,

[1] published in *Nat. Hazards Earth Syst. Sci.*, 2022, with A. Karwat as co-author.
[2] currently under review in *Weather Clim. Dyn.*, 2023, with A. Karwat as co-author.

storms cross the North Atlantic and usually begin to occlude in the Northeastern Atlantic (Shaw et al., 2016). Here, storms tend to move slower and have a higher potential to appear as groups of cyclones, hence to cluster (Dacre and Pinto, 2020). Sometimes newly developing and fast-moving cyclones may also cluster in these regions (Mailier et al., 2006; Dacre and Pinto, 2020).

1.3.4 North Pacific

The counterpart to the North Atlantic – European storm track is the North Pacific storm track (see areas within thick black contour lines on left side of Fig. 1.1, Shaw et al. (2016)). Its main cyclogenesis region typically emerges east of Japan and sometimes extends to a more central part of the North Pacific (Sickmöller et al., 2000). Changes in the storm track over the North Pacific depend on the position and intensity of the Aleutian Low (Salathé Jr, 2006). As the North Pacific ocean is highly susceptible to the interaction of aerosols and clouds throughout the winter, there is a strong link between Asian pollution and an enhanced North Pacific storm track (Zhang et al., 2007). In the past, the eastern North Pacific has also experienced a second storm track aside from the main cyclone track where cyclones partly propagated toward the US Pacific Northwest and British Columbia (Bancroft, 2016).

On average, and while developing further, cyclones track over the North Pacific and occlude, for example, in the Bering Sea, across the Aleutian Islands or in the Gulf of Alaska (Trenberth and Hurrell, 1994). Here, there is a particularly high chance that cyclones may cluster as groups (Mailier et al., 2006; Blender et al., 2015).

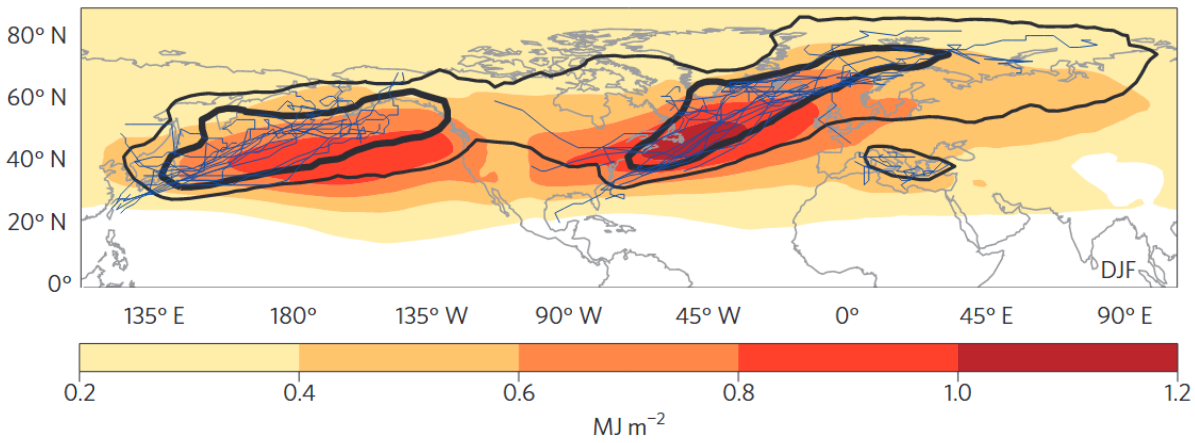

FIGURE 1.1: Wintertime (December-February) (DJF) storm tracks in the Northern Hemisphere. Averaged 10-day high-pass filtered eddy kinetic energy (EKE) [MJ m^{-2}] from the ERA-Interim reanalysis (coloured shading). Black contours show cyclone track density and blue lines show individual cyclone tracks for the top 0.5% most intense cyclones ranked by minimum sea level pressure (shown separately for the North Pacific, North Atlantic, and Mediterranean). Figure and caption adapted from Shaw et al. (2016) and reproduced with permission from Springer Nature.

1.4 Cyclone Clustering

Storms that occur completely at random are comparable to a homogeneous Poisson process with constant intensity (Cox and Isham, 1980) (see details on the Poisson process in Section 2.4.2). However, this is not the case for regularly occurring storms and storms that are observed as sequences, so-called clustered cyclones. The theoretical approach (relative metric) to separate clustered from non-clustered cyclone activity is by a dispersion statistic, which was introduced by Mailier et al. (2006) (for details see Section 2.4.3). The main idea is that cyclones either appear regularly (i.e., variance less than mean) or clustered (i.e., variance greater than mean) (Mailier et al., 2006). Thus, the dispersion can be interpreted as the standard deviation of a Poisson process. It has been an established and useful tool in many studies to distinguish between regular and clustered cyclones (e.g., Mailier et al. (2006), Vitolo et al. (2009), and Economou et al. (2015)).

These storm sequences, groups or 'cyclone families' are more specifically referred to as a phenomenon called cyclone clustering (Mailier et al., 2006; Priestley et al., 2020; Dacre and Pinto, 2020). From a practical perspective, cyclone clustering describes the passage of several, typically at least 2, 3, 4 or more intense cyclones tracking through a preferred geographical region (absolute metric), mostly originating over the eastern ocean basins in the Northern Hemisphere (see Sections 1.3.3 and 1.3.4). Indeed, clustered cyclone activity is more common over the eastern North Atlantic and northwestern Europe as well as in the eastern North Pacific including the Gulf of Alaska and the Pacific Northwest than in other regions (Mailier et al., 2006; Blender et al., 2015).

Vitolo et al. (2009) found that the most intense cyclones cluster near the exit of the North Atlantic storm track, specifically over Great Britain, the Benelux countries, France, and northern Germany. This is because of a number of reasons: in the North Atlantic, cyclone clustering is based on a very strong jet stream, which is flanked to the north and to the south during Rossby wave breaking (Pinto et al., 2014; Priestley et al., 2017). It is caused by a steering of the large-scale flow, which directs storms in a similar direction and generates conditions favourable for a fast intensification. It is also produced through secondary cyclogenesis (Pinto et al., 2014; Ziv et al., 2015; Priestley et al., 2020). These factors all contribute to the cyclone clusters seen over the northeastern Atlantic and western Europe. Although the dynamics behind clustering are less studied concerning the North Pacific, it is argued that the North Pacific storm track is also flanked during times of clustering (Mailier et al., 2006; Blender et al., 2015).

The following section elaborates on studies that analyzed cyclone clustering in climate models. Pinto et al. (2013) analyzed a large coupled Global Climate Model (GCM) ensemble for present-day climatic conditions, demonstrating that the GCM can mainly reproduce the geographical locations of clustered cyclones, although with certain biases: the areas where clustered cyclones are detected, for example, are more zonal in the GCM ensemble than in the reanalyses. Under future climate conditions, using data from the Coupled Model Intercomparison Project 3 (CMIP3), cyclone clustering decreases over the North Atlantic storm track and over parts of western Europe, as well as for more extreme cyclones. However, results were often not statistically significant in either present-day or in future scenarios (Pinto et al.,

2013). Pinto et al. (2013) concluded that the impact of anthropogenic climate change may be underestimated, since the study considered only a single GCM, and that a multi-model CMIP5 ensemble was required to further assess the uncertainties in future cyclone clustering.

Cyclone clustering using historical ERA40 reanalysis data (1958-2001) and 17 CMIP5 models for the RCP4.5 scenario during 2069-2099 was studied by Economou et al. (2015). Economou et al. (2015) stated that the typical aspects of the underdispersion (regularly occurring cyclones along the east coast of the US and near Newfoundland) and overdispersion (clustered cyclones in the eastern North Atlantic and over western Europe) of cyclone occurrences were captured by the models, which were in line with previous studies (e.g., Mailier et al. (2006) and Vitolo et al. (2009)). Moreover, the CMIP5 models were also able to reproduce the increase in overdispersion as shown for more extreme storms in the reanalyses (similar to Vitolo et al. (2009)). Future changes in the dispersion, however, were generally found to be minor and inconsistent between the models (Economou et al., 2015). In the RCP4.5 scenario, the multi-model mean dispersion demonstrated an increase in more intense storm clusters over Northern Europe and Scandinavia. But the 30-year overdispersion statistic was also characterized by large sample uncertainty and did not provide a strong indication of anthropogenic climate change (Economou et al., 2015).

Storm data sets often contain considerable sample and observational errors, which require a thorough quality control. Using 8 different storm data sets, Cusack (2016) showed that by reducing large uncertainties, such information provides a novel approach to evaluate cyclone clustering. This confirmed, in particular, that cyclone clustering increases with storm severity (Cusack, 2016).

Pinto et al. (2016) found that the overall features of underdispersion and overdispersion over the North Atlantic and western Europe, as well as the dipolar pattern of the North Atlantic Oscillation (NAO)'s influence on the dispersion, are essentially independent from the choice of the cyclone tracking method. Indeed, this emphasizes that clustering does not depend on the definition of a cyclone. Yet, the magnitude of the dispersion may still vary between different methods (Pinto et al., 2016).

To conclude, it is of utmost importance to examine and quantify the feedback from strong clustered cyclones over different regions in the Northern Hemisphere. The concept of the dispersion statistic opens up new possibilites to investigate cyclone clustering in various reanalysis data sets and climate models.

1.5 Impacts from Individual and Clustered Cyclones

1.5.1 Environments and Sectors

Extra-tropical cyclones pose severe socio-economic consequences for different environments such as the agriculture and forest habitats, as well as urban, transport and energy sectors (Fig. 1.2). In the following section, we will present an overview of the specific sectors and how they are affected by the occurrence of single individual or clustered cyclones (for a detailed review see Gliksman et al. (2022)[3]).

Cyclone-generated strong winds can damage or destroy urban areas including buildings, personal property, bridges, parks, trees, and turning loose debris into harmful flying objects. The severity and type of damage depends on the level of exposure as well as the vulnerability of the individual objects that are affected by local severe winds. For example, a city's infrastructure (i.e., railroads, roads, sidewalks) might largely be disrupted by overturning cars as an immediate consequence of emerging crosswinds or even floods (Alert Air Worldwide, 2022a).

In addition to damaging property, wind gusts from cyclones may harm the natural environment by causing storm surges that knock down trees, cause rivers and lakes to overflow, and create coastal erosion along beaches (Russell, 1993; Gliksman et al., 2022). Storm surges are generated by an unusual rise of water induced by strong winds from storms. This is particularly dangerous for houses built in coastal areas. Slow moving cyclones may accumulate large amounts of precipitation over the same area, leading to unprecedented rainfall and flooding (Sillmann et al., 2021; Koks et al., 2022).

Not only urban and transport sectors are affected, but also the energy sector: cities and rural environments all rely on an uninterrupted supply of energy, but this is a critical vulnerability when storms damage wind turbines (Kettle, 2020; Kettle, 2021). Similarly, solar panels might not withstand extraordinary wind gusts (Patt et al., 2013).

Another sector that human societies depend on is agriculture. Crops and plants are very sensitive towards an above-average supply of wind and water. Therefore, any losses in the production of, for example, wheat, might have socio-economic consequences (Gliksman et al., 2022).

Last but not least, storms may harm different flora and fauna in forest habitats. Windthrow, for instance, can increase the risk of fire, insect, and fungal damage in managed forests, as well as the damage to lakes and watercourses (Gardiner et al., 2010).

To summarize this overview, cyclone-related impacts such as wind gusts, storm surges, and flooding may be destructive to human-made structures and different environments. Indeed, the more exposed and vulnerable a sector, the larger the damage. This implies that (individual or clustered) cyclones can lead to significant socio-economic losses.

[3] currently under review in *Nat. Hazards Earth Syst. Sci.*, 2022, with A. Karwat as co-author.

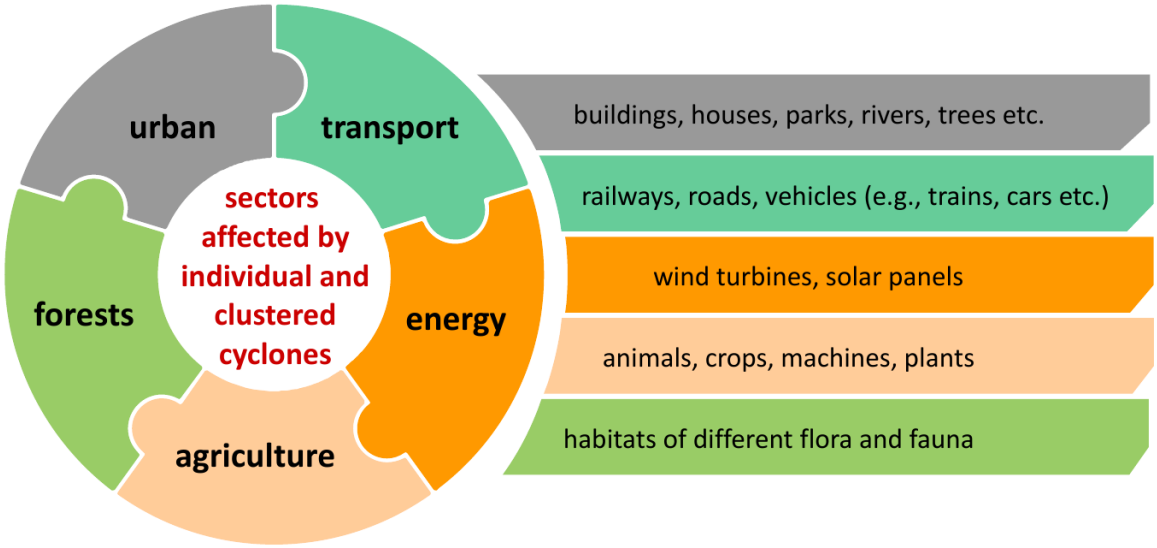

FIGURE 1.2: A schematic of all the sectors affected by individual and clustered cyclones (own creation).

1.5.2 Socio-Economic Losses

Since storms have the potential to cause large damage across different sectors, insurance companies provide protection to people and property against storm-related losses. There have been several damaging cyclones in the past, for example, Lothar and Martin, Kyrill, Ciara, and most recently Dudley and Eunice (Munich Re, 2002; Alert Air Worldwide, 2009; Alert Air Worldwide, 2022a). In the event of a storm, the insurance companies rely on an accurate storm model to estimate the claims resulting from that particular storm. According to Alert Air Worldwide (2022a), the insured losses of past cyclone cluster events since 1990 have reached approximately up to 17 bn € if they were to happen again today (Tab. 1.1). As a result, understanding the risk of previous storm occurrences is crucial for providing greater protection to socio-economies and reducing the cost of these natural hazards. Therefore, it is important to shed light on the long-term behaviour of storms in order to prevent and prepare our environments from hazardous and land-falling cyclones (Karwat et al., 2022). Developing climate-economy models that take into account the response of global warming might also help policy-makers to adapt societies in the future (Klawa and Ulbrich, 2003; Schwierz et al., 2010; Donat et al., 2011; Franzke, 2017; Franzke, 2021; Franzke et al., 2022).

TABLE 1.1: Insured losses of past cyclone cluster events if they were to happen again today as modeled with the "Verisk Extratropical Cyclone Model for Europe" (Table and caption adapted from Alert Air Worldwide (2022a)).

historical season	clustered extra-tropical cyclones	Verisk modeled insured loss (in bn €)
1990	Daria and Herta	14.5
1990	Vivian and Wiebke	8.9
1999	Lothar and Martin	17
2007	Hanno and Kyrill	6.6
2015	Elon and Felix	1.1
2015	Mike and Niklas	1.8
2022	Dudley and Eunice	approx. 3-5

1.6 The Shared Socioeconomic Pathways

An international team of climate scientists, economists and energy systems modellers have developed a number of new "pathways" that look at how societies, economies and demographies may evolve under different atmospheric greenhouse gas emissions scenarios until 2100. These pathways are referred to as "Shared Socioeconomic Pathways" (SSPs) and are separated into 5 main categories (O'Neill et al., 2016; Riahi et al., 2017):

- SSP1: Sustainability ("Taking the Green Road")
- SSP2: Middle of the Road
- SSP3: Regional Rivalry ("A Rocky Road")[4]
- SSP4: Inequality ("A Road divided")
- SSP5: Fossil-fueled Development ("Taking the Highway")

Each of these categories differs in terms of socio-economic developments and thus leads to different climate policies. Using a predetermined selection of these scenarios, climate change simulations have been carried out by international climate

[4]This SSP scenario was used in Chapter 4.

research organizations (O'Neill et al., 2016; Riahi et al., 2017). The Intergovernmental Panel on Climate Change's sixth assessment report (IPCC AR6) from 2021, for example, is also based on these SSPs (Masson-Delmotte et al., 2021).

The first narrative, SSP1, illustrates a sustainable and "green" world where the limits of nature are being respected. Human welfare is given more priority than economic expansion. Income disparities within and across states are decreasing. The consumption of energy and resources is minimized as much as possible. This scenario is the only one that meets the Paris Agreement's goal of keeping global warming in 2100 to around 1.5°C above preindustrial temperatures of 1850-1900 (O'Neill et al., 2016; Riahi et al., 2017).

The SSP2 scenario takes into account developments and emissions from the past and present. There are major differences between income patterns among nations. Although collaboration between countries is present, it is barely increased. The world population will gradually decline in the second half of the 21st century. There is a certain deterioration of environmental systems. After 2050, global CO2 emissions will have drastically decreased but not as quickly as in the SSP1 narrative. As the progress toward sustainability is slow, average temperatures rise about 2.7°C by the end of the century (O'Neill et al., 2016; Riahi et al., 2017).

Following the SSP3 scenario, global issues are put aside due to national and regional conflicts. Policymakers focus more on these conflicts and security issues, whereas education and technological advancement are given less attention. Thus, inequality is significantly increasing and some areas experience severe environmental harm. On this path, CO2 emissions roughly double compared to preindustrial times. As countries become more competitive with one another, average temperatures rise by approximately 3.6°C (O'Neill et al., 2016; Riahi et al., 2017).

The SSP4 narrative describes a pathway of inequality. The difference between industrialized countries that cooperate on a global scale and those who remain at a lower developmental stage, with low income and poor education levels, is growing. In some areas, environmental policies work well to address local issues, but not in others. Here, temperatures are increasing by roughly 3.7°C in 2100 compared to preindustrial temperatures of 1850-1900 (O'Neill et al., 2016; Riahi et al., 2017).

The last one, SSP5, leads to a scenario with very high fossil fuel use, energy demand and CO2 emissions. Since global markets become more interconnected in this scenario, innovations and technical advancement are increasing. However, the global energy-intensive lifestyle and an increased usage of fossil fuel resources are the foundations of social and economic progress. Thus, the global economy is expanding, while local environmental issues like air pollution are being individually addressed. By 2100, the average global temperature is about 4.4°C higher (O'Neill et al., 2016; Riahi et al., 2017).

All of these SSPs can be further divided into specific subcategories that describe the additional radiative forcing of future greenhouse gas emissions by 2100, ranging typically from 1.9 to 8.5 W/m^2 dependent on the scenario (see e.g. O'Neill et al. (2016)). In this study, we concentrate on the SSP3-7.0[5] scenario.

[5] see details in Chaper 4

1.7 Current Knowledge Gaps

In the last years, a considerable number of studies have been conducted on extra-tropical cyclone activity, with many of them focussing on how these storms will change in a warming climate. For example, Ulbrich et al. (2009) reported that in most studies the number of winter cyclones decreases under anthropogenic climate change, but in specific regions, over the Northeast Atlantic and the British Isles, as well as in the North Pacific, the number of intense cyclones increases in the climate models. However, cyclone frequency and intensity often are the only two main cyclone features considered, but less attention is given to other storm parameters such as the storms' radii and depths, which are crucial for cyclone development and intensification (Schneidereit et al., 2010). Cyclone propagation speed, direction and overall travelled distance of the storms are also factors that could change under global warming. The linkage between these features and a warmer climate has been partially explored by Jiang and Perrie (2007): under enhanced CO2 emissions, autumn storms were able to develop larger radii, become more intense and propagate faster, although these results were often not statistically significant.

Moreover, not many studies have addressed the combined effect of changes in storm impacts related to long-term trends in cyclone characteristics. These aspects are frequently regarded as independent issues, but are clearly interconnected. Therefore, it remains yet to be seen whether wind gusts and heavy precipitation associated with extreme winter storms have significantly changed in the last decades.

Studies on the Northern Hemisphere cyclone tracks have determined that storms might shift more poleward in the future (Bengtsson et al., 2006; Tamarin and Kaspi, 2017; Harvey et al., 2020), whereas there is a substantial lack of studies focussing on quantifying storm changes in historical reanalyses (e.g., using the state-of-the-art extended ERA5 reanalysis). Indeed, no robust estimations on various cyclone characteristics for different cyclone intensities have been determined. To capture the full spectrum of long-term behaviour in storms, long and consistent data sets are needed to predict future storm activity.

In a review by Catto et al. (2019), the authors have noted that the general interacting processes that might lead to changes observed in extra-tropical cyclones in a warmer climate are known. But despite this, no study has been able to precisely evaluate the regional-to-local when-and-where component with high statistical significance. Exploring such ties also applies to Northern Hemisphere storminess.

Apart from an individual storm perspective, clustered cyclone activity has gained more importance in recent decades due to excessive socio-economic costs (see Section 1.5.2). While the dynamics behind clustering are largely known, at least for the North Atlantic cyclone track (Priestley et al., 2020; Dacre and Pinto, 2020), the statistical quantification of clustering in historical and projected winter climates remains still unanswered. Using a dispersion statistic to characterize cyclone clustering, Karremann et al. (2014b) concluded that a constant overdispersion factor cannot be identified for storm losses, since the factor varies with intensity and between data sets. It is yet unclear whether alternative, more intuitive methods would be able to provide answers to this question.

Dacre and Pinto (2020) summarized that there are large sample uncertainties in clustered cyclone activity in climate change studies. It is yet to be determined how

different projections among the climate models are related to changes in clustered cyclones. This amplifies the increasing demand for new studies on multi-model or large ensemble evaluations of, for example, CMIP6 data. Nevertheless, as climatological analyses rely on consistent and long data sets, including a high, temporal and spatial, resolution to perfom cyclone tracking – such data have to be available. As a result, options often are limited because the resolution of climate models is not high enough; there is a lack in different future emissions scenarios or the climate models are restricted by time (they might not necessarily be available for a constant period, e.g., 2060-2100), which make direct comparison and quantifying cyclone clustering difficult. These are all critical research gaps.

1.8 Thesis Aims and Structure

The aim of this thesis is to address the knowledge gaps and questions highlighted above. The main research questions (RQ) that will be answered are as follows:

RQ1: Are the different ERA5-BE and ERA5 data sets compatible to perform a long-term trend analysis on storms and impacts in the full period 1950-2021?

RQ2: To what limit does a Lagrangian-based analysis allow for a comprehensive assessment of cyclone characteristics, for example, frequency, size, and intensity in the extended ERA5 reanalysis?

RQ3: Are there significant trends in the Northern Hemisphere storm tracks that provide us with new data on the atmospheric circulation response to global warming?

RQ4: How is clustered cyclone activity in the Northern Hemisphere mid-latitudes characterized in the ERA5 reanalysis and CESM2-LE in 1980-2020?

RQ5: How is extra-tropical cyclone clustering projected to change by 2060-2100 compared to 1980-2020 based on two metrics?

RQ6: What are possible reasons in terms of large-scale dynamics and cyclone characteristics for these projected changes?

Following these questions, the remaining part of this thesis is structured as follows:

Chapter 2 addresses the cyclone tracking method of Blender et al. (1997), which was applied in this thesis. Furthermore, the main data sets used for the analysis of historical long-term trends in Northern Hemispheric winter cyclones, as well as of clustered cyclone activity in recent and future winter climates, are presented. In addition, the background of the statistical methods for identifying trends in cyclones and how to differentiate between random, regular, and clustered cyclone activity are discussed. An overview of several statistical tests for quantifying results is provided.

Chapter 3 concentrates on the extensive analysis of long-term trends of Northern Hemispheric winter cyclones using a Lagrangian-based approach. The analysis shows the compatibility between ERA5-BE and ERA5 with a study focus of the cyclone characteristics and related impacts in the North Atlantic and North Pacific. Moreover, statistical significant trends are identified. This chapter was published in full in *JGR Atmospheres* as Karwat et al. (2022).

Chapter 4 examines clustered cyclone activity in recent and future winter climates. Cyclone clustering is characterized by two different metrics, and applied to the ERA5 reanalysis and CESM2-LE to identify preferred geographical regions for cyclone clustering in 1980-2020. Moreover, CESM2-LE simulations including an upper-level greenhouse gas emissions scenario are used to predict and quantify cyclone clustering in 2060-2100 compared to 1980-2020 and 1850-1890, respectively. This chapter has been submitted to the *Journal of Climate* and is currently in review as *Karwat et al. (2023)*.

Chapter 5 discusses the main results of this thesis. The implications and limitations are summarized. In addition the key conclusions of this thesis are presented. Finally, directions for potential future work in this field and beyond are proposed.

Chapter 2

Data and Methods

2.1 Cyclone Tracking Algorithm

As extra-tropical cyclones can largely differ in size (100-1000 km) and structure (often asymmetric), their velocities and other characteristics may also vary (Neu et al., 2013). Tracking the same physical features at different times acknowledges that one cyclone can sometimes split into different features or that two will merge into one, which may be a challenge for automated algorithms that are designed to identify and track the cyclones. Over the years, several tracking algorithms have been developed to track cyclones (e.g., Murray and Simmonds (1991), Sinclair (1994), Hodges (1995), Pinto et al. (2005), and Wernli and Schwierz (2006)). For a recent review see Neu et al. (2013).

The most common tracking scheme is based on a nearest-neighbour search where the trajectories of individual cyclones are connected at subsequent time steps as shown by Blender et al. (1997). Blender et al. (1997) define cyclones as local minima of the 1000 hPa geopotential field (as applied in Chapter 3) or as local minima of the mslp field (as applied in Chapter 4). This tracking algorithm assumes no preferred propagation direction and speed in the preceding field, making it a reliable and robust method to identify cyclones.

To conclude, multiple cyclone tracking algorithms have been established in the past, which have enabled studies on different storm aspects including storm features, connections to impacts, dynamics, and related mechanisms. Each tracking scheme has both advantages and disadvantages. As there is no universal definition of a cyclone, the tracking ultimately depends on how the storm was defined prior to analysis (Raible et al., 2008; Neu et al., 2013).

2.2 ERA5 Reanalysis

Reanalysis data are an assimilation of heterogeneous observations coupled with a numerical weather prediction model to reconstruct the historical weather and climate (Bollmeyer et al., 2015). Due to the reanalysis's temporally and spatially high resolution, these data sets can be applied to an increasing range of earth science disciplines such as the long-term study of cyclones. Although commonly used in many different fields, reanalysis data sets may intrinsically show some uncertainties, for example, global reanalysis data sets often underestimate the observed daily precipitation extremes (Hu and Franzke, 2020), since the difficulties lie in the (statistical or dynamical) downscaling in order to receive data in a specific resolution. Therefore,

the regional enhancement of global reanalysis data is very important. Reanalysis data sets are continuously being improved, updated and re-evaluated, since they provide a reliable source of historical weather and climate conditions in the atmosphere.

In this thesis, ERA5, a global atmospheric reanalysis produced by the European Centre for Medium-Range Weather Forecasts (ECMWF) (2020) was used. ERA5 is the latest state-of-the-art reanalysis by the ECMWF and the successor of the well-known ERA-Interim dataset (Hersbach et al., 2020).

In November 2020, the ECMWF released an ERA5 Back Extension (ERA5-BE)[1] ranging from 1950 to 1978 for the first time (European Centre for Medium-Range Weather Forecasts (ECMWF), 2020). In addition to the standard ERA5 reanalysis data from 1979 to 2021 (Hersbach et al., 2020), after some quality control and compatibility tests[2], a consistent and extended data series from 1950 to 2021 was used for detecting long-term trends in extra-tropical cyclones and related impacts.

The ERA5-BE and ERA5 reanalysis data sets have a horizontal resolution of 0.25° and a temporal resolution of one hour. For the cyclone tracking, 1000 hPa geopotential fields were interpolated on a 2° x 2° grid using three-hourly data for the winter months: December through February (DJF). Other studies in the past have used, for example, 850 hPa relative vorticity, which might be less influenced by the background state but more suitable for smaller (geographical) spatial scales due to its very high vortex resolution. A potential drawback of choosing relative vorticity rather than the geopotential or sea level pressure is that it is more noisy and could imply detecting some 'fake cyclones'. To estimate impacts related to the tracked cyclones hourly ERA5 data of 10m wind gust, the 10m u- and v-components of the wind, and total precipitation with a 0.25° spatial resolution were used. Cyclones were analyzed in the Northern Hemisphere with a focus on the North Atlantic and North Pacific sectors. Consequently, cylones were tracked over the North Atlantic and Europe (80°W to 30°E and 25°N to 75°N) and in the North Pacific (120°E to 120°W and 25°N to 65°N).

For studying clustered cyclone activity, ERA5 mean sea level pressure data from 1980 to 2020 (Hersbach et al., 2020) was used in the same spatial resolution, but for six-hourly data. The study areas of Europe (10°W to 15°E and 50°N to 60°N), the west coast of the US states and western Canadian provinces (120°W to 135°W and 30°N to 60°N) and the Gulf of Alaska (135°W to 165°W and 50°N to 60°N) were considered as most relevant for the cluster analysis.

2.3 CESM2 Large Ensemble

For projections on cyclone clustering, the CESM2 Large Ensemble (CESM2-LE) (Rodgers et al., 2021) was used. The CESM2-LE is based on the Community Earth System Model (CESM, version 2) and has a horizontal resolution of 1° (Danabasoglu et al., 2020). The model is forced by the CMIP6 historical forcing from 1850 to 2014 and a higher Shared Socioeconomic Pathways forcing scenario (SSP3-7.0) from 2015 to 2100. The SSP3-7.0 scenario relates to an additional radiative forcing of 7 W/m^2

[1] preliminary until June 2022
[2] see details in Chapter 3

by 2100 (Masson-Delmotte et al., 2021). On this path, temperatures rise steadily and CO2 emissions roughly double from current levels by 2100. By the end of the century, average temperatures have risen by approximately 3.6°C compared to pre-industrial temperatures of 1850-1900 (Masson-Delmotte et al., 2021). This scenario is in the upper-middle part of all the scenarios in CMIP6. It was introduced to close the gap between the RCP6.0 and RCP8.5 scenarios in CMIP5.

The same conditions for the cyclone tracking as conducted with ERA5 were used. Overall, the focus was on three different time slices: pre-industrial times (1850-1890), recent past (1980-2020), and future (2060-2100).

2.4 Statistical Approaches

The background of the statistical methods for identifying long-term trends in cyclones and differentiating random from regular or clustered cyclones are discussed in the following sections.

2.4.1 Quantile Regression

In predictive analysis, a commonly used method to detect trends is linear regression, which relies on specific assumptions about the model data. For example, data that is normally or Gaussian distributed. A Gaussian distribution is symmetric (i.e., bell-shaped) and has a constant mean and variance[3] (Wilks, 2011). It is one of the most frequently observed data distributions in nature. Thus, it is often called normal or standard distribution.

However, data does not always follow a clear linear trend where the data come from a normal distribution. Quantile regression does not imply such an assumption (Koenker and Hallock, 2001). It is a parametric method[4] to estimate, for example, the median, the 90th percentile and other quantile thresholds. In literature, quantiles are usually referred to as fractions (0.9) and percentiles to percents (90 %) (Coles, 2001). Quantile regression estimates the median or other quantiles of the dependent variable by solving the simplex algorithm (Koenker and Hallock, 2001). Thus, the aim is to minimize a sum of residuals[5], with n as the length of the time series y, ρ_p as the check function and p as the specified percentile, x^T as the vector of time points and β as the regression coefficients to be estimated. Consequently, it is defined by Koenker and Hallock (2001) as follows:

$$\sum_{i=1}^{n} \rho_p(y_i - x^T\beta). \tag{2.1}$$

The advantage of using quantile regression is that it is robust against outliers (Koenker and Hallock, 2001). In this study, a quantile regression analysis was performed in an almost identical manner to linear regression with one exception that an extra argument called τ, for example, $\tau = 0.9$ for the 90th percentile, is used to specify the quantile (Coles, 2001). The applied method is defined by eq. 2.2 with

[3] Variances measure the dispersal of the data points around the mean.

[4] see details in Section 2.5.2

[5] Residuals describe the difference between an observed value and a predicted value.

y(storm variable[6]*)* as the dependent variable, x as the slope, t as the independent time step and ε as the intersection with the y-axis:

$$y(storm\ variable) = x_1 t_1 + x_2 t_2 + ... + x_n t_n + \varepsilon + \tau. \tag{2.2}$$

Using quantile regression, the study's aim is to estimate the effect of an independent variable like the seasonal period of boreal winter (December, January, and February) on a specified quantile, for example, the 90th percentile of the dependent variable (i.e., a storm variable such as the cyclones' intensity) in Northern Hemisphere storm tracks.

2.4.2 Homogeneous vs. non-homogeneous Poisson Process

The homogeneous Poisson (point) process is a stochastic process, which assumes that a number of points in a region of finite size is a random variable that fits a Poisson distribution (Stoyan et al., 2013; Ross, 2020). In other words, it models the occurrence of random events in time and thus assumes that the arrival of any event is independent of the number of preceding events and the amount of time since the preceding event (Stoyan et al., 2013; Ross, 2020). The homogeneous Poisson process implies a constant rate parameter λ (Mailier et al., 2006). Here, it is assumed that storms occur at random and that the waiting times between storms are exponentially distributed.

In contrast, a non-homogeneous Poisson process can have a variable rate parameter λ(t) that is a function of time. This implies that the increments between events are non-stationary (Ross, 2020). Hence storms occur at specific times, depending on the intensity function defined in the process.

For example, storms that appear in clusters during high frequency periods are therefore more adequately represented by the Poisson cluster process, which is based on the assumption that many cyclones track over the same region in a short amount of time (Mailier et al., 2006). This case will be reviewed in the next section.

2.4.3 Dispersion Statistic

Mailier et al. (2006) introduced the concept of the dispersion statistic derived from a variable rate Poisson process to model cyclone occurrences. The probability of a number of occurrences (N) with a fixed rate λ during a time interval (ΔT) is defined as follows:

$$P(N = n) = (\lambda \Delta T)^n e^{-\lambda \Delta T} / n!, n = 0, 1, 2, ... \tag{2.3}$$

Thus, the deviation from a Poisson process is given by the dispersion index that is defined as

$$\psi = \text{Fano factor} - 1 = (\sigma^2 / \mu) - 1 \tag{2.4}$$

where σ^2 and μ are the variance and mean of the number of cyclone occurrences at each grid point, respectively. A value of ψ = 0 (Fano factor = 1) corresponds to a

[6] for example, the storms' intensity or radius

homogeneous Poisson process, which implies that the occurrences are uncorrelated and thus random events (eq. 2.4). For values of $\psi < 0$, cyclone occurrences are underdispersive and thus cyclones occur regularly; for values of $\psi > 0$ the occurrences are more clustered than random and hence overdispersive (Mailier et al., 2006).

To summarize, cyclone clustering can mathematically be described by the Poisson cluster process. In the cluster process, regions with high clustered activity have a large number of cluster events, whereas regions with low clustered activity show a small number of cluster events.

2.5 Statistical Significance, Tests and Quantification

In order to have a robust estimate of results, it is necessary to quantify and thereby demonstrate the statistical significance of the data. Here, the concept of hypothesis testing and the differences between parametric and non-parametric methods are presented. In addition, an overview of the most commonly used significance tests are given, focusing on the standard methods, such as t-tests, the modified Mann-Kendall trend test, and the alternative method of bootstrapping with replacement.

2.5.1 Hypothesis Testing

In statistics, hypothesis testing is the process of determining whether an assumption regarding a certain sample or data set is statistically significant. Statistical significance indicates that the outcome cannot be explained purely by chance or random variables. It is used to provide an educated guess about the data based on a specific assumption prior to testing. Thus, there are two mutually exclusive hypotheses: the null and the alternative hypothesis (Wilks, 2011; Ross, 2020). The null hypothesis states that there is no difference between groups or no relationship between variables. When there is adequate evidence for statistical significance in the data sample, the null hypothesis can be rejected and it is concluded that the result is statistically significant. In this case, the alternative hypothesis is accepted. Statisticians often denote the null hypothesis as H_0 and the alternative hypothesis as H_a (Wilks, 2011; Ross, 2020).

As the alternative hypothesis is the most intriguing one, because it assumes a significant difference in the two samples, a statistical test is run on the data to show that the null hypothesis can be rejected and that the data are statistically significant. This is accomplished by determining the probability (p-value) of a hypothesis to be true and comparing it to a specific threshold (significance level), where the null hypothesis can be rejected (Wilks, 2011; Ross, 2020). The p-value is an important component of statistical results, because it measures how strongly the data sample contradicts the null hypothesis. A significance level, typically $\alpha = 0.05$, for example, represents a 5% probability that a difference in the data exists. If the data provide solid evidence, e.g., the p-value is less than or equal to the significance level α, the null hypothesis can be rejected and the alternative hypothesis is accepted. Hence, the data is assumed to be statistically significant. In contrast, p-values greater than α suggest that there is not sufficient evidence for the data to be significantly different (Wilks, 2011; Ross, 2020).

2.5.2 Parametric or non-parametric?

Before choosing the most appropriate significance test, it is important to distinguish whether to employ a parametric or a non-parametric test, because these tests rely on different assumptions about the data (Wilks, 2011; Ross, 2020). A parametric test assumes that

1. the data is normally distributed,
2. the data in each group is sampled independently or randomly,
3. there are no extreme outliers in the data,
4. the variance of the data in each group should be almost the same.

Conversely, a non-parametric test (sometimes also referred to as a distribution-free test) does not assume anything about the underlying distribution of the data.

To assure that the parametric method is the most suitable for further analysis, the above mentioned conditions should, if possible, be validated. For example, there are two tests to check whether the data is normally distributed: the Shapiro-Wilk and the Kolmogorov-Smirnov test (Shapiro and Wilk, 1965; Wilks, 2011; Ross, 2020). For both of these tests, the null hypothesis states that the data come from a normal (or Gaussian) distribution. In the Shapiro-Wilk test, a test statistic of the sample's variance is calculated and then compared to critical thresholds. If the test statistic is less than the critical threshold, the null hypothesis must be rejected (Wilks, 2011; Ross, 2020). In other words, the regression line for the estimated values should be almost equal, resulting in a quotient close to 1, to assume that the data are normally distributed (e.g., visually solved by a QQ-plot).

In contrast, the Kolmogorov-Smirnov test compares the data's observed and expected, therefore normal, cumulative relative frequencies. The cumulative relative frequency is the cumulative frequency divided by the sample size. As a result, the maximum absolute difference between these curves is used as the test statistic (Wilks, 2011; Ross, 2020).

To summarize, the Shapiro-Wilk test is a more appropriate method for small sample sizes ($n < 50$ samples), while the Kolmogorov-Smirnov test is typically used for larger sample sizes of $n \geq 50$ when attempting to demonstrate that the data is normally distributed (Shapiro and Wilk, 1965; Wilks, 2011; Ross, 2020).

A parametric approach assumes not only normality, but also implies that the variances of the data sets are almost the same. For example, the F-test is used to check whether the variance of two groups of data is significantly different. The term F-test assumes that this test uses a F-statistic (inherently it is a test statistic), which is the ratio of two variances. If the variances are identical, the variance ratio equals 1 and the condition is fulfilled (Wilks, 2011; Ross, 2020). Since variances have squared units, they might be difficult to interpret. By taking the square root of the variance, the standard deviation of the data is obtained, which may be a more straightforward way for interpreting the results (Wilks, 2011; Ross, 2020).

Having checked the above conditions of a parametric method, a significance test is chosen. There are two main tests to compare the means of two independent groups of data and show whether the data are statistically significant: the Student's

t-test and Welch's t-test (Wilks, 2011; Ross, 2020). Both tests state in their null hypothesis that there is no statistically significant difference between the data ($H_0 = 0$). The following sections now examine the differences between these two tests.

2.5.3 Student's t-test

The Student's t-test assumes that both groups of data come from samples that follow a normal distribution and that those two groups have the same variance (Wilks, 2011). This is probably the most frequently used test to show significance. Here the test (t-)statistic is defined as follows:

$$(\bar{x}_1 - \bar{x}_2)/s_p(\sqrt{1/n_1 + 1/n_2}) \tag{2.5}$$

where x_1 and x_2 are the sample means, n_1 and n_2 are the sample sizes for sample 1 and sample 2, respectively, and where s_p is calculated as:

$$s_p = \sqrt{(n_1 - 1)s_1^2 + (n_2 - 1)s_2^2/(n_1 + n_2 - 2)} \tag{2.6}$$

where s_1 and s_2 are the sample variances. After determining the t-statistic and the degrees of freedom (i.e., the number of independent values in a data sample), a p-value may be found using a table of values from Student's t-distribution (Wilks, 2011). If the calculated p-value is less than the statistical significance threshold (e.g., the 95th percentile level), then the null hypothesis is rejected in favor of the alternative hypothesis. Thus, the result is concluded to be statistically significant.

2.5.4 Welch's t-test

The Welch's t-test also assumes that both groups of data are taken from samples that follow a normal distribution (Derrick et al., 2016). However, unlike the Student's t-test, it does not assume that those two groups have the same variance (Derrick et al., 2016). The test statistic is therefore defined as follows:

$$(\bar{x}_1 - \bar{x}_2)/(\sqrt{s_1^2/n_1 + s_2^2/n_2}) \tag{2.7}$$

where x_1 and x_2 are the sample means, and n_1 and n_2 are the sample sizes for sample 1 and sample 2, respectively. Here, the t-statistic and degrees of freedom are computed similarly to the Student's t-test, and the resulting p-value is compared to the pre-determined significance threshold. Employing this test has the advantage that it can be used on data where different variances are expected. Welch's t-test also remains robust for skewed distributions and large data samples (Derrick et al., 2016).

2.5.5 Pearson's chi-square goodness of fit test

The Pearson's chi-square goodness of fit test evaluates whether an observed distribution differs from the expected distribution (Wilks, 2011; Ross, 2020). Here, the null hypothesis states that data follow the specified distribution, whereas the data

do not follow the specified distribution in the alternative hypothesis. Consequently, the test statistic for the chi-square goodness of fit test is defined as follows:

$$x^2 = \sum \frac{(O - E)^2}{E} \tag{2.8}$$

where O are the observed and E the expected values (Wilks, 2011; Ross, 2020). The larger the difference between the observations and the expectated data, the bigger the chi-square x^2. Similarly to the t-tests, the resulting p-value, obtained from the test statistic and the degrees of freedom, is compared to the significance level (Wilks, 2011; Ross, 2020). If the p-value is less than the significance level, the null hypothesis can be rejected and it is concluded that the differences are statistically significant. Thus, the hypothesized distribution would not follow the expected distribution.

If many of the expected data are very small, the approximation of the p-value may be poor in Pearson's chi-square goodness of fit test. In this case, an alternative test such as the G-test or Fisher's exact test might be more suitable (Upton, 1992; McDonald, 2009).

The G-test, like previous tests, employs a test statistic that enables the computation of the p-value and subsequently, the comparison with the significance threshold. A p-value larger than the threshold would imply that the data do not follow the hypothesized distribution (McDonald, 2009)

Fisher's exact test, on the other hand, is used to find the total number of contingency tables (i.e., frequencies for combinations of two variables), which might have the same rows and columns (i.e., marginal distributions – the distribution of each of the individual variables) as the observed table. By calculating the percentage of hypothetical tables that are more extreme than the observed table, it is possible to determine the probability for the p-value (Upton, 1992; McDonald, 2009). The p-value can thus be compared to the significance level. If it is concluded that the alternative hypothesis is true and that the two variables are not independent, then the results are statistically significant (Upton, 1992; McDonald, 2009).

2.5.6 Modified Mann-Kendall trend test

The Mann Kendall trend test is used to analyze time series data for the quantification of increasing or decreasing trends (Mann, 1945; Kendall, 1975). It is a non-parametric method that does not assume a normal distribution. The null hypothesis in the Mann-Kendall test states that the data are independent and randomly ordered ($H_0 = 0$) (Mann, 1945; Kendall, 1975).

For a value other than $H_0 = 0$, the alternative hypothesis suggests a trend in the data. However, time series data are often affected by autocorrelation and therefore excluded in some trend detection tests, because the error would be transferred from one period to the next (Mann, 1945; Kendall, 1975).

In this study, a modified Mann-Kendall trend test by Hamed and Rao (1998) was used. In the modified test, a correction term is applied to avoid the effect of autocorrelation (ρ). This is done by using only significant values of ρ_s to calculate the variance correction factor n/n_s^*, since the variance of the Kendall test statistic ($V(S)$) is underestimated when the data are not serially independent. The number of observations n, and the 'effective' number of observations n_s^* account for autocorrelation

in the data, and $\rho_s(i)$ is the autocorrelation function of the observations. Thus, the empirical expression by Hamed and Rao (1998) is defined as follows:

$$n/n_s^* = 1 + \frac{2}{n(n-1)(n-2)} \sum_{i=1}^{n-1} (n-i)(n-i-1)(n-i-2)\rho_s(i). \tag{2.9}$$

The parent autocorrelation function of the observations, $\rho(i)$, is given by Kendall (1975):

$$\rho_s(i) = \sin^{-1}(\frac{\rho(i)}{2}). \tag{2.10}$$

Consequently, the corrected variance $V^*(S)$ by Hamed and Rao (1998) is then computed as follows:

$$V^*(S) = V(S)n/n_s^* \tag{2.11}$$

with *V(S)* obtained from the number of observations n and ties t up to sample i (Mann, 1945):

$$V(S) = \frac{[n(n-1)(2n+5) - \sum_t t(t-1)(2t+5)]}{18}. \tag{2.12}$$

The Kendall test statistic S (Kendall, 1975) is given as:

$$S = \sum_{k=1}^{n-1} \text{sgn}(x_j - x_k) \tag{2.13}$$

where $\text{sgn}(x_j - x_k)$ is the signum function. The remaining process of the trend analysis is included in the Mann-Kendall test by the corrected variance in the standardized test statistics (Z_{mk}), also denoted as z-score, which is estimated by Mann (1945) and Kendall (1975) as follows:

$$Z_{mk} = \begin{cases} \frac{S-1}{\sqrt{V(S)}} & \text{if S} > 0 \\ 0 & \text{if S} = 0 \\ \frac{S+1}{\sqrt{V(S)}} & \text{if S} < 0 \end{cases} \tag{2.14}$$

Z_{mk} shows the direction of the trend, since the sign values of the Kendall test statistic S will tend to increase or decrease continuously. A positive value of the z-score indicates an upward trend and a negative value indicates a downward trend. If S = 0, then no trend is detected.

Furthermore, it is noteworthy that by applying more data points n, the probability to find a trend is higher (Hamed and Rao, 1998). In this study, significance levels of 5 % and 10 % were used for the autocorrelation of $\rho_s(i)$, which produce the best overall empirical significance levels. The advantage of applying a corrected variance is that there is no need to either normalize data or their autocorrelation function (Hamed and Rao, 1998). The Mann-Kendall trend test is a common method used in the analysis of trends as shown, for example, by Gavrilov et al. (2016).

2.5.7 Bootstrapping with replacement

An alternative method to quantify results is by applying a bootstrap. Bootstrapping with replacement is the process of resampling a single data set to generate many simulated samples (Wilks, 2011; Ross, 2020). This also implies that all values in the sample have an equal probability of being selected, including multiple times. Thus, bootstrapped data could have duplicates. Bootstrapping follows this logic: resample, calculate a statistic (e.g., the mean), repeat this hundreds or thousands of times and a precise uncertainty of the mean of the data's distribution can be estimated (Wilks, 2011; Ross, 2020). The most important advantage over traditional hypothesis testing is that this method does not rely on any test statistic or a priori assumptions about the data's distribution.

Instead of looking at p-values, like with any classical t-test, the significance of the bootstrapped data can be determined by examining whether the confidence intervals for each group of data overlap (Schenker and Gentleman, 2001; Wilks, 2011). An overlap means that a sample of group 1 is in the interval of group 2. If they overlap, the null hypothesis would be accepted and it is concluded that there is no statistically significant difference between the groups. In contrast, if there is no overlap of the bootstrapped confidence intervals, the null hypothesis must be rejected and the alternative hypothesis is accepted, which suggests that the data are statistically significant. For the confidence intervals usually the 95th and 5th percentiles are considered (e.g., Daniels et al. (2014)). This is similar to the 95% significance level of t-tests.

Chapter 3

Long-Term Trends of Northern Hemispheric Winter Cyclones in the Extended ERA5 Reanalysis[1]

The research questions that are addressed in this chapter are as follows:

RQ1: Are the different ERA5-BE and ERA5 data sets compatible to perform a long-term trend analysis on storms and impacts in the full period 1950-2021?

RQ2: To what limit does a Lagrangian-based analysis allow for a comprehensive assessment of cyclone characteristics, for example, frequency, size, and intensity in the extended ERA5 reanalysis?

RQ3: Are there significant trends in the Northern Hemisphere storm tracks that provide us with new data on the atmospheric circulation response to global warming?

3.1 Abstract

Understanding how historical extratropical cyclone tracks respond to global warming is crucial for predicting future storm activity. Thus, long reanalysis data sets are needed to investigate long-term changes in storm features and their impacts. By using a systematic change-point analysis, we provide evidence that the presatellite ERA5 data of the Backward Extension (covering 1950–1978) is highly compatible with the standard ERA5 (1979–2021) data set. The joint ERA5 data from 1950 to 2021 is consistent in all storm-related quantities, consequently allowing long-term studies. Our trend analysis suggests that the intensity of extratropical cyclones has increased significantly during 1950–2021. The number of North Pacific storms has increased, and while they have longer life cycles and travel larger distances, they grow more slowly. For 1979–2021, we find notable increases in wind gusts for North Atlantic storms and in precipitation extremes for North Pacific storms. Our results also indicate an increase in Northern Hemispheric storminess based on an index of an extreme percentile of the central geopotential. Finally, we show potential impact locations using the findings of our trend analysis.

[1] published in *J. Geophys. Res. Atmos.*, 2022, with A. Karwat as first-author.

3.2 Plain Language Summary

To understand how midlatitude storms change in the context of global warming, long-term trends in the historic storm behavior need to be examined. This requires long data sets that are consistent over time. By using a recently extended data set that covers the years 1950–2021 for the first time, we look for inconsistencies in their time series of several storm characteristics. Our results indicate continuous behavior in all storm measures, allowing us to use the full period for the long-term study of midlatitude storms and their impacts. We perform a trend analysis and show that midlatitude storms have intensified from 1950 to 2021. The number of North Pacific storms has increased, and while they have longer life cycles and travel larger distances, they grow more slowly. Since 1979 wind gusts and storm-related precipitation have notably increased. We show potential impact locations using the findings of our trend analysis. Future storm adaptation planning should take these results into account.

3.3 Key Points

- We provide evidence that ERA5 data of the Backward Extension is highly compatible with ERA5 for midlatitude storms and, thus, their combination can be used for long-term studies
- We find significant trends in both Northern Hemispheric storm tracks for more poleward storms, longer distance traveled, and a speed decrease
- We find significant positive trends for 1979–2021 in wind gusts for the North Atlantic and in precipitation extremes for the North Pacific

3.4 Introduction

Extratropical cyclones are one of the major natural hazards affecting the midlatitudes, especially large economies in Europe. For instance, the economic damage caused by the European wind storm Ciara in February 2020 caused at least €1.9 billion in insurance claims (Alert Air Worldwide, 2020) and was recently surpassed by insurance claims ranging from €3 billion to €5 billion in the aftermath of the storms Dudley and Eunice in February 2022 (Alert Air Worldwide, 2022a). These storms are among the most expensive storms since storm Kyrill hit Northern and Central Europe in January 2007. Furthermore, hurricane-force wind gusts and heavy precipitation accompanied the North Pacific Hanukkah Eve wind storm in December 2006 and the Great Coastal storm in December 2007; both caused havoc in the US states of Oregon and Washington and the Canadian province of British Columbia (Mass, 2008). In December 2020, an intense extratropical cyclone moved across the North Pacific toward the Aleutian Islands of Alaska. This storm developed rapidly by bombogenesis and set a new record for the lowest central pressure in Alaska (National Environmental Satellite Data and Information Service, 2021). These events show how important it is to understand how extratropical cyclones have changed in the last few decades to gauge probable future storm behavior.

To estimate the impacts of extreme storms, current research focuses on developing economic damage functions and high-resolution wind damage models (Franzke, 2017; Franzke, 2021; Franzke and Czupryna, 2019; Koks and Haer, 2020). An important question from a predictability point of view is the estimation of storm losses for potential long-term impacts; studies show that there are significant trends in socio-economic damages (Franzke, 2021; Franzke and Czupryna, 2019). Current research is also interested in cyclone-related compound precipitation and wind extreme events and their relationship to extratropical cyclones (Messmer and Simmonds, 2021; Owen et al., 2021). Owen et al. (2021) show that these events are frequently observed over Europe.

A Lagrangian perspective is particularly crucial for linking wind gust and precipitation extremes to Northern Hemispheric storms, since this kind of approach incorporates the tracking of cyclonic features, e.g., storm speed and intensity, at any point in space and time. Therefore, only Lagrangian trajectories sustain spatial and temporal representativeness of cyclones that allows for a comprehensive analysis of storms and impacts (Walker et al., 2020). The Eulerian method, however, provides less information about the individual cyclone characteristics but instead indicates how a given location will experience these changes (Walker et al., 2020).

Indeed, winter storm activity of the Northern Hemisphere is of great interest: an increase in storminess over the Northeast Atlantic and Northern Europe during 1960–1995 was identified (Alexandersson et al., 1998; Alexandersson et al., 2000), while studies on longer time scales often could not confirm significant trends (Storch and Weisse, 2008). Thus, long-term trends in storminess are still an active area of research (Feser et al., 2015; Krueger et al., 2019; Matulla et al., 2008). Trends in extratropical cyclones have been investigated, for instance, using the ERA-20C and NOAA-20CR reanalyses (Befort et al., 2016; Krueger et al., 2013; Wang et al., 2012) or the ERA-Interim reanalysis (Lee et al., 2019). Dullaart et al. (2019) show that ERA5 can be used to simulate probable surge heights of historical storm events, albeit Dullaart et al. (2019) also indicate that a longer ERA5 record could reduce uncertainties.

In a recent study, Bell et al. (2021) show that the extension of the ERA5 reanalysis back from 1979 to 1950 continues coherently with the latter period of 1979-present. For example, there is high confidence in the back extension due to the precise representation of the North Sea Storm of 1953 (Bell et al., 2021). Additionally, the variability of precipitation is consistent with observations; the distribution of winds agrees in most parts (Bell et al., 2021). However, neither long-term trends of midlatitude storms nor storm-related impacts are addressed by Bell et al. (2021). As a result, it is still unclear if the reanalysis can be used for a more in-depth study of extratropical cyclones in the full period 1950–2021. Here, we aim to close that knowledge gap. No studies have investigated trends of extratropical cyclones and related impacts like extreme precipitation and wind gusts using the most recently extended ERA5 reanalysis that spans about 71 years of data. In our study, we provide evidence that ERA5 data of the Backward Extension (ERA5-BE; 1950–1978) and ERA5 (1979–2021) can be combined for the long-term study of extratropical cyclones and their impacts.

To achieve this, we define our study objectives as the following:

1. We explore whether there are quantitative changes between the two ERA5 data sets using a systematic change-point analysis and temporal histograms of all storm-related variables in the full period 1950–2021.
2. We apply a Lagrangian-based analysis that allows for a comprehensive assessment of the cyclone characteristics, e.g., frequency, size, and intensity in the extended ERA5 reanalysis.
3. Finally, we quantify significant trends in the Northern Hemisphere storm tracks that provide us with new data on the atmospheric circulation response to global warming.

The remainder of this paper is organized as follows: In Section 3.5, we introduce the ERA5 data sets and the methodology; in Section 3.6, we present our results, and in Section 3.7, we discuss the conclusions of this study.

3.5 Data and Methods

3.5.1 ERA5 Reanalysis Data

We use the ERA5 back extension reanalysis data from 1950 to 1978 (preliminary version, hereafter referred to as ERA5-BE) and the ERA5 reanalysis data from 1979 to 2021 (European Centre for Medium-Range Weather Forecasts (ECMWF), 2020; Hersbach et al., 2020). ERA5-BE has been a preliminary version since its release in November 2020. This is because the quality control showed that tropical cyclones were overly intense. A recent update from June 2022 corrected the issue with tropical cyclones in ERA5-BE. Nevertheless, we only study extratropical cyclones so this issue does not affect us. The ERA5-BE and ERA5 reanalysis products have a horizontal resolution of 0.25° and a temporal resolution of 1 hour. For the Lagrangian cyclone tracking we interpolate the 1,000 hPa geopotential fields on a 2° × 2° grid and use 3-hourly data for the winter months December-February (DJF). To estimate impacts related to the cyclones, we use hourly ERA5 data of 10-m wind gust, the 10 m u-component and v-component of the wind, and total precipitation with a 0.25° spatial resolution. We analyze cyclones in the Northern Hemisphere and focus on the North Atlantic and North Pacific sectors. Cyclones are tracked over the North Atlantic and Europe (80°W–30°E and 25°–75°N) and in the North Pacific (120°E–120°W and 25°–65°N; Figure 3.1).

3.5.2 Methods

To show how compatible ERA5-BE and ERA5 are, we will introduce a change-point detection analysis of all storm-related variables, followed by the methods for identifying trends in cyclone characteristics, the storm tracking methodology and impact measures.

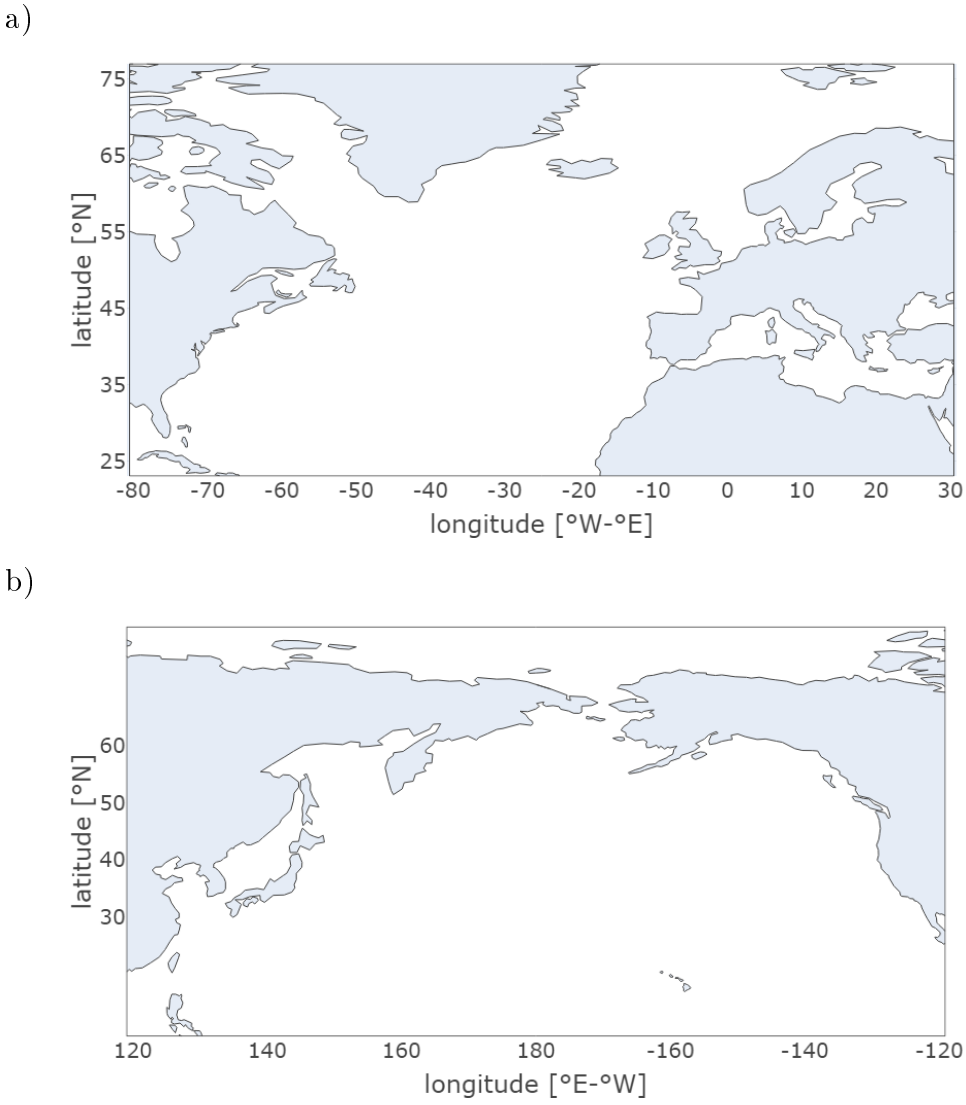

FIGURE 3.1: Study areas of the (a) North Atlantic and (b) North Pacific sectors. Cyclones are tracked over the North Atlantic and Europe (80°W–30°E and 25°–75°N) and in the North Pacific (120°E–120°W and 25°–65°N).

Compatibility of ERA5-BE and ERA5

In order to evaluate whether we can combine ERA5-BE and ERA5 for a long-term cyclone analysis, we apply a change-point detection analysis, which is a method to detect systematic changes in the mean or variance of different variables at some a priori unknown time. Here, we use a binary segmentation-based change-point analysis method (Killick and Eckley, 2014).

The inclusion of satellite data starting in 1979 has the potential to introduce a significant change in the reanalysis. If the change-point analysis does not detect any significant change-point around 1979 we claim that we can combine both reanalysis data sets for a long-term analysis. For a single change-point detection, the test statistic is defined as $\lambda = 2[\max_{\tau_1} ML(\tau_1) - \log p(y_{1:n}|\hat{\theta})]$, where $ML(\tau_1)$ is

the maximum log-likelihood of the change-point position τ and $\log p(y_{1:n}|\hat{\theta})$ is the log-likelihood of the probability density function p. This function depends on the data y for 1:n years and the maximum likelihood estimate $\hat{\theta}$. Thus, for a specific threshold c, if $\lambda > c$, a single change-point in the data is detected (Killick and Eckley, 2014). This concept can be further extended to detect multiple change-points within a data series by minimizing the function $\Sigma_{i=1}^{m+1}[C(y_{(\tau_{i-1}+1):\tau_i)}] + \beta f(m)$ where C is a cost function based on the log-likelihood and $\beta f(m)$ is a multiple change-point indicator of the threshold c (Killick and Eckley, 2014). To minimize this function, a binary segmentation (Edwards and Cavalli-Sforza, 1965; Killick and Eckley, 2014) is used, which is one of the most common algorithms in change-point analysis. In the binary segmentation algorithm, a single change-point test statistic is applied to the full data series. If it identifies a change-point in the data, the data are split into two at the location of the change-point. This concept is then repeated on the two new data sets and the algorithm continues splitting the data sets until no more change-points are identified (Edwards and Cavalli-Sforza, 1965; Killick and Eckley, 2014). Here, we look explicitly for single change-points in our storm-related variables, however, considering multiple change-points do not change our conclusions. If there are change-points, we use a bootstrap to estimate a probability on whether these change-points are significant. Here, we use a Bootstrapping with resampling (Wilks, 2011). By doing this n times (here: n = 1,000), we are able to determine a probability of the mean (confidence interval) of the data distribution.

Furthermore, we analyze the distribution of the geopotential (in regions and along the tracks), relative vorticity at 850 hPa, mean sea level pressure, 10-m wind gust, and the 10 m u-component and v-component of the wind through different time series of histograms for both parts of the Northern Hemisphere. This is a powerful approach to visualize possible changes within the different distributions of the variables (Potter et al., 2020). Just like a classical probability distribution function (PDF), the temporal histograms take into account every single data point of the geopotential, whereby the histogram bins are computed for the full (DJF) period 1950–2021. Finally, the data are displayed as bin density (instead of counts) and plotted against time (1950–2021). A great advantage of this approach is that it reveals shifts in the data and that it can be used independently of location or time scale (Potter et al., 2020).

Trend evaluation

As we want to cover the whole range of cyclones and the impacts, we use the arithmetic mean and take various percentiles into account. Trends in cyclone characteristics and impacts are identified with quantile regression (Chatterjee and Hadi, 2000; Koenker and Hallock, 2001). Therefore, we look at trends in both mean and percentiles. Furthermore, trends in extremes can be estimated when specified as high or low percentiles (e.g., 5th or 95th percentile). This is a useful method to characterize trends in extremes (Donner et al., 2012; Franzke, 2015; Gao and Franzke, 2017; Karwat and Franzke, 2021).

Moreover, examining various percentiles also enables us to gauge how the whole distribution evolves over time. As a result, we investigate several percentiles for assessing the full spectrum of cyclones and their impacts. This can be helpful for different cyclone intensities and goes beyond the insight one can gain using just linear regression.

Due to the auto-correlation of climate data (Franzke, 2012), statistical trend estimation methods need to take account of this property. Here, we use the nonparametric modified Mann-Kendall trend test (Hamed and Rao, 1998). The test can be applied on specific percentiles as shown, e.g., by Gao and Franzke (2017) and Karwat and Franzke (2021). For most significance tests, we provide the actual p-values. However, we consider the significance levels of 5% and 10% as relevant for our discussion of trends.

Cyclone Tracking and Impacts

Different algorithms to identify tracks of cyclones have been developed by, e.g., Murray and Simmonds (1991), Sinclair (1994), Hodges (1995), Wernli and Schwierz (2006), and Neu et al. (2013). Here, we use the Lagrangian cyclone tracking algorithm of Blender et al. (1997). In the tracking algorithm cyclones are defined as local minima of the 1,000 hPa geopotential field (z1000). The cyclone tracks are computed by a nearest-neighbor search in the z1000 field where the trajectories of individual cyclones are connected at subsequent time steps. Note that we distinguish between the central geopotential (actual cyclone tracks) and the geopotential (entire regions) for illustrative purposes. The central geopotential describes the intensity of the storms from the tracking while the entire geopotential represents the intensity in the whole regions including the cyclones. In our study, we only consider cyclones with a minimum lifetime of 24 hr and which have traveled at least a distance of 1,000 km.

To estimate the impacts of wind and precipitation, we use a comoving Lagrangian cyclone-box, which uses the latitude, the longitude, the radius of each cyclone, and the 2° grid spacing as the likely impact region of the cyclone. Within this box, the impacts are calculated at 0.25° resolution at every hourly time step to track the full movement of each individual cyclone.

The severity of storms is an important indicator in the analysis of long-term trends of extratropical cyclones (Feser et al., 2015; Matulla et al., 2008).

We define storminess by a seasonal storm index as a function of time

$$S(t) = \frac{z_{c,0.2}(t) - \overline{z_c}(t)}{\sigma(z_c(t))} \tag{3.1}$$

where t is time and represents a value for each DJF in each year. We use the DJF time series of the second percentile of the central geopotential $z_{c,0.2}(t)$ (2° resolution data) from all tracked cyclones in a given year and season and from which the seasonal average $\overline{z_c}(t)$ is subtracted; then divided by the standard deviation $\sigma(z_c(t))$. We use the second percentile of the central geopotential since we are interested in the most intense storms. This is similar to a *Storm Severity Index* (SSI; Roberts et al. (2014)), which is important for damage and loss estimates. While the SSI depends on the wind speed over land or the wind gusts, the area affected and the duration of the storm, our storminess is directly associated with the intensity of the cyclones. The central geopotential represents the intensity of the cyclones. Therefore, it is intrinsically linked to storminess and a derivative of the Lagrangian cyclone tracking. Our storminess index is robust with regard to the particular choice of the percentile (not shown).

We also compute a cyclone deepening rate for each cyclone: $D(t) = \Delta z_c(t)/\Delta t$, where $\Delta z_c(t)$ is the difference of the central geopotential between two consecutive time steps and Δt is the time step size. Second, we also use the mean gradient of the geopotential instead of the central geopotential as an alternative method for a deepening rate.

Trends in cyclone movement are studied by computing their propagation speed from the great-circle distance between two points using the spherical Pythagorean theorem (Haversine formula). Cyclone speed is then computed at every hourly time step using $v = \Delta d/\Delta t$, where distance is d and time is t.

Aside from the deepening and propagation speed, we also examine the 10 m *eddy kinetic energy* (EKE) for each time step of the propagating cyclones and then compute the respective percentiles of all cyclones per winter. The EKE is a common measure for storm track intensity (Montoya Duque et al., 2021; Rivière et al., 2014); $EKE = (u^2 + v^2)/2$, where u and v are the 10 m zonal and meridional velocity components, respectively. An increasing EKE could provide information on the long-term trends in cyclonic growth processes.

3.6 Results

3.6.1 Change-Point Analysis

First, we examine whether we can combine both ERA5 periods and whether there is a systematic change-point between 1978 and 1979 due to the use of satellite data in the latter period. It is important to check whether the mean or variance differs between the two periods. Overall, the transition between ERA5-BE and ERA5 is homogeneous in all North Atlantic and North Pacific cyclone-related parameters across the distinct time series (see Figures A.1 and A.2 in Appendix A.1). The continuous behavior in the time series implies that the joint ERA5 data from 1950 to

2021 is consistent, and is supported by the binary segmentation, which yields no change-points in any bin density of the different variables.

The only exception is relative vorticity at 850 hPa. In 1978/1979, we find very few change-points and only in the North Atlantic. To show how significant these change-points are, we use a bootstrap analysis with 1,000 samples. Only in 1.41% of our bootstrap samples we find evidence for a change-point detected in 1978/1979, indicating that the change-point is outside the 95th percentile. Furthermore, the vorticity time series is consistent despite some occasionally appearing change-points (Figure 3.2). These change-points could be caused by internal variability of the investigated period. Since our cyclone tracking algorithm does not depend on vorticity, we now can examine all other cyclone-related parameters in the full time series.

Analyzing the cyclone activity from 1950 to 2021 we find single change-points for the seasonal number of extratropical cyclones in 1952 (North Atlantic) and 1974 (North Pacific); however, no change-point in the transition phase of 1978/1979, which suggests that the time series is continuous (Figure 3.3a). In summary, the combined ERA5 data can be used to study long-term trends in extratropical cyclones.

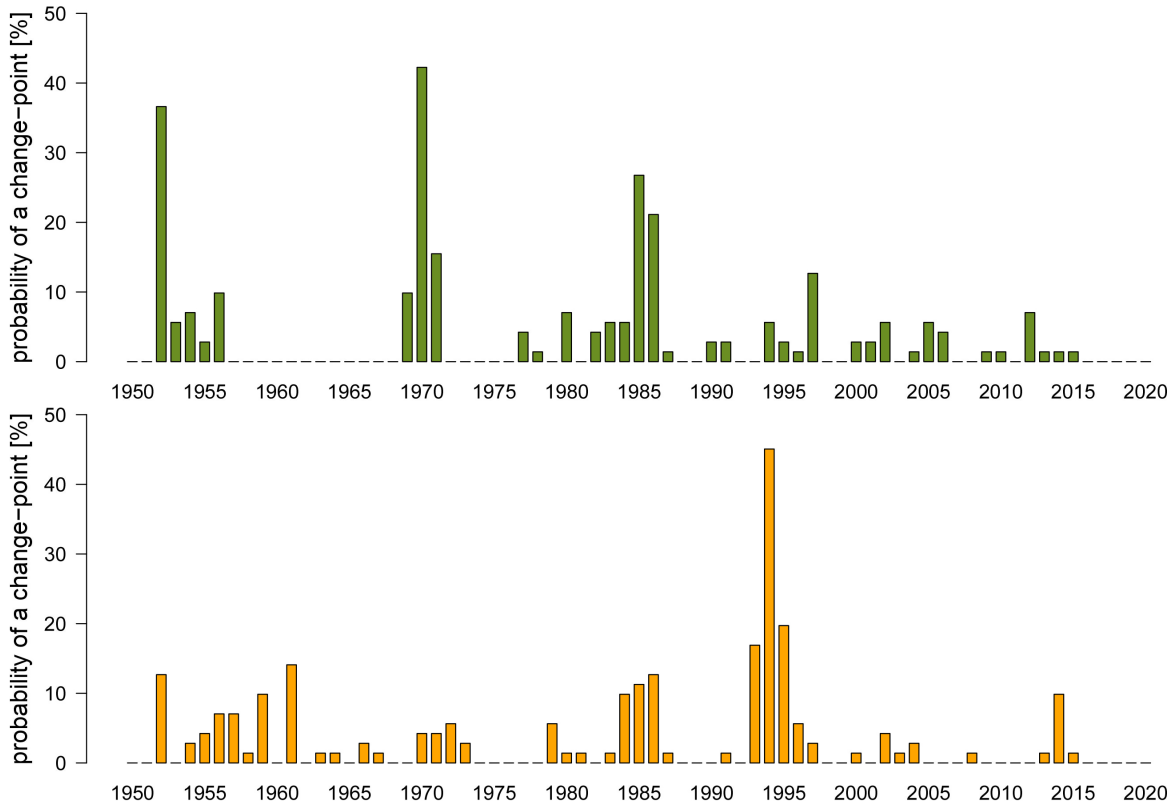

FIGURE 3.2: Probability of a change-point in ERA5's relative vorticity at 850 hPa for the North Atlantic (green bars, upper panel) and North Pacific (yellow bars, lower panel) study areas in 1950–2021. The probability for a change-point in 1978/1979 is 1.41% in the North Atlantic, indicating that the change-point is outside the 95th percentile and not significant. In the North Pacific, there is no change-point in 1978/1979.

a)

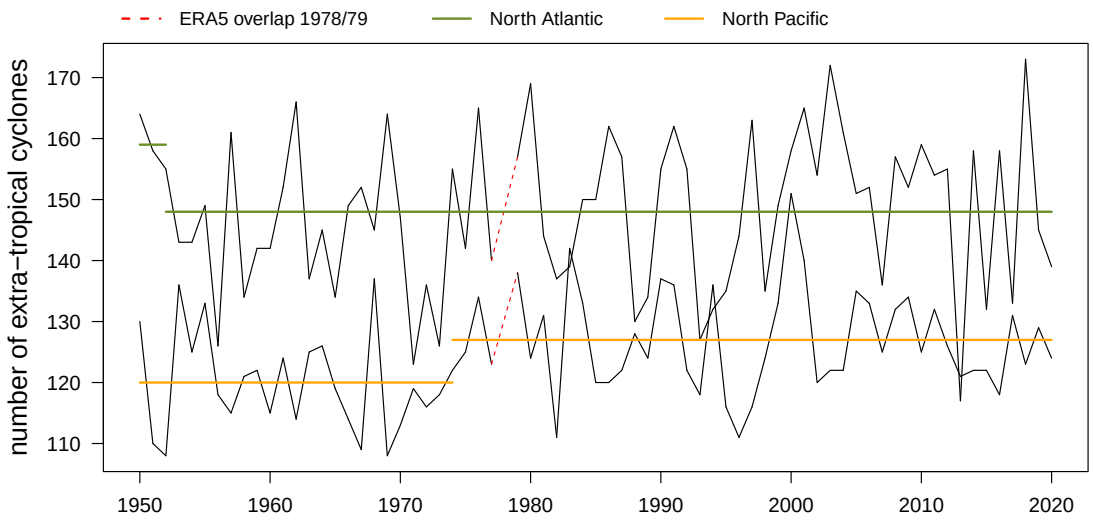

b)

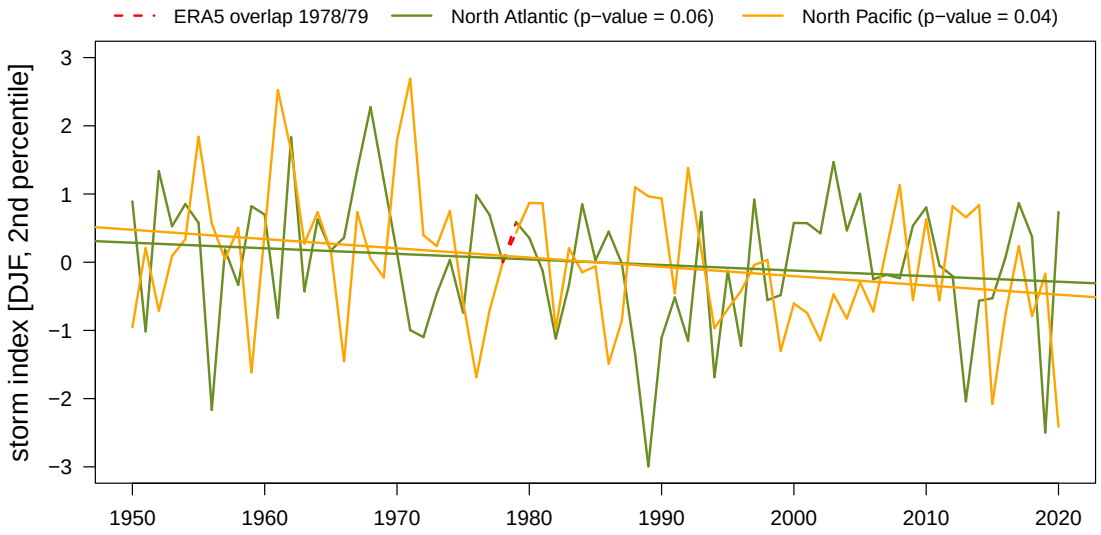

FIGURE 3.3: (a) Binary segmentation change-points in mean analysis of Northern Hemispheric extratropical cyclone counts and (b) storminess indices for the North Atlantic and North Pacific sectors in 1950–2021. Note that positive indices relate to less storminess while negative indices are connected to more storminess.

3.6.2 Significant trends in cyclones

Having shown that there is no systematic change-point around 1978/1979, we can examine the combined time series for trends. We find a change in the frequency in both North Atlantic and North Pacific cyclones in 1950–2021 (Figure A.3 in Appendix A.1). The modified Mann-Kendall test indicates a positive significant trend of ~1.1 cyclones per decade in the North Pacific. Although the number of cyclones seems to increase in the North Atlantic also, albeit at a slower pace, the trend is not significant here. The increase in numbers may be a slower process in this case; however, the trend in these two study areas is rather similar (Figure A.3 in Appendix A.1). Furthermore, the *F*-test (Wilks, 2011) implies no significant differences in the variance between both periods for neither North Atlantic (p-value = 0.65) nor North Pacific cyclones (p-value = 0.89). This suggests that our results are robust. Since any trends in the entire geopotential (z1000 field) might affect the tracking of cyclones, we also check the background state of the geopotential for significant trends using standard linear regression. We find that the geopotential is decreasing in 1950–2021, e.g., at 30°W 57°N in the North Atlantic sector: ~1.88% per decade in 1950–2021 (p-value < 2.2 x 10^{-16}). This suggests that the background state of the geopotential might affect the intensity of the tracked cyclones. We see this is also true for the geopotential in the North Pacific, e.g., at 200°E 61°N the geopotential is decreasing by 0.73% per decade (p-value < 2.2 x 10^{-16}). As a result, we expect that the further cyclone trend analysis will be influenced by the background state of the geopotential.

Following the change in cyclone frequency, we examine whether there are also trends in Northern Hemispheric storminess. The storm indices based on the second percentile of the central geopotential in 1950–2021 are shown in Figure 3.3b. Note that positive indices relate to less storminess while negative indices are connected to more storminess. Indeed, the indices suggest an increase in North Atlantic and North Pacific storminess. The largest (negative) storminess in the North Atlantic is observed in the winter of 1989/1990 (Figure 3.3b). Here, the storminess is a result of the storm series of 1990—with cyclones Daria (January 1990, McCallum (1990)) and Vivian (February 1990, Schüepp et al. (1994)) falling into our spectrum of winter storminess. The second-largest storminess in the North Atlantic is associated with wind storms Ciara (February 2020, Alert Air Worldwide (2020)) and Dennis (February 2020, German Weather Service (DWD) (2020)) in the 2019/2020 winter season (Figure 3.3b). The stormy winter of 2013/2014 (Figure 3.3b) represents yet another season affected by large storminess and is closely linked to the cyclones Bernd, Dirk and Erich (all December 2013, Priestley et al. (2017)), and Tini (February 2014, Priestley et al. (2017)).

The North Pacific saw the highest (negative) storminess in 2020/2021 (Figure 3.3b), when a triplet of extratropical cyclones developed over the North Pacific and another storm set a new record for the lowest pressure in Alaska (National Environmental Satellite Data and Information Service, 2021). Storminess was also large during the 2015/2016 winter (Figure 3.3b), which was a particularly active season (Bancroft, 2016). Strong North Pacific cyclones formed around Japan, before weakening close to or in the Gulf of Alaska. Some cyclones moved across the North Pacific, with one strong system moving into the Bering Sea in January 2016 (Bancroft, 2016). The Eastern North Pacific also experienced a second storm track aside

from the main cyclone track where cyclones partly turned toward the US Pacific Northwest and British Columbia (Bancroft, 2016).

Thus, we find that the Northern Hemispheric storminess has significantly increased for the most intense cyclones from 1950 to 2021. Our findings reveal that the trends in increasing Northern Pacific storminess and their seasonal numbers of cyclones are slightly more robust (p-values ≤ 0.05) than the trends in North Atlantic cyclones (p-values ≤ 0.1). Finally, the links between well-known storms and high-active winter storm seasons in relation to large storminess indices also emphasize that impacts are increasing since the 1990s. This is a critical factor to consider in future storm adaptation planning.

3.6.3 Significant trends in cyclone characteristics and impacts in 1950-2021

We further examine trends in mean characteristics and impacts of North Atlantic and North Pacific cyclones (Figure 3.4). The cyclone characteristics are the central geopotential, mean gradient of the geopotential, radius, depth, age, distance traveled, propagation speed, EKE, storm location (coordinates), the 10 m u-component and v-component of the wind, wind gust, and total precipitation.

We find a significant positive trend in the mean traveled distance of North Atlantic cyclones of ~21 km (0.93%) per decade (p-value = 0.02, Figure 3.4a). Moreover, these storms shift northward from ~54.05°N to 54.8°N on average, which relates to a change of 0.2% per decade (p-value = 0.07, Figure 3.4a). The latitude band affected by this shift includes central Northern Ireland, Northern England (e.g., North Pennines), and the German-Danish border in Northern Germany. The change also affects the largest German island in the North Sea, Sylt, as well as the Baltic Sea islands of Southern Denmark, and the Polish Baltic coast. This trend suggests that wind damage and flooding could become more common in these regions. It also affects intrinsically larger areas north of the mean cyclone shift, such as Scotland, Denmark, Scandinavia, and the Baltic nations (Figure 3.5), because cyclones frequently make landfall in these particular regions. In 1950–2021, the mean analysis of wind gusts shows no significant trends. There is a tendency toward a decline in the mean amount of total precipitation in the Northern Hemispheric cyclones by ~0.7% per decade. However, this trend is also insignificant (not shown). Therefore, we find that long-term trends in mean impacts cannot confirm any changes to the lysis regions yet. This could be due to the cyclone-related impact measures being underestimated in ERA5 or it may be a result of the high-interannual variability in the (mean) time series.

Moreover, we check whether the impacts change in a wider cyclone-box since this could imply different trends in, e.g., heavy precipitation. The instantaneous total, maximum, and mean amount of precipitation increases with the box size, however, the trends are not altered when extending the cyclone-box. This is an important finding as it shows that the distribution of precipitation around the cyclone does not change in a wider impact region. Thus, the accumulated precipitation is proportional to the cyclone-box size. Similarly, we find that for wind gusts a bigger cyclone-box does not lead to changes in the trends in any part of the Northern Hemisphere, which indicates that our results are robust. Consequently, our cyclone-box

method is showing reasonable skill in capturing the cyclone-related precipitation and wind gust extremes.

In connection with impacts, it is also important to look at the propagation speed of cyclones, since slow-moving storms may cause severe damage. The mean analysis shows that North Atlantic cyclones are decreasing significantly in speed by ~0.2 km/hr (0.29%) per decade (p-value = 0.003, Figure 3.4a). This suggests that on average, North Atlantic cyclones are able to travel longer distances, albeit at a lower speed, which might be due to changes to the jet stream and Arctic amplification (Cohen et al., 2014; Meleshko et al., 2016). Both of which could influence the speed and direction of cyclones. For instance, the steering of the large-scale flow drives storms in a particular direction while a strong jet stream may even amplify this mechanism (Priestley et al., 2017). Consequently, resulting in a more poleward shift of cyclones. Furthermore, increased nonlinear advection and latent heat release are hypothesized as two possible physical processes that would lead to storms moving more northward (Tamarin and Kaspi, 2017). As cyclones prefer to develop in areas where surface temperature gradients are large, changes in heat fluxes and growth circumstances might also be a factor for extended cyclone tracks. The reduction in cyclone propagation speed is most likely due to a slowdown of the atmosphere (Kossin, 2018; Lai et al., 2020; Zhang et al., 2020) or simply a combination of the former mentioned physical processes. More research is needed to address this question.

Concerning North Pacific cyclones, we find significant positive trends in the mean age of cyclones by ~0.5 hr (0.84%) per decade (4 hr overall in 1950–2021; p-value = 0.06, Figure 3.4b), which is only one time step longer than our temporal cyclone tracking resolution of 3 hr. Moreover, we find significant positive trends in the mean traveled distance by ~23 km (1.16%) per decade (p-value = 0.006, Figure 3.4b), in the mean u-component of the wind by ~0.05 m/s (5.24%) per decade (p-value = 0.1, Figure 3.4b) and in the mean v-component of the wind by ~0.06 m/s (7.65%) per decade (p-value = 0.04, Figure 3.4b). However, there are no trends in the EKE—we assume that this is due to the very minor absolute trends in the 10 m u-wind and v-wind components. Our results reveal that on average, North Pacific cyclones show a similar behavior in the traveled distance, which is here connected to longer life cycles. Unfortunately, long-term studies on life cycle lengths of cyclones analyzed in terms of atmospheric dynamics and processes focus solely on the intensity and deepening in tropical cyclones.

In conclusion, these results illustrate that we can find robust long-term trends in mean cyclone characteristics, which might stem from changes in atmospheric conditions. Compared to North Atlantic cyclones, cyclone-related impacts in the North Pacific show a similar pattern in their mean values: the sum of total precipitation appears to be decreasing while wind gusts remain stationary in this time series, however, these trends are not significant (not shown). This suggests that it may be important to look at how various and more extreme percentiles change over time, since they may be more helpful to evaluate the complete spectrum of different cyclone intensities.

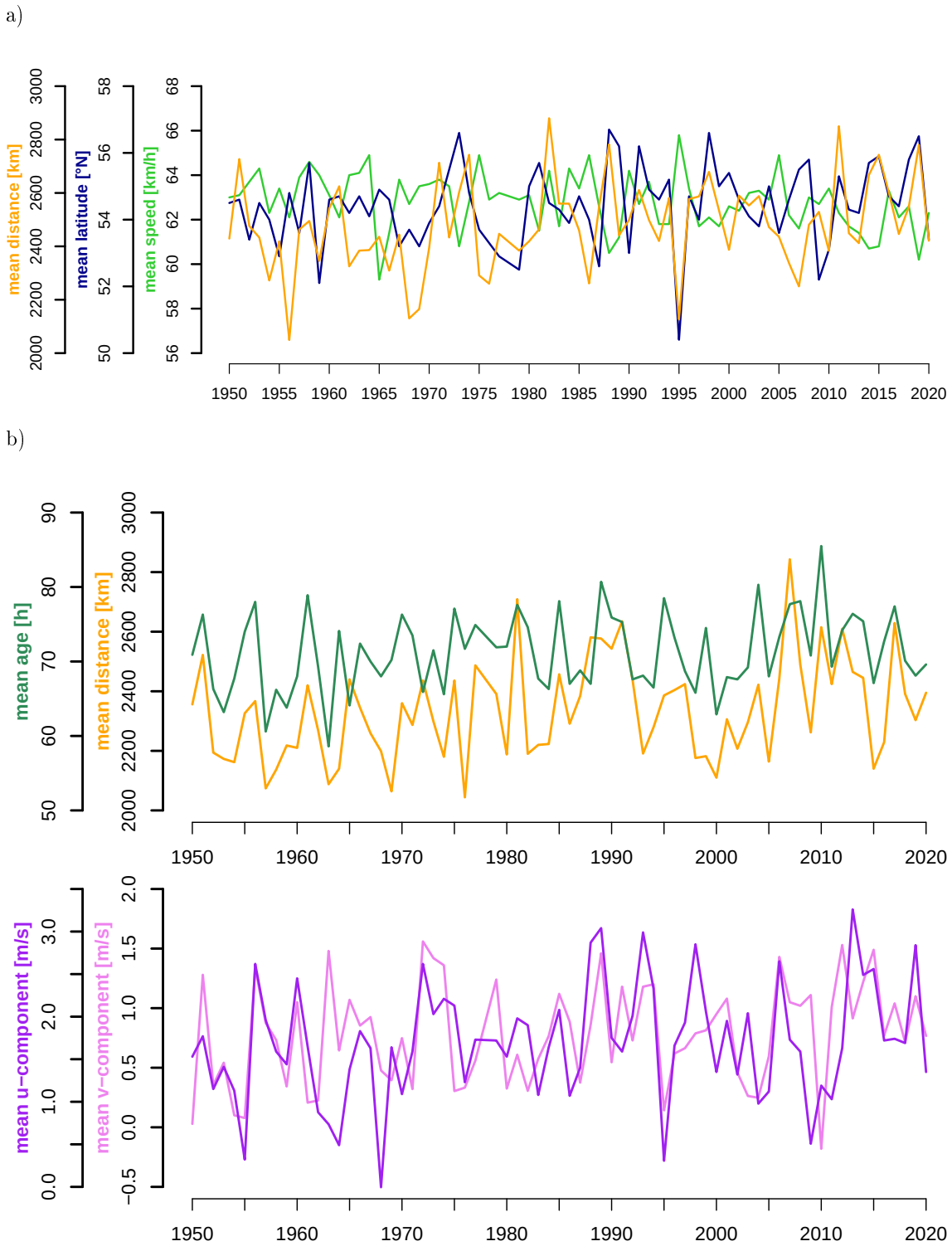

FIGURE 3.4: Mean values of significant cyclone characteristics in the (a) North Atlantic and (b) North Pacific in 1950–2021. The cyclone characteristics are age, latitude, speed, distance traveled, u-component and v-component of the wind.

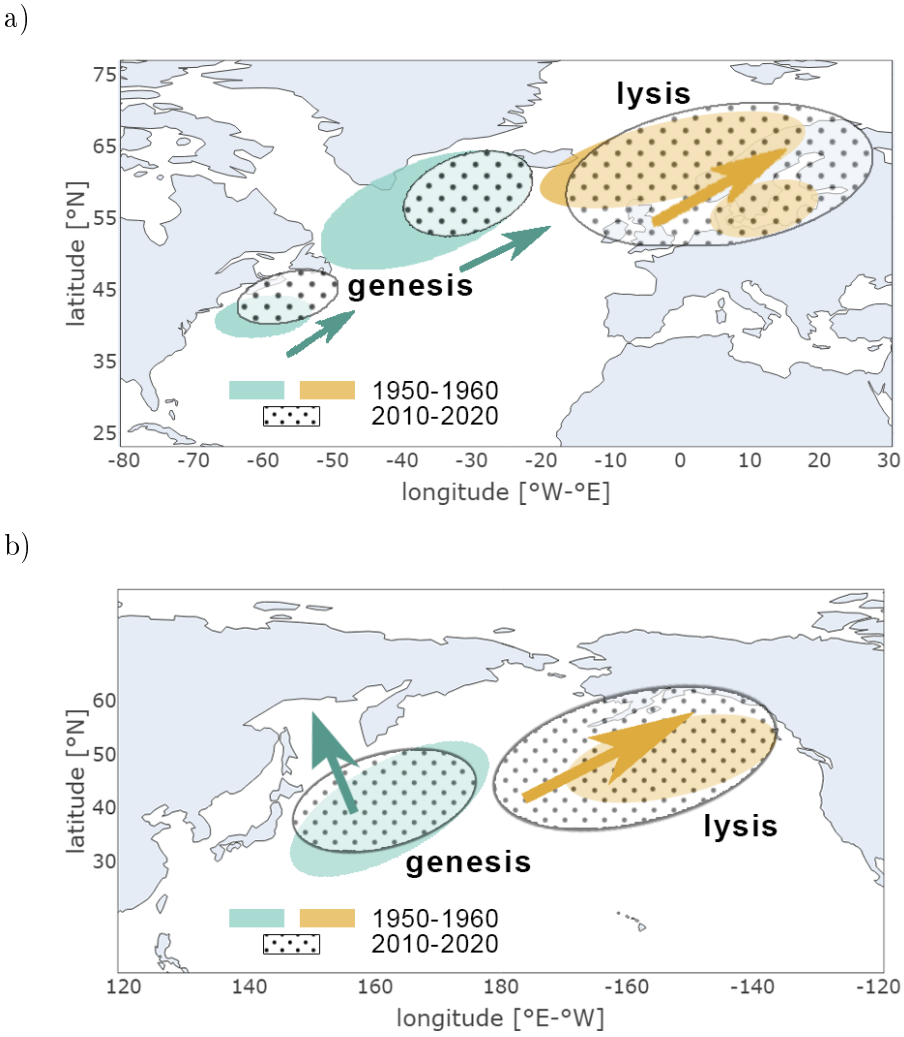

FIGURE 3.5: Schematic of the trends in extratropical cyclone genesis (green shades) and lysis (yellow shades) in 1950–1960 (colored shades) compared to 2010–2020 (dotted shades) for (a) the North Atlantic and (b) the North Pacific. Our trend analysis shows significant trends in both Northern Hemisphere storm tracks for more poleward storms, longer distance traveled, and a speed decrease from 1950 to 2021. As indicated by the arrows on the schematic, cyclone genesis areas are shifting northward (green arrows) and lysis regions are expanding over broader areas (yellow arrows) in the last decades. The most affected regions are located approximately between 51°N and 62°N. This concerns large regions across Europe such as the Northern parts of Ireland, Scotland, England, and Germany, as well as Southern Denmark, several islands in the Baltic Sea and the Polish Baltic coast cities. In the North Pacific, mainly the Bering Sea, the Gulf of Alaska, and Northwestern Canadian provinces are affected by the cyclone shifts. Trends also suggest that Northern Hemisphere storms are significantly intensifying and storminess is increasing from 1950 to 2021. Finally, we find significant positive trends for 1971–2021 in wind gusts for the North Atlantic and in precipitation extremes for the North Pacific. The trends in extratropical cyclone features and their impacts highlight the importance of adapting societies for future storm losses.

North Atlantic

Significant trends in different percentiles of cyclone characteristics of North Atlantic cyclones are shown in Figure 3.6. We find significant trends in our intensity measures: the mean gradient of the geopotential (from the edge to the center of the cyclone) is increasing by ~0.57%, 0.63%, and 0.54% per decade in the 80th, 90th, and 95th percentiles (Figure 3.6a). On the other hand, the deepening rate based on the mean gradient shows a decrease between 0.92% and 2.63% per decade in the 60th, 70th, and 80th percentiles (Figure 3.6b). Although these trends are comparatively small, they suggest that North Atlantic cyclones intensify significantly in the higher percentiles and intensify more slowly.

North Atlantic cyclones shift northward not only on average, but also in other percentiles of the latitude that include different cyclone intensities. We find that there are trends in the whole distribution, e.g., in the median and in upper extreme percentiles of latitude, as well as in the 60th percentile of the latitude: from ~58.7°N to 60.4°N (Figure 3.6c). This relates to a poleward shift of 0.41% per decade. We see this shift at the level of, e.g., Southern Greenland, the Shetland Islands, over Bergen in Norway, and over several Finnish islands. These regions are likely more prone to wind gusts and heavy rainfall (Figure 3.5). Interestingly, this cannot be seen in the impacts: long-term trends suggest that wind gusts may be increasing only since 1979 (Figure 3.8).

Another cyclone shift can be seen in the 40th percentile from ~51.4° to 53.1° (Figure 3.6c), which represents a distance of about 260 km and relates to a change of 0.47% per decade. Here the West Frisian Islands and Northern Germany are notably affected by this shift. We also find a significant westward shift in the fifth percentile from ~75.5°W to 76.3°W (Figure A.4 in Appendix A.1), which refers to a shift of 0.16% per decade. This implies that cyclones form closer to the east American coast, e.g., at the level of the US city Norfolk. Combined with the mean northward shift, these findings suggest a general displacement of cyclones. Studies on present and future changes in (extra)tropical cyclones argue this to be a direct impact of anthropogenic climate change on Northern Hemispheric cyclone tracks (Ciasto et al., 2016; Mbengue and Schneider, 2016; Wang et al., 2017; Woollings et al., 2012). The accelerating warming and sea ice loss brought on by Arctic amplification may increase the latitudinal movement of storms. According to observations and model projections, storms may move poleward as a result of the increase in anthropogenic greenhouse gas emissions (Studholme et al., 2022).

Indeed, the release of latent heat and the increase of nonlinear advection are argued to be two important physical processes leading to the cyclone poleward shift as shown by Tamarin and Kaspi (2017). However, it is still unclear how changes in, e.g., latent heat fluxes and sea surface temperatures contribute quantitatively to the migration of storms.

Moreover, we find that not only does the mean distance increase, but also the higher percentiles: cyclones travel ~32 km/1.23% (70th percentile), 44 km/1.49% (80th percentile), and 69 km/1.26% (95th percentile) more per decade (Figure 3.6d). This means that long living cyclones tend to live even longer now. Cyclone speed is decreasing not only in the mean, but also in the median: ~0.3 km/hr (0.85%) per decade (Figure 3.6e). Thus, there are significant long-term trends concerning the traveled distance and the slower speed of cyclones. A likely mechanism could

be Arctic amplification, which might induce changes in the speed and travel direction of cyclones. As a result of a warming atmosphere, a potential change in the intensity and position of the Icelandic Low and the Azores High could be key to answering this question, since a reduced baroclinic instability might then determine how storms develop in the future. Changes could also likely originate from alterations in the cyclonic growth rates and development processes (e.g., Besson et al. (2021) and Pinto et al. (2009)). Further research is needed to evaluate the dynamics and mechanisms behind this.

Having shown that the distribution of impacts does not change in a wider impact region, we find that precipitation is decreasing significantly by ~1.3 mm (1.34%) per decade in the 95th percentile in 1950–2021, but the years with extremes are increasing (Figure 3.6f). For example, during the winter seasons 1990/1991 and 2013/2014 the storms that affected Northwestern and Central Europe brought heavy rainfall and strong wind gusts to the European mainland (Priestley et al., 2017). This indeed led to flooding over large parts of England such as at the Somerset Levels.

Overall, the North Atlantic storm track experiences changes not only in the mean and median, but also in different, upper and more extreme percentiles: cyclones are intensifying, moving more poleward, and showing increased track lengths. We also find that impacts appear to be increasing more in recent decades. This emphasizes the need for more studies between midlatitude storms and their impacts in longer time series; especially in high-resolution climate models to estimate future socio-economic impacts.

North Pacific

The significant trends in North Pacific cyclones are presented in Figure 3.7. The central geopotential is decreasing by 1.27% per decade in the 5th and 10th percentiles (Figure 3.7a). This suggests that these storms are significantly intensifying, similar to the North Atlantic cyclones. Furthermore, North Pacific cyclones are showing longer life cycles not only on average: we find significant positive trends of ~1.41% longer life cycles per decade in the median (Figure 3.7b). The trend toward longer life cycles can also be observed in the extreme 95th percentile for the most intense North Atlantic cyclones, however, the trend was not significant there (not shown).

The cyclone deepening rate based on the central geopotential increases significantly by ~0.85% and 1.09% per decade in the 10th and 20th percentiles (Figure 3.7c). This is consistent with the deepening rate based on the mean gradient, which decreases by ~1.2% per decade in the 90th and 95th percentiles (Figure 3.7d). Thus, these findings reveal a slower growth rate in 1950–2021. This trend can also be seen in North Atlantic cyclones, which suggests that both Northern Hemispheric storm track areas likely undergo similar processes due to alterations in the atmospheric circulation as part of natural variability and anthropogenic global warming.

There are significant positive trends in the traveled distances in all percentiles. Here, cyclones travel between 1.7 and 86 km (0.87%–2.03%) more per decade (Figure 3.7e). Not only do cyclones in the median have longer tracks, but also those in upper percentiles such as in the 80th, 90th, and 95th percentiles. The significant trends in cyclone track lengths affect both storms of medium strength and those with higher intensity, as indicated by the extreme percentiles. Nonetheless, the largest trend

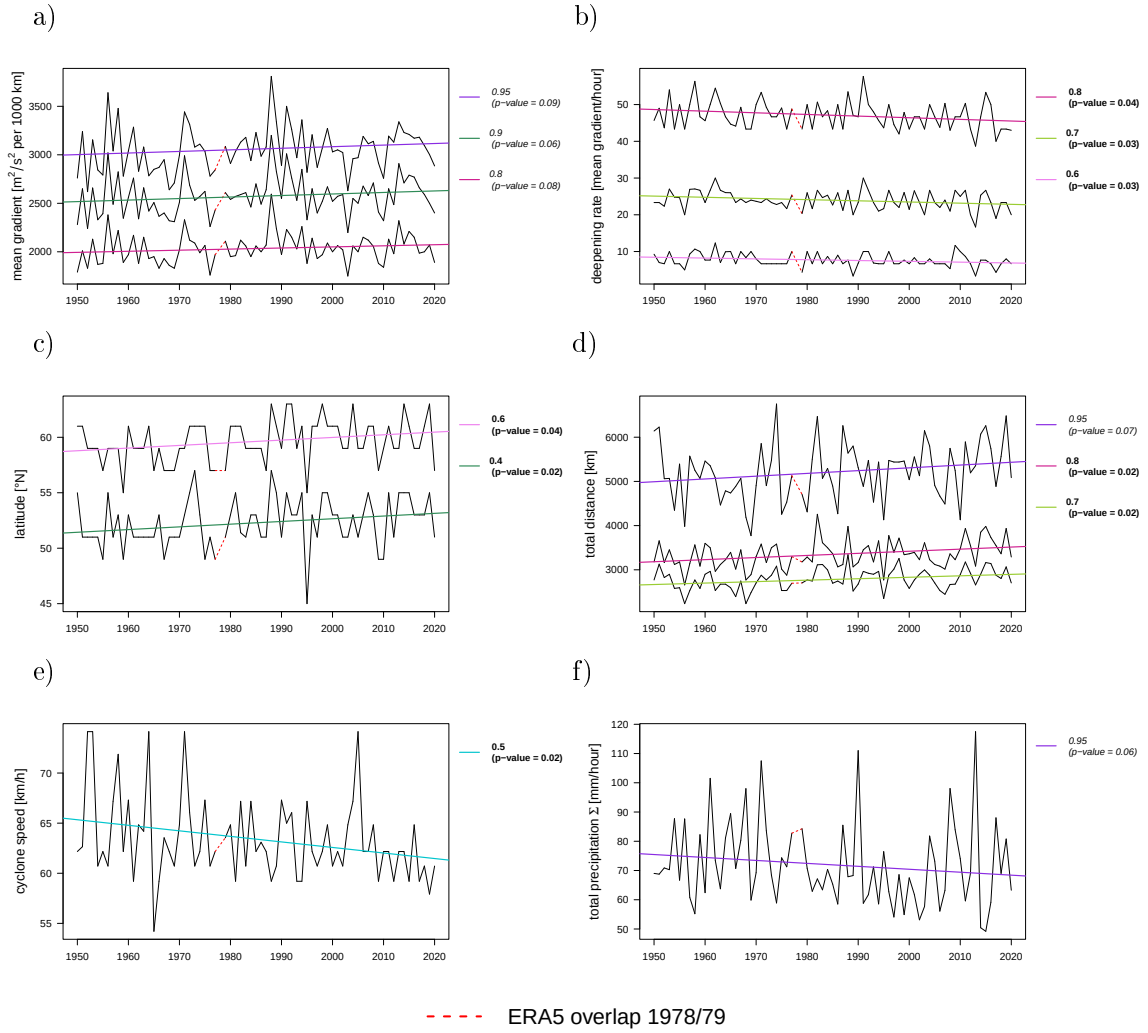

FIGURE 3.6: Trends in North Atlantic cyclones in 1950–2021. The variables are (a) mean gradient of the geopotential, (b) deepening rate based on mean gradient, (c) latitude, (d) distance traveled, (e) speed, and (f) sum of total precipitation. p-values ≤ 0.05 are marked in bold and p-values ≤ 0.1 are in italic.

of 2.03% per decade is seen in the most intense cyclones (95th percentile, Figure 3.7e). This seems to be in accordance with the decrease in the cyclonic deepening and the longer life cycles; hence, these results appear to be robust. We can also see this pattern of change in North Atlantic cyclones, which suggest that cyclones in the Northern Hemisphere exhibit comparable trends in the long period.

Our trend analysis additionally suggests a northward shift of the strongest North Pacific cyclones in the 95th percentile from ~61.04°N to 61.82°N (Figure A.5a in Appendix A.1; 0.18% per decade), which is the level of Anchorage, Alaska's biggest city. Indeed, the Gulf of Alaska and the Bering Sea are the main affected areas (Figure 3.5). Similar shifts were found in the North Atlantic-European region; this implies possible changes for lysis regions (Figure 3.5). North Pacific storms are decreasing in speed by ~0.13 km/hr (0.14%) per decade in the 95th percentile (Figure A.5b in Appendix A.1). Long-term trends toward slower cyclone speeds were also

observed in the North Atlantic.

Moreover, the v-component of the wind is increasing by ~0.05 m/s per decade in the median, which relates to an increase of 10.06% per decade (Figure 3.7f). Comparable trends were found in the mean wind components, but not in the EKE. Most likely this is a result of the very minor trends we have seen previously.

In conclusion, our results indicate that North Pacific cyclones are not only traveling longer distances, they also have longer life cycles and a slower speed. Correspondingly, this seems to be in accordance with North Atlantic cyclones, which suggests that in the long term, both storm track areas experience significantly better growth conditions for cyclone development. In cyclone-related impacts, however, this response is not seen, neither in the original cyclone-box nor in any extension of it.

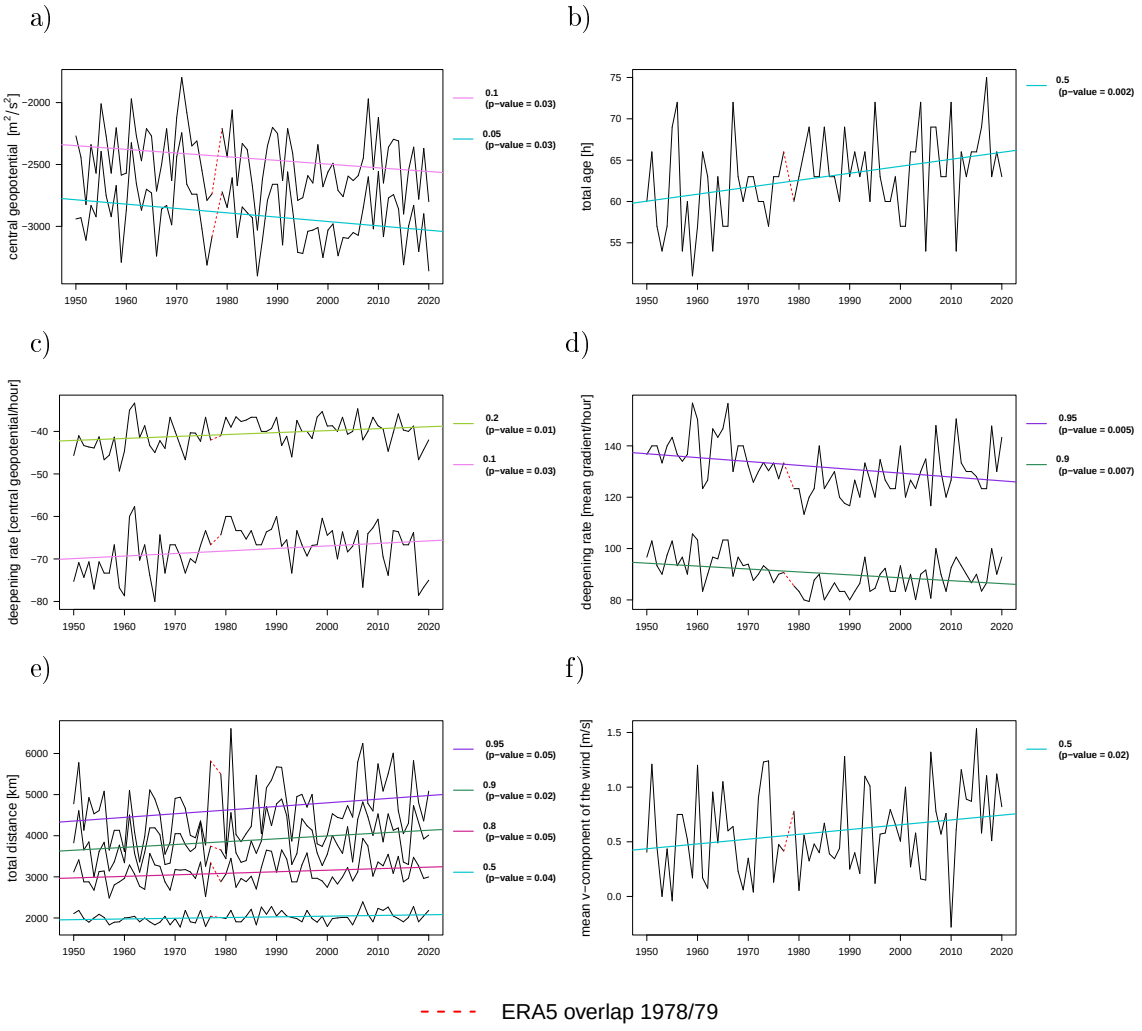

FIGURE 3.7: Trends in North Pacific cyclones in 1950–2021. The variables are (a) central geopotential, (b) cyclone age, (c) deepening rate based on central geopotential, (d) deepening rate based on mean gradient, (e) distance traveled, and (f) mean v-component of the wind.

3.6.4 Significant trends in cyclone characteristics and impacts in 1979-2021

As more recent changes in the dynamics of the atmospheric circulation could be attributable to increased anthropogenic warming since the 1980s, it is important to check whether this is the case for extratropical cyclones and their impacts, specifically in 1979–2021. For both Northern Hemispheric storm track areas, the majority of the trends observed in 1979–2021 are consistent with the trends in 1950–2021. In the following sections, we will now focus on the trends in 1979–2021 that differ from the long-term trends in 1950–2021.

North Atlantic

We find a significant increase in the maximum wind gust by ~0.2 m/s (0.71%) per decade in the 95th percentile for the most intense cyclones (Figure 3.8). Although this trend is small, there is a tendency visible that the maximum wind gust increases also in the other percentiles (not shown). This is a more recent trend, since it could not be detected in the full period 1950–2021. It could be attributable to enhanced warming and increases in atmospheric moisture since the 1980s (Climate Signals, 2021; Santer et al., 2007; Stocker et al., 2013).

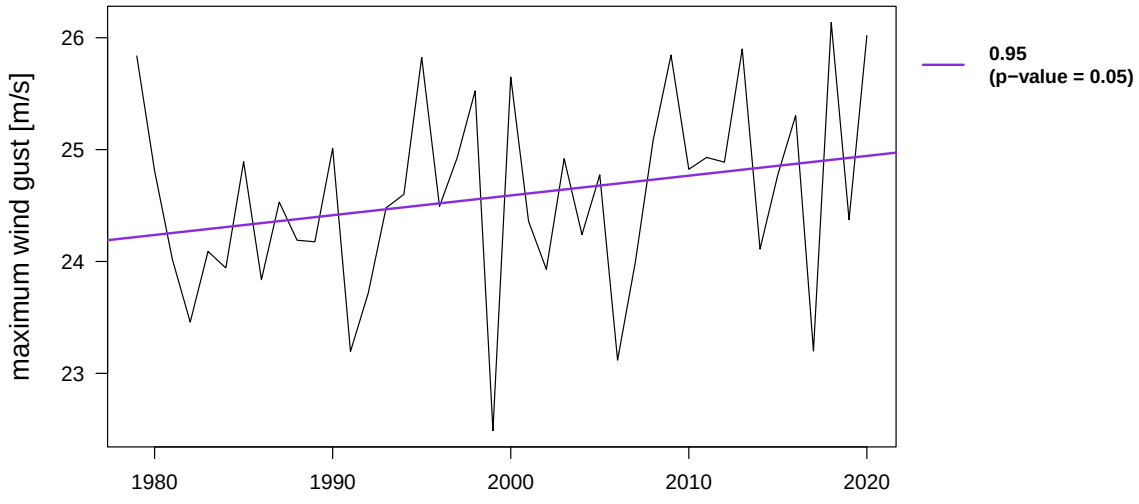

FIGURE 3.8: Significant trend in the 95th percentile of maximum wind gust in North Atlantic cyclones in 1979–2021.

North Pacific

Trends in cyclone radii suggest increases approximately between 2 and 9 km (0.45%–1.59%) per decade in the median and higher percentiles (Figure 3.9a). These results indicate that North Pacific storms have intensified since 1979, which can also be seen by the central geopotential in the full period 1950–2021 (Figure 3.9a), but not in the cyclone radii or mean gradient therein. This supports the trend toward more recent intense storms since 1979. Moreover, the cyclone deepening rate based on the central geopotential decreases significantly approximately between 2% and 2.77% per decade in the 5th and 10th percentiles (Figure 3.9b). Similarly, the deepening rate based on the mean gradient increases by ~2.73% and 2.47% per decade in the 90th and 95th percentiles (Figure 3.9c). This suggests that North Pacific cyclones in more extreme percentiles are deepening more since 1979. Interestingly, the trends in 1950–2021 suggest a slower growth rate. Therefore, this trend here is related to more recent anthropogenic warming.

We also identify significant positive trends in the total precipitation: the sum increases by ~2.4 mm (5.26%) per decade in the 90th percentile (Figure 3.9d). These findings illustrate that the increases in cyclone-related precipitation are due to atmospheric processes that favor the accumulation and occurrence of precipitation. In the full period 1950–2021, this trend was insignificant, which suggests that the increase in total precipitation of the most intense cyclones is a more recent trend, similar to North Atlantic cyclones. It is related to anthropogenic global warming and the increasing amount of atmospheric moisture since the 1980s (Climate Signals, 2021; Santer et al., 2007; Stocker et al., 2013).

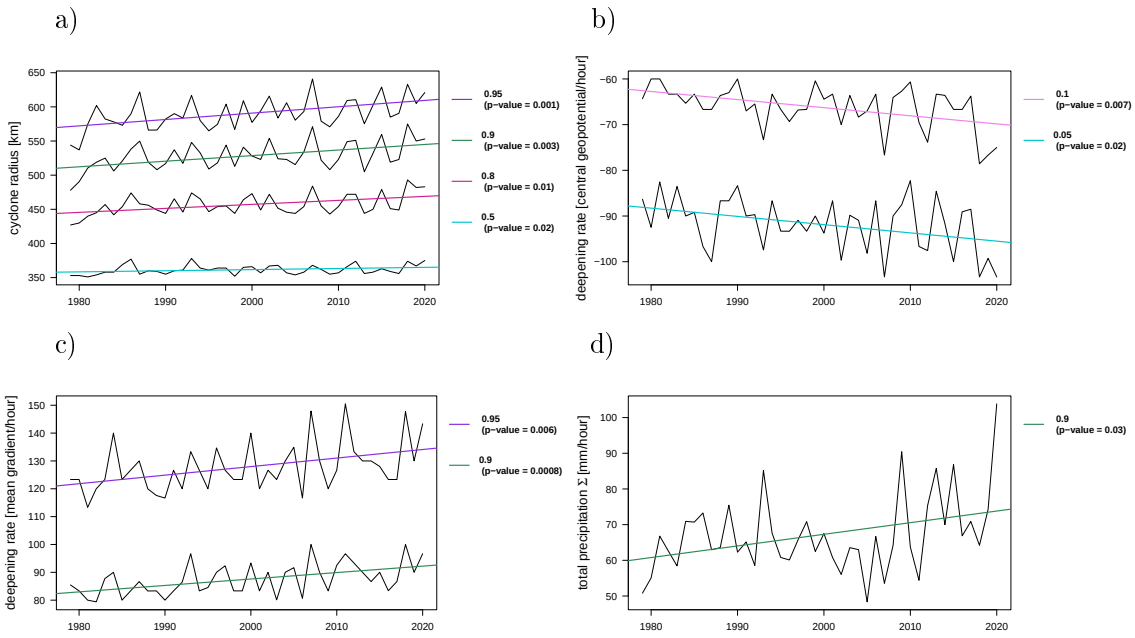

FIGURE 3.9: Significant trends in North Pacific cyclones in 1979–2021: (a) cyclone radius, (b) cyclone deepening based on the central geopotential, (c) cyclone deepening based on the mean gradient of the geopotential, and (d) sum of total precipitation related to North Pacific cyclones.

3.7 Conclusions

In this study, long-term trends of extratropical cyclones and their impacts were analyzed in the recently extended ERA5 reanalysis, which spans about 71 years of data (Figure 3.5).

The first aim of our research was to explore whether there are quantitative changes between the two ERA5 data sets using a systematic change-point analysis and temporal histograms of all storm-related variables in the full period 1950–2021. Our results showed continuous behavior between ERA5-BE and ERA5 in any cyclone-related parameters and, thus, that the extended reanalysis can be used in long-term studies of midlatitude cyclones and their impacts. Using a different tracking metric other than the geopotential, such as relative vorticity at 850 hPa, may be less appropriate due to a change-point in 1978/1979.

As a second study objective, we performed a Lagrangian-based analysis that allowed us to comprehensively assess cyclone characteristics, e.g., frequency, size, and intensity in the extended ERA5 reanalysis. Finally, directly linked and combined with our previous aim, our third study objective was to identify significant trends in the Northern Hemisphere storm tracks in order to provide us with new data on the atmospheric circulation response to global warming.

Overall, our results suggest that extratropical cyclones have intensified in both Northern Hemispheric storm track areas in 1950–2021. These trends are in line with the latest international climate assessment, which shows that the intensity of storms increases as global temperatures rise (Masson-Delmotte et al., 2021).

Long-term trends derived from the extended ERA5 reanalysis indicate a significant northward (poleward) shift of the North Atlantic cyclone track in 1950-present, which agrees with other studies (e.g., Bengtsson et al. (2006) and Harvey et al. (2014)). Interestingly, these shifts are observed in the mean and in the 40th/60th percentiles, but not in the extreme upper or lower percentiles. This trend has an impact on a number of locations, e.g., Northern England, Scotland, islands in Northern Germany and Southern Denmark as well as on Polish Baltic coast cities. A key finding is that we were able to identify more recent significant increases in wind gusts (North Atlantic) and cyclone-related precipitation (North Pacific) in 1979–2021. These results have important implications for both storm track and lysis regions; as more socio-economic damages can be expected in the future (Franzke, 2021; Ranson et al., 2014). We believe further research is needed to quantify whether these trends are due to natural variability or anthropogenic forcing.

Nevertheless, our trend analysis also revealed that the number of North Pacific cyclones is significantly increasing; these storms show longer life cycles and travel longer distances, while they grow more slowly in 1950–2021. The longer cyclonic life cycles might be due to changes in atmospheric conditions over the North Pacific (ocean), while the slow growth rate might be more related to a weakening of the atmospheric circulation. Moreover, atmospheric processes like latent heating could in turn still favor the cyclonic development. While one would initially expect higher growth rates in more favorable conditions for cyclone development, the influence of a slower atmospheric circulation in a warmer climate may play an important role in early growth stages. Slower growth rates might also be caused by changes in baroclinicity, which is the major determinant of the growth rate. However, there are

no trends in the EKE that could give clues on how cyclones grow through baroclinic instability and subsequently decay over land. We assume that this is due to the very minor trends in the 10 m u-wind and v-wind components, implying that any trend in EKE would equally be small. Large ensemble simulations might be helpful for this question, since they might enable a higher signal-to-noise ratio to find small trends. This is research we plan to pursue in the future.

Furthermore, we find similarities in both storm track regions, e.g., a decrease in cyclone speed. Unsurprisingly, as the atmospheric circulation weakens under anthropogenic warming, a slowdown is expected: This is a significant trend that has also been observed in tropical cyclones, hurricanes and typhoons (Kossin, 2018; Lai et al., 2020; Zhang et al., 2020).

In light of the importance we have placed on impacts, our results emphasize the critical link between increasing Northern Hemisphere storminess and more recent increases in heavy precipitation and wind gusts from winter storms.

Thus, these findings call for stronger efforts on part of policymakers to adapt societies to the impacts of intense cyclones making landfall; particularly in the most vulnerable and densely populated regions.

3.8 Data Availability Statement

The data that support the findings of this study are openly available in the Climate Data Store of the ECMWF at https://cds.climate.copernicus.eu/cdsapp%23%21/search%3Ftype%3Ddataset.

3.9 Acknowledgments

AK and RB were supported by the Federal Ministry of Education and Research (BMBF) project ClimXtreme. CF was supported by the Institute for Basic Science (IBS), Republic of Korea, under IBS-R028-D1, and Pusan National University Research Grant 2021.

Chapter 4

Northern Hemisphere Extra-Tropical Cyclone Clustering in ERA5 Reanalysis and the CESM2 Large Ensemble[1]

The research questions that are addressed here are as follows:

RQ4: How is clustered cyclone activity in the Northern Hemisphere mid-latitudes characterized in the ERA5 reanalysis and CESM2-LE in 1980-2020?

RQ5: How is extra-tropical cyclone clustering projected to change by 2060-2100 compared to 1980-2020 based on two metrics?

RQ6: What are possible reasons in terms of large-scale dynamics and cyclone characteristics for these projected changes?

4.1 Abstract

Extra-tropical cyclones are a dominant feature of the mid-latitudes, and often occur as storm sequences. Such a phenomenon is known as cyclone clustering, and is common over regions like the eastern North Atlantic and western Europe. Intense clustered cyclones may lead to large cumulative socio-economic impacts. There are several different approaches to quantify cyclone clustering, but a wide evaluation on how clustering may change in a warmer climate is missing. Here, we perform a cyclone clustering analysis for the Northern Hemisphere mid-latitudes using the ERA5 reanalysis to characterize clustering during 1980-2020. Moreover, we use Large Ensemble simulations of the Community Earth System Model version 2 following the SSP3-7.0 scenario to compare clustering during 2060-2100 to 1980-2020. Our model simulations show significant enhancement in cyclone clustering over Europe for 3 and 4 cyclones within 7 days in the future decades, which is increasing by up to 25% on average during 2060-2100 compared to 1980-2020. In contrast, cyclone clustering decreases along the west coast of the US and Canada by up to 24.3% and by 10.1% in the Gulf of Alaska for the same periods. Clustered cyclones

[1] currently under review in *J. Clim.*, 2023, with A. Karwat as first-author.

are generally intensifying in a warmer climate due to lower minimum pressure and larger radii and depths compared to non-clustered events. Our findings suggest that cyclone clustering may change under global warming, with implications for the cumulative windstorm risk.

4.2 Significance Statement

Storm sequences like the one of December 1999 (Anatol, Lothar, and Martin) have led to large socio-economic impacts in Europe. It is still unclear how such events will change under global warming. We analyze storm sequences in a reanalysis and a large climate model ensemble for recent (1980-2020) and future climate conditions (2060-2100). Our results show a significant enhancement of storm sequences over Europe for 3 and 4 storms within 7 days, while a decrease is found along the west coast of the US, western Canada and in the Gulf of Alaska in future decades. Our findings suggest that the characteristics of cyclone clustering may change in a warmer world, and thus also the associated impacts.

4.3 Key Points

- Uncertainties in the quantification of future cyclone clustering can be reduced by using large ensembles of global climate simulations.
- We find significant increases in cyclone clustering over Europe for 3 and 4 cyclones within 7 days by up to 25% on average during 2060-2100 compared to 1980-2020.
- Cyclone clustering along the west coast of the US and Canada decreases on average significantly by up to 24.3%, and by 10.1% in the Gulf of Alaska during 2060-2100 compared to 1980-2020.

4.4 Introduction

Sequences of intense extra-tropical cyclones have led to large socio-economic damage in Europe in the last few decades. For example, the storm series of December 1999 - including Anatol, Lothar and Martin (Ulbrich et al., 2001) caused approximately €18.5 billion in economic damage over continental Europe (Munich Re, 2002; Alert Air Worldwide, 2009). The stormy winter of 2013/14 was the stormiest on record for the British Isles (Matthews et al., 2014) and was characterized by cluster periods, in particular in late December 2013 and mid-February 2014 (Priestley et al., 2017). Many of these storms brought a lot of precipitation to Europe and resulted in some notable flood events, for instance, in southern England (Kendon and McCarthy, 2015; Schaller et al., 2016). A recent example occurred on 16-20 February 2022, when three major storms (Ylenia, Zeynep and Antonia) hit the European continent and caused much destruction over large areas of northwestern and central Europe (Mühr et al., 2022). More than 20 storm-related deaths have been reported across Europe, and the insured wind losses from the first two winter storms range

between €3 billion and €5 billion, primarily in Germany, the UK, and the Netherlands (Alert Air Worldwide, 2022a).

The concepts of cyclone series (also known as cyclone sequences, cyclone families, temporal clustering or temporally compounding cyclones) is not new (Schultz et al., 2019). For example, Bjerknes (1922) had already recognized the importance of cyclone families about a century ago, and described their synoptic characteristics. In the present study, we focus on temporal clustering of extra-tropical cyclones, i.e. sequences of cyclones affecting a certain area in a specific time window. Following Dacre and Pinto (2020), there are several methods how to quantify clustering. The first corresponds to absolute metrics based on synoptic knowledge, e.g., defining a threshold of 4 or more cyclones over a certain location within a week as cyclone clustering (Pinto et al., 2014). The second option is to consider relative metrics, where clustering is defined as a positive deviation from a stochastic process, where more cyclones occur than expected by chance (Mailier et al., 2006; Blender et al., 2015). The last possibility is to assume impact metrics and determine the relationship between the more intense loss per year (occurrence exceedance probability, OEP) and the cumulative loss per year (annual exceedance probability, AEP) (Priestley et al., 2018).

For the North Atlantic basin, there is a large consensus that clustered cyclone activity is found primarily on the flanks and exit region of the North Atlantic storm track (overdispersion), including the UK, the Benelux countries, France, Germany, and occasionally Scandinavia, while regions like the entrance of the North Atlantic storm track are characterized by a regular process (underdispersion) (Dacre and Pinto, 2020). There is evidence that clustering increases for more intense cyclones (Vitolo et al., 2009; Pinto et al., 2013; Economou et al., 2015). While fast-moving storms may produce strong wind gusts in a short period of time, slow-moving storms can be just as damaging, since these storms can accumulate huge amounts of precipitation during their development, and hence, result in severe floods (e.g., winter 2013/14 in the UK (Priestley et al., 2017)). Accordingly, the clustering of extra-tropical cyclones may be stronger for more extreme storms, and countries further from the storm track are likely to be more affected than others (Cusack, 2016). Other regions such as the Northeast Pacific, including the west coast states of the US and the western Canadian provinces are also regions affected by clustering due to the Northeastern Pacific storm track (Santos Mesquita et al., 2010). As strong cyclones often pass across the Aleutian Island chain, the Gulf of Alaska is another important storm-prone region, which might provide information on the future changes in cyclone clustering (Santos Mesquita et al., 2010). Still, there is a large knowledge gap in studies assessing cyclone clustering outside of the North Atlantic basin. In fact, only two studies have investigated cyclone clustering in the North Pacific in climatological terms (Mailier et al., 2006; Blender et al., 2015). While both studies agree that the preferred regions for cyclone clustering are the Gulf of Alaska and the west coast of Canada and the US, large uncertainties remain.

Concerning historical periods, e.g. the last 40 years, clustered extra-tropical cyclone activity was examined only a few times and exclusively in the ERA-Interim reanalysis or older reanalyses (Mailier et al., 2006; Pinto et al., 2013; Economou et al., 2015; Priestley et al., 2018). The ERA5 reanalysis (Hersbach et al., 2020) have recently been made available, and features both higher spatial and time resolution,

and an improved data assimilation methodology. Thus, ERA5 is one of the best reanalysis products suitable for reliable cyclone tracking and storm analyses, for example, as in Karwat et al. (2022).

Another important question is how extra-tropical cyclone clustering will change in a future climate under different greenhouse gas emissions scenarios. In the Coupled Model Intercomparison Project Phase 5 (CMIP5), future changes were found to be minor and inconsistent between models, whereas for more extreme storms clustering increases over northern Europe and Scandinavia in the RCP4.5 scenario (Economou et al., 2015). This is in line with Pinto et al. (2013), which focussed on a single GCM large ensemble with 20 members. Other studies find shorter return times for severe winter storms and related losses for western Europe in the future (Della-Marta and Pinto, 2009; Pinto et al., 2012; Karremann et al., 2014a). Here, the number of (clustered) cyclones is expected to increase, while overall the total number of non-clustered cyclones is projected to decrease in the future (e.g. Bengtsson et al., 2006; Pinto et al., 2009; Ulbrich et al., 2009; Zappa et al., 2013b; Priestley and Catto, 2022). However, many of these studies that address clustering focus on Europe.

There is also a substantial lack of available large ensembles of future climate simulations with CMIP6 models with sufficient temporal and spatial high-resolution to perform cyclone tracking from 2050 onwards, and a general lack of studies assessing all ocean basins except the North Atlantic (Dacre and Pinto, 2020). The 50-member CESM2 Large Ensemble (CESM2-LE) (Rodgers et al., 2021) provides thus an excellent opportunity to investigate how cyclone clustering may change from pre-industrial times (e.g., 1850-1890) until the end of the 21st century in many different realizations. Moreover, two clustering metrics will provide us with more insights into clustering from 1850 to 2100 focussing on both the North Pacific and the North Atlantic basins. Therefore, the specific aims of this paper can be summarized by the following three questions:

1. How is clustered cyclone activity in the Northern Hemisphere mid-latitudes characterized in the ERA5 reanalysis and CESM2-LE in 1980-2020?

2. How is extra-tropical cyclone clustering projected to change by 2060-2100 compared to 1980-2020 based on two metrics?

3. Can we identify reasons in terms of large-scale dynamics and cyclone characteristics for these projected changes?

The remainder of this paper is organized as follows: in Section 4.5, we introduce the ERA5 and the CESM2-LE data and the methodology; in Section 4.6, we analyze the cyclone statistics and mean sea level pressure (mslp) fields for recent and future climate conditions. Section 4.7 examines clustering based on the dispersion metric, and Section 4.8 is dedicated to clustering based on absolute measures. Possible links to large-scale patterns and cyclone characteristics are explored in Section 4.9. Finally, we discuss the conclusions of this study in Section 4.10.

4.5 Data and Methods

4.5.1 ERA5 Reanalysis Data

We use the European Centre for Medium-Range Weather Forecasts - ERA5 reanalysis data from 1980 to 2020 (Hersbach et al., 2020). ERA5 has a horizontal resolution of 0.25°. For the Lagrangian cyclone tracking we interpolate the mslp fields on a 2° x 2° grid and use six-hourly data for the winter months December through February (DJF). We analyze clustered cyclones in the North Atlantic and North Pacific sectors. Cyclones are tracked over the North Atlantic and Europe (80°W to 30°E and 25°N to 75°N) and in the North Pacific (120°E to 120°W and 25°N to 65°N). We consider the areas of Europe (10°W to 15°E and 50°N to 60°N), the west coast of the US states and western Canadian provinces (120°W to 135°W and 30°N to 60°N) and the Gulf of Alaska (135°W to 165°W and 50°N to 60°N) (Fig. 4.1).

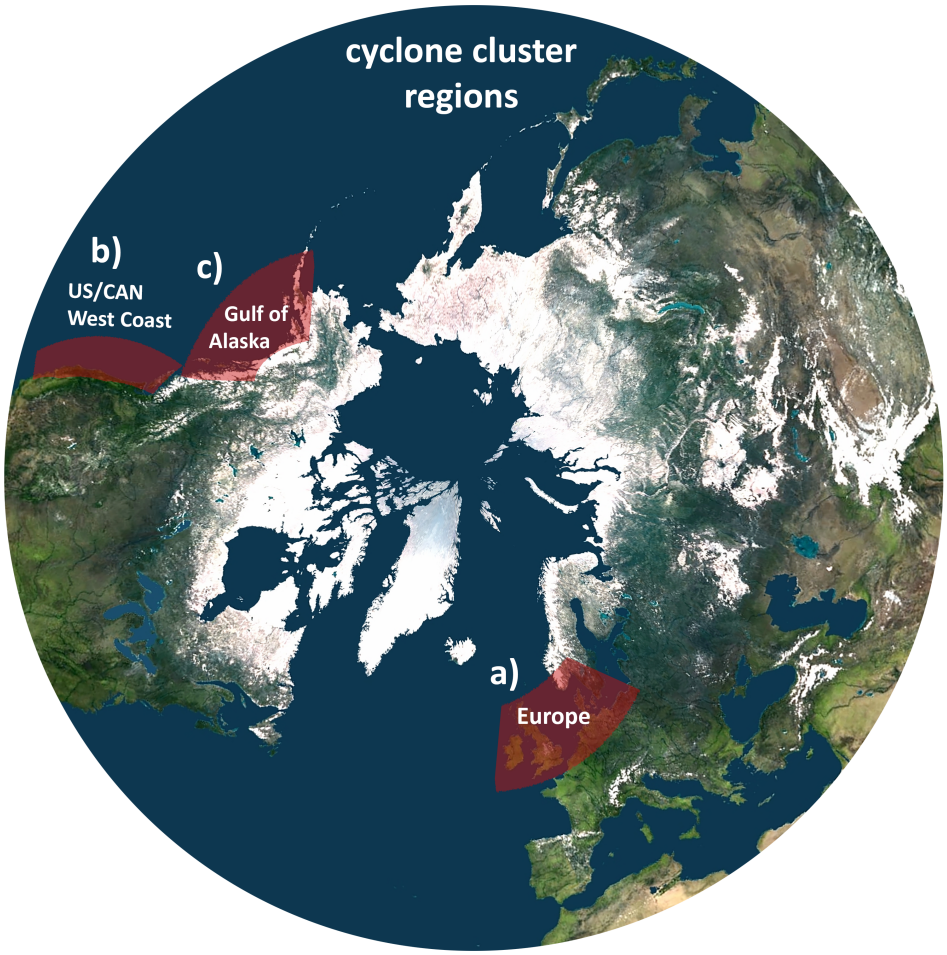

FIGURE 4.1: Map of the cyclone cluster regions in this study: a) Europe (10°W to 15°E and 50°N to 60°N), b) the west coast of the US states and western Canadian provinces (120°W to 135°W and 30°N to 60°N), and c) the Gulf of Alaska (135°W to 165°W and 50°N to 60°N).
Map credit: own creation.

4.5.2 CESM2 Large Ensemble

We use model simulations with the Community Earth System Model - version 2 (CESM2) (Danabasoglu et al., 2020). The large ensemble (CESM2-LE) is documented in Rodgers et al. (2021). The CESM2-LE has a horizontal resolution of 1° and is forced by the CMIP6 historical forcing from 1850 to 2014 and the Shared Socioeconomic Pathways forcing scenario (SSP3-7.0) from 2015 to 2100. The SSP3-7.0 scenario relates to an additional radiative forcing of 7 W/m^2 by 2100 (Masson-Delmotte et al., 2021). On this SSP, temperatures rise steadily and CO2 emissions roughly double from current levels by 2100. By the end of the century, global average temperatures have risen by approximately 3.6°C compared to pre-industrial temperatures of 1850-1900 (Masson-Delmotte et al., 2021). This scenario is in the upper-middle part of all the scenarios in CMIP6. It was introduced to close the gap between the RCP6.0 and RCP8.5 scenarios in CMIP5. We use the 50 of 100 CESM2-LE ensemble members which have six-hourly mslp output fields chosen from a set of different combinations of atmosphere and ocean initial states (Rodgers et al., 2021). Overall, we focus on three different time slices: pre-industrial times (1850-1890), recent past (1980-2020), and future (2060-2100).

4.5.3 Cyclone Tracking Methodology

Several algorithms for identifying cyclone tracks have been developed, for example, by Murray and Simmonds (1991), Sinclair (1994), Hodges (1995), and Wernli and Schwierz (2006). Here, we use the Lagrangian cyclone tracking algorithm of Blender et al. (1997). In the tracking algorithm cyclones are defined as local minima of the mslp field. The cyclone tracks are computed by a nearest-neighbour search in the mslp field where the trajectories of individual cyclones are connected at subsequent time steps. In our study, we only consider cyclones with a minimum life time of 48 hours and which have traveled at least a distance of 1000 km. The cyclone statistics from this tracking method compare well with others (Neu et al., 2013), also in terms of metrics related with cyclone clustering (Pinto et al., 2016). We use the same conditions for the cyclone tracking for ERA5 and CESM2-LE.

4.5.4 Cyclone Statistics and Clustering Metrics

We compare ERA5 and CESM2-LE to investigate if the overall number of cyclones per winter is comparable for recent climate conditions and if there are any significant changes between the different CESM2-LE time slices (1850-1890, 1980-2020, and 2060-2100). In particular, we analyze the storm characteristics for ERA5 and CESM2-LE in 1980-2020. Therefore, we look at the ensemble spread (defined as twice the standard deviation of all ensemble members) of the cyclone counts, life time, mslp, radius, depth, and distance. Since our tracking depends on the mslp fields, any trends in mslp are likely to affect our cluster analysis. Thus, we examine the differences in the mslp fields of the North Atlantic and North Pacific storm tracks in 2060-2100 compared to 1980-2020 and 1850-1890, respectively. To quantify our results we use a Welch Two-Sample t-test (Wilks, 2011). We compare the local cyclone mean counts from the large ensemble between the future winter climate

and the current climate. Here we apply a bootstrapping with resampling (n = 1000) (Wilks, 2011).

To assess cyclone clustering, we use two methods: a dispersion statistic ψ (following e.g., Mailier et al. (2006)) and the number of cyclone occurrences per week, e.g., 3-6 cyclones in 7 days (following e.g., Pinto et al. (2014)). In the dispersion statistic (see details in *Appendix* B), a value of $\psi = 0$ corresponds to a homogeneous Poisson process, which means that the occurrences are uncorrelated random rare events. For values of $\psi < 0$, occurrences are less clustered than random and thus underdispersive cyclones occur regularly; for values of $\psi > 0$ the occurrences are more clustered than random and hence overdispersive (Mailier et al., 2006). We also investigate the decadal dispersion at specific grid points in genesis and cluster regions under present climate conditions, and then use CESM2-LE to compare the future climate in 2060-2100 to 1980-2020. For the second metric we use 5° x 5° grid boxes (similar to Mailier et al. (2006)) in which we count the number of cyclone occurrences and differentiate whether there are 3, 4, 5 or 6 cyclones at the respective grid location during 7 days. These high numbers are necessary because of the already high number in weekly cyclone occurrences (see details in *Appendix* B). We define 'ensemble agreement' as the cumulative percentage of ensemble members that predict a trend (positive, negative, or none) in the different type of cluster events and specifically analyze the lower (more extreme) 5th, 10th, 15th, and 20th percentiles and the median. Finally, we summarize the mean cyclone clustered activity and relate their significance to our ensemble agreement, corresponding to i.e. 60% (medium), 70% (high), and 80% (very high) of all individual ensemble members in 2060-2100 compared to 1980-2020.

Moreover, we examine the large-scale patterns that have been caused by cyclone clustering in 2060-2100 and compare them to patterns from historical clustering during 1980-2020. Here, we concentrate on the 3 cyclones within 7 days scenario to capture the most severe cyclone cluster events using CESM2-LE. Finally, we investigate specific cyclone characteristics that help us understand whether cyclones are more intense in the future by evaluating the mslp, the storms' radii and depths, life times, and the distances traveled. With this aim, we use the Welch Two-Sample t-test (Wilks, 2011) to show significance between 2060-2100 and the recent climate in 1980-2020.

4.6 Cyclone and Large-Scale Evaluation of ERA5 and CESM2-LE

4.6.1 Cyclone statistics for recent climate conditions

Our analysis starts with comparing the number of all cyclone occurrences in ERA5 and CESM2-LE. We find that for 1980-2020 CESM2-LE reproduces the cyclone frequency in both study areas compared to ERA5 well (Tab. 4.1). The slightly underestimated number of cyclones from the ensemble mean of CESM2-LE could be related to ERA5 being more sensitive towards tracking cyclones or internal variability in the large ensemble. Overall, there is evidence that the number of all cyclones is decreasing in the Northern Hemisphere within the 40-year period (Tab. 4.1). This

trend is clearer when considering the three time slices, i.e., 2060-2100 in comparison with 1980-2020 and 1850-1890, respectively (p-values ≤ 0.05, Tab. 4.1). Only in the North Pacific between 1980-2020 and 1850-1890 the number of cyclones remains stationary (Tab. 4.1). The significant trends in cyclone occurrences suggest that their numbers have been decreasing since pre-industrial times and that there will be less cyclones by the end of the current century. These findings are in line with other studies, which also have identified a reduction in the number of cyclones in future decades (e.g., Bengtsson et al. (2006), Pinto et al. (2009), Ulbrich et al. (2009), Zappa et al. (2013b), and Priestley and Catto (2022)).

The characteristics of the North Atlantic storm track are almost identical in ERA5 and CESM2-LE in 1980-2020 in terms of the typical north-east south-west tilt of the main storm track (Fig. 4.2a-b). In both data sets the maximum in the number of seasonal cyclone counts is located between Greenland and Iceland (e.g., Denmark Strait). Furthermore, the number of cyclones is decreasing from northern to central Europe, with the lowest numbers occurring between 25°N to 40°N (Fig. 4.2a-b). In CESM2-LE, a higher number of up to 2 cyclones per grid point is detected between Iceland and Great Britain (Fig. 4.2e). Here, ERA5 identifies fewer cyclones (Fig. 4.2a). With the exception of a few minor differences (e.g., Baffin Bay and eastern Mediterranean), CESM2-LE reproduces the North Atlantic storm track rather well.

The storm track features in the North Pacific are very well replicated by CESM2-LE in 1980-2020 compared to ERA5 (Fig. 4.2c-d). Although the maximum in seasonal cyclone counts may be slightly more specific in terms of where the maxima are located in ERA5 (Fig. 4.2c) as in CESM2 (Fig. 4.2d), the storm track is well captured. A somewhat higher number of up to 2 cyclones is detected over Siberia and Alaska in ERA5 (Fig. 4.2f).

Moreover, we compare ERA5 to the ensemble spread (defined as twice the ensemble standard deviation) of the large ensemble in 1980-2020 to ascertain how cyclone characteristics are represented in both data sets. The ensemble spread of cyclone counts matches well with the number of cyclones in ERA5, especially for North Pacific cyclones (Tab. 4.2). Northern Hemispheric winter cyclones have slightly longer life times and therefore larger radii and depths, and travel longer distances in the large ensemble than in ERA5 (Tab. 4.2). However, these differences are comparably small – as is the ensemble spread. This indicates high confidence in the ensemble.

To conclude, CESM2-LE provides an accurate estimate on the Northern Hemisphere storm tracks and storm characteristics in 1980-2020 compared with the tracks and characteristics in ERA5. We assume that the internal variability between the 50 ensemble members might be responsible for the regional differences.

We further evaluate the mslp fields of both Northern Hemisphere storm tracks to show whether ERA5 and CESM2-LE are comparable during 1980-2020. The most noticeable differences in the North Atlantic mslp are found between Iceland and Scotland, where ERA5 shows higher mslp of up to 3 hPa and over the western Mediterranean with lower mslp of up to 5 hPa (Fig. B.1a in *Appendix* B). In the recent climate of the North Pacific, mslp in ERA5 is higher over the Bering Sea than in CESM2-LE (Fig. B.1b in *Appendix* B). Thus, some of these differences might account for changes in storms that originate in these regions.

TABLE 4.1: Statistical significance of the cyclone frequency in the North Atlantic and North Pacific in ERA5 and in CESM2-LE.

North Atlantic	**no. per DJF**	**relation**	**p-value**	**trend**
1850-1890	113	1850-1890 vs 1980-2020	0.04	decrease
1980-2020	111 (124 in ERA5)	1980-2020 vs 2060-2100	$6.2{\cdot}10^{-20}$	decrease
2060-2100	103	1850-1890 vs 2060-2100	$2.5{\cdot}10^{-24}$	decrease
North Pacific	**no. per DJF**	**relation**	**p-value**	**trend**
1850-1890	89	1850-1890 vs 1980-2020	0.2	-
1980-2020	89 (93 in ERA5)	1980-2020 vs 2060-2100	$1.5{\cdot}10^{-15}$	decrease
2060-2100	84	1850-1890 vs 2060-2100	$1.2{\cdot}10^{-13}$	decrease

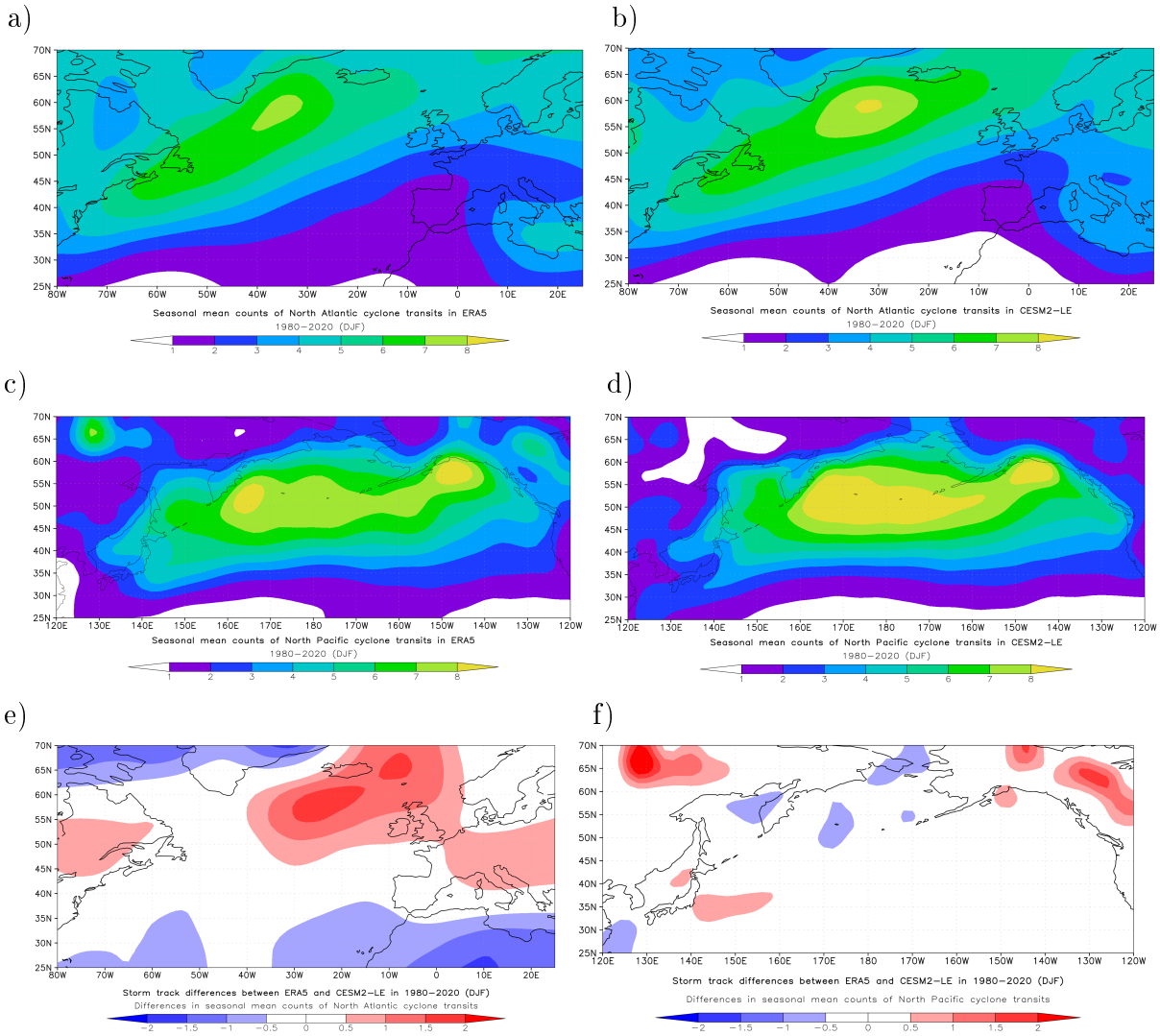

FIGURE 4.2: North Atlantic storm track in a) ERA5 and b) CESM2-LE; c) and d) same but for the North Pacific storm track, e) and f) storm track differences between ERA5 and CESM2-LE in 1980-2020.

TABLE 4.2: Mean cyclone counts per winter, life time, minimum and mean mslp, mean radius, depth and distance in ERA5 and CESM2-LE in 1980-2020. We compare ERA5 to the ensemble spread of CESM2-LE.

North Atlantic	**ERA5**	**CESM2-LE (Ensemble Spread)**
mean cyclone counts per winter	124 cyclones	111 $\pm$ 8 cyclones
mean life time	3.3 days	3.5 $\pm$ 0.05 days
min mlsp	917 hPa	919 $\pm$ 8.8 hPa
mean mslp	994 hPa	991 $\pm$ 1.2 hPa
mean radius	388 km	398 $\pm$ 3.5 km
mean depth	643 m	692 $\pm$ 11.6 m
mean distance	2998 km	3391 $\pm$ 71 km
North Pacific	**ERA5**	**CESM2-LE (Ensemble Spread)**
mean cyclone counts per winter	93 cyclones	89 $\pm$ 7 cyclones
mean life time	3.4 days	3.6 $\pm$ 0.06 days
min mlsp	927 hPa	922 $\pm$ 8.7 hPa
mean mslp	994 hPa	992 $\pm$ 0.9 hPa
mean radius	384 km	396 $\pm$ 4 km
mean depth	685 m	704 $\pm$ 11.7 m
mean distance	2698 km	3057 $\pm$ 68 km

4.6.2 Mean Sea Level Pressure conditions in ERA5 and CESM2-LE

Having shown that ERA5 and CESM2-LE are highly compatible in cyclone frequency, characteristics and mslp, we investigate the differences in the mslp fields of both storm tracks in 2060-2100 compared to 1980-2020 to see whether they can (partly) explain changes in storm intensities (Fig. 4.3).

We find that in the North Atlantic region mslp is decreasing over the Hudson Bay and central to northern Scandinavia by up to 4 hPa (Fig. 4.3a). A t-test shows that these trends are statistically significant as indicated by the black dots. A strengthening eastern trough associated with cyclogenesis over the eastern Hudson Bay implies that storms in or emerging from these areas are more intense (Fazel-Rastgar, 2020). The melting of ice caps in Canada might also contribute to the changes in pressure in these regions (Serreze et al., 2017). Moreover, pressure is significantly increasing over Greenland by up to 3 hPa. These trends indicate that storms that have their cyclogenesis, for example, over Greenland or in the Denmark Strait, have a higher initial pressure before they intensify as they are propagating towards the European mainland. Greenland is one of the fastest-warming regions on Earth and its ice sheet is melting more rapidly in the higher global warming SSP3-7.0 scenario (Xie et al., 2022). As a result of Arctic warming, this might lead to an increase in mslp. Furthermore, this might also affect the baroclinicity and therefore the intensity of cyclones. Note that changes in mslp over Greenland should be treated carefully, since estimates may be less accurate.

In the Mediterranean, we also find that pressure is increasing (Fig. 4.3a). A t-test

confirms that there is a significant difference between the two periods (p-values $<$ 0.05). This region has been identified as drying up with fewer numbers of cyclones in the future (Ulbrich et al., 2009; Reale et al., 2022). With the exception of a very few minor shifts and more extended areas, the future changes in mslp we have seen here between 2060-2100 and 1980-2020 are almost identical with those of 2060-2100 compared to 1850-1890. This means that mslp in 1980-2020 is very similar to 1850-1890 (not shown).

Significant changes in mslp are also found in the North Pacific region (see black dots in Fig. 4.3b). Here, the central part of the North Pacific ocean experiences an increase in pressure by approximately 3 hPa (Fig. 4.3b). Higher greenhouse gas emissions in the SSP3-7.0 scenario might cause this amplifying effect. Over Siberia and in the Bering Sea we find that pressure is significantly decreasing by up to 5 hPa (Fig. 4.3b), which means that cyclones propagating over the Northern part of the North Pacific and towards Alaska and Canada are more intense. There is a decline in the sea-ice extent over this particular region (Jeong et al., 2022; Huang et al., 2022), similar to the ice sheet melting over Greenland (Zheng et al., 2022). Interestingly, the trend here is negative. One possible reason could be changes in stratification or in the meridional temperature gradient, which in turn could affect the baroclinicity. This could explain alterations in the cyclones' intensities. Future research is needed to identify the processes behind these opposite trends between a decline in sea-ice mass and changes in mslp. We find that the differences here are similar to those of 2060-2100 and 1850-1890 with the exception of one small area near the west coast of the US (located approximately at 130°W and 40°N) where pressure is decreasing by up to 2 hPa. It might be a derivative of the climate response between 1980-2020 and 1850-1890 (not shown). This eastern part of the North Pacific storm track is more prone to cyclone clustering. Hence, cyclones in this particular region might be more intense.

While a statistically significant decrease in mslp is found for some areas under future climate conditions (e.g., northeastern Canada, Scandinavia, the Bering Sea, and Alaska), other regions show an increase (e.g., Greenland, the Mediterranean, and central part of the North Pacific ocean), thus changing the large-pressure gradients in the mid-latitudes. In conclusion, our findings suggest that the climatological background state, the mslp fields, influences the intensity of cyclones under future conditions.

4.6.3 Future Cyclone Mean Counts in CESM2-LE

We are also interested in the future cyclone mean counts, since they are highly affected by the changes in the intensity of the climatological background states. To study the number of cyclones in more detail, we examine the mean cyclone transits in 2060-2100 and compare them to 1980-2020 (Fig. 4.4). We find that the number of the mean cyclone transits is decreasing over Greenland and in the eastern Mediterranean (Fig. 4.4a), where we found that cyclones have a higher initial pressure (Fig. 4.3a). These are the only differences identified by the large ensemble. Comparing the different confidence intervals shows that the decrease in the number of cyclones is, however, only statistically significant for cyclones in the eastern Mediterranean. The future changes in mean cyclone counts we have seen here between 2060-2100

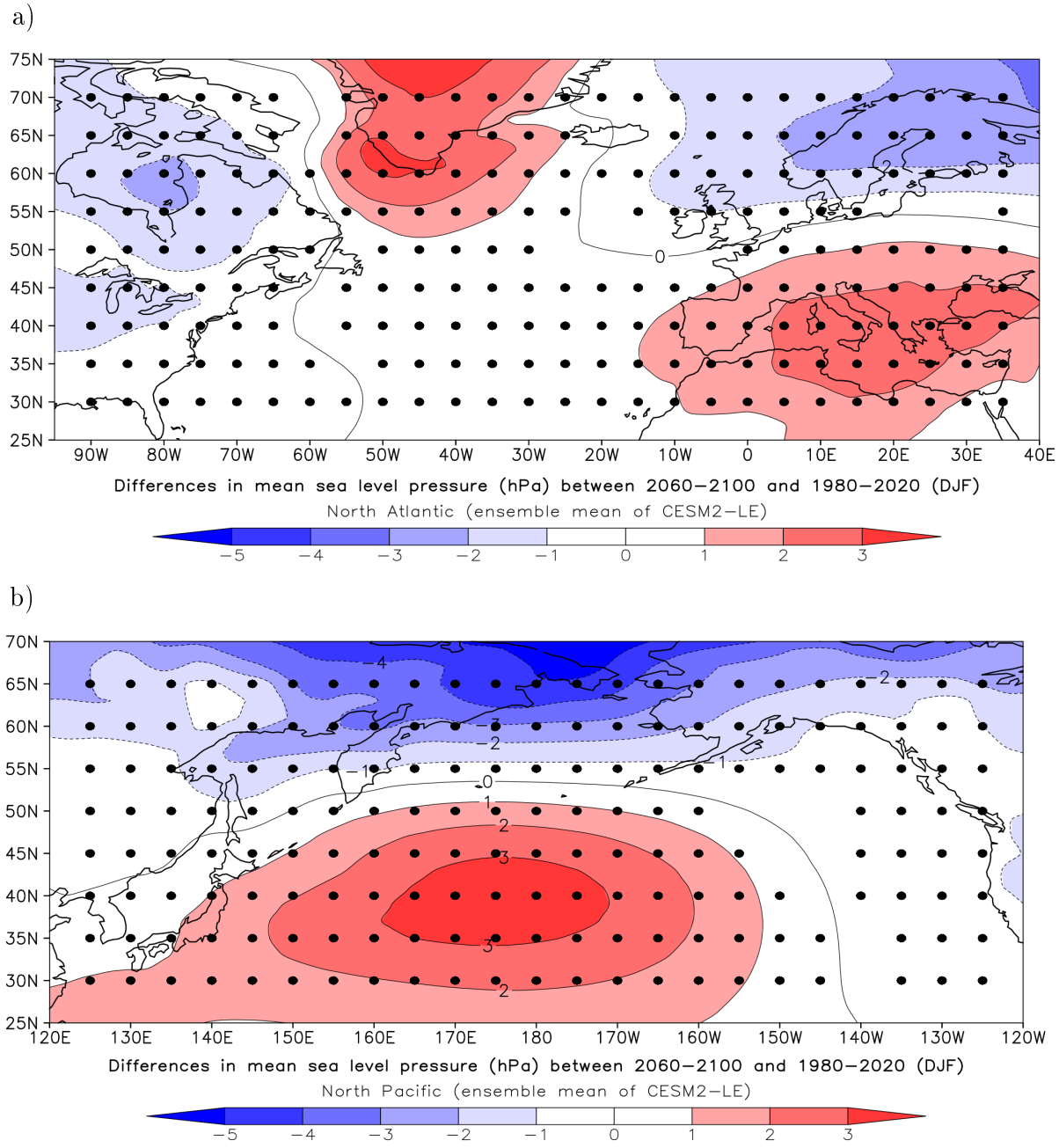

FIGURE 4.3: Differences in mean sea level pressure between 2060-2100 and 1980-2020 in the a) North Atlantic and b) North Pacific storm track regions using CESM2-LE. The black dots mark grid points where differences are significant at the 95% confidence level.

and 1980-2020 are similar to those of 2060-2100 and 1850-1890 (not shown). In the latter period, the decreases in cyclone counts are statistically significant for both southern Greenland and the eastern Mediterranean.

In the following sections, we only focus on the Pacific Northwest, since we are particularly interested in cyclone clustering in the eastern part of the North Pacific including the Gulf of Alaska and the west coast states of the US and Canada. CESM2-LE shows less cyclone transits in the future (Fig. 4.4b). This reduction in cyclone transits is argued to be a result of global warming (e.g., Bengtsson et al. (2006), Pinto et al. (2009), Ulbrich et al. (2009), Zappa et al. (2013b), and Priestley and Catto (2022)). The only exception is western Canadian provinces, where it is indicated that the numbers of cyclones are slightly increasing (Fig. 4.4b). Both results are statistically significant as indicated by the black dots. There are no significant differences between 2060-2100 and 1850-1890 that differ from 1980-2020 (not shown). This suggests robust findings in future North Pacific cyclone counts.

To conclude, climate simulations show that the number of cyclones decreases particularly over rapidly warming regions, such as Greenland and the eastern Mediterranean. In addition the central Northeast Pacific will experience significantly less cyclone transits in the future. It is likely that dynamic changes are responsible for these changes.

4.7 Clustering Analysis based on dispersion statistics

4.7.1 ERA5 and CESM2-LE in recent climate conditions

Following Mailier et al. (2006)'s definition of the dispersion statistic we compare the dispersion of cyclone counts during 1980-2020 for both our study areas in ERA5 and CESM2-LE (Fig. 4.5). Along the east coast of the US and in the western North Atlantic we find regularly occurring (underdispersive) cyclones denoted by the negative values of the dispersion (Fig. 4.5a). Following the storm track from the southwest to the northeast Atlantic the dispersion is increasing (Fig. 4.5a). This is in line with the increasing dispersion along the storm track axis as found by Blender et al. (2015). A maximum in dispersion of up to 0.5 is found near the Iberian Peninsula and over the British Iles – these are preferred regions of clustered cyclones (Fig. 4.5a). Comparing ERA5 to CESM2-LE, we find that the large ensemble generally reproduces the dispersion seen in ERA5 well (Fig. 4.5b). While the overdispersion in ERA5 has a more dipole structure in north-south direction, it is more zonal and west-east oriented in CESM2-LE. This might be due to the peculiarity of the model data. In the North Pacific cyclones occur regularly over the central part of the North Pacific (see negative values in Fig. 4.5c). Overdispersive cyclone occurrences, therefore cluster areas, are identified along the west coast of the US and Canada (Fig. 4.5c). The large ensemble deviates from ERA5 here: in CESM2-LE, the overdispersion is characterized as largest in the central Northeast Pacific (Fig. 4.5d). We assume that this is due to internal variability in the ensemble.

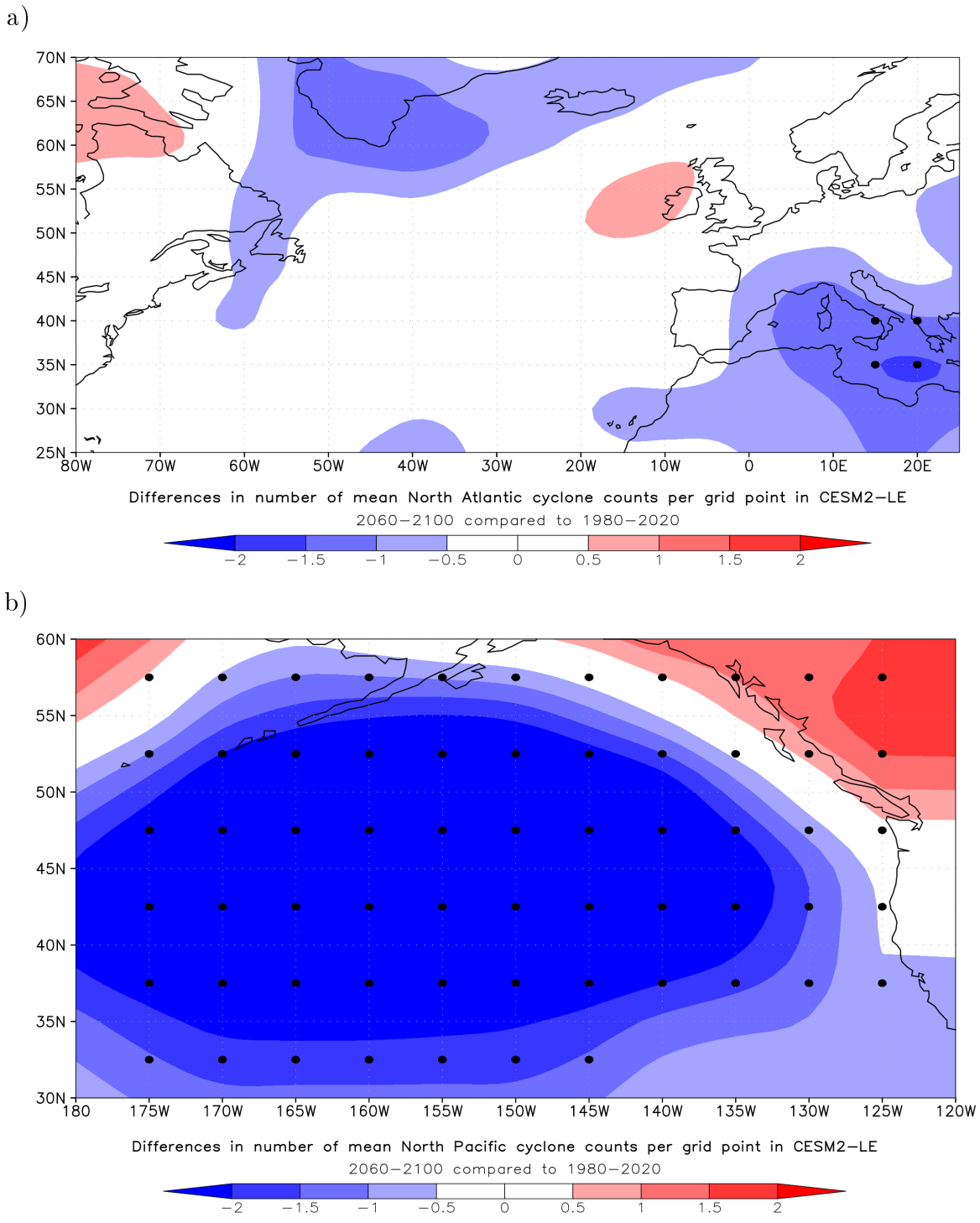

FIGURE 4.4: Differences in the number of mean cyclone counts per grid point of a) North Atlantic and of b) Northeast Pacific cyclone transits during 2060-2100 compared to 1980-2020 using CESM2-LE. The black dots mark grid points where differences are significant at the 95% confidence level.

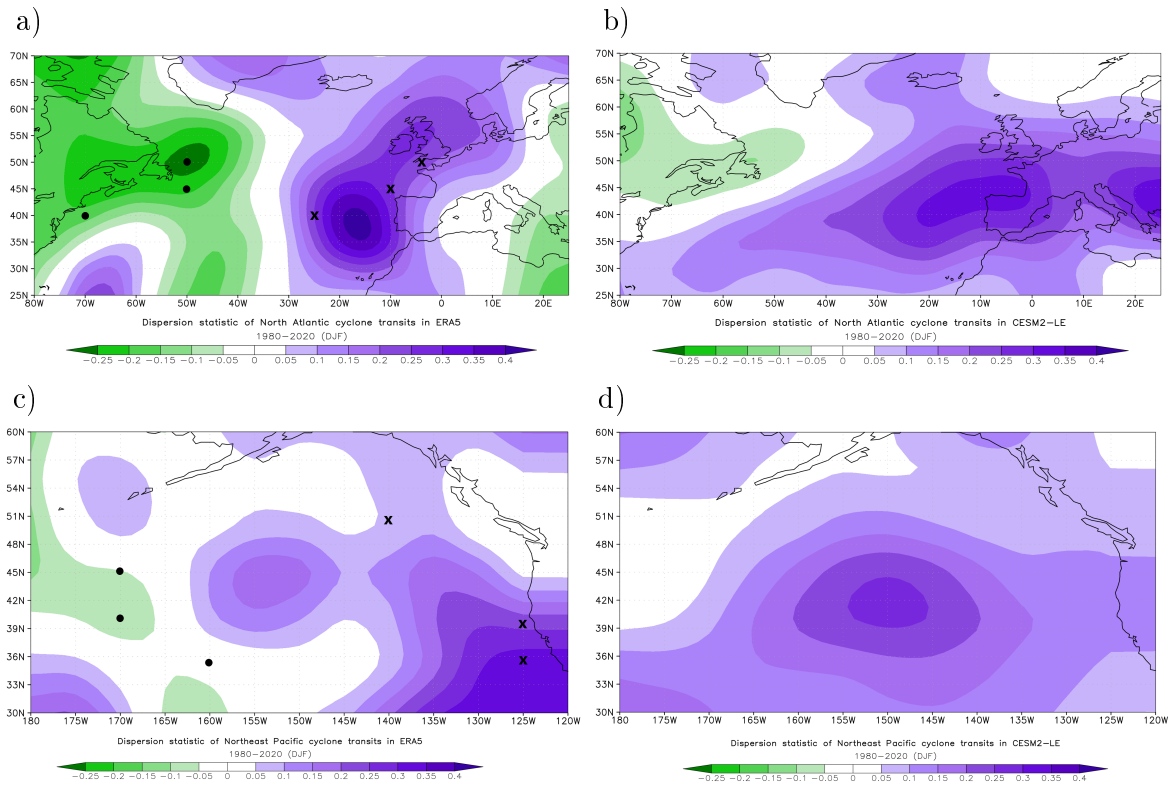

FIGURE 4.5: Dispersion statistic of North Atlantic and Northeast Pacific cyclone transits in 1980-2020 from the ERA5 reanalysis (left row) and CESM2-LE (right row). The dispersion statistic is the standard deviation of a Poisson process and describes whether cyclones occur regularly (negative values), randomly (near zero values) or in clusters (positive values). The black dots (genesis regions) and crosses (cluster regions) in a) and c) mark specific grid points where the dispersion is changing in 1980-2020 (see Fig. 4.7).

4.7.2 Possible changes in dispersion statistics in CESM2-LE

Now we explore possible future changes in the dispersion as projected by the large ensemble (Fig. 4.6). Over central and southern Iceland we find that the dispersion is decreasing during 2060-2100 compared to 1980-2020, relating to more regularly occurring cyclones in the future (Fig. 4.6a) (p-values < 0.05). Other regions are characterized by more randomly occurring cyclones during 2060-2100, for example, in the cyclogenesis regions: along the east coast of the US (Fig. 4.6a). This suggests that physical processes associated with global warming may be important for the transformation or shift towards more regular or clustered occurrences (or vice versa). The temperature gradient might also play a role. From 2060-2100 to 1850-1890, we find that the projected changes in the dispersion are rather similar to the results we have seen before. The only exception is a small area located approximately over northern Germany at 5-15°W and 50°N where more regularly cyclones are occurring in comparison with pre-industrial times (not shown). The changes in the dispersion might already represent the current climate change during 1980-2020.

In the Northeast Pacific, the large ensemble identifies mostly values close to zero, except along the east coast of the Aleutian Island chain where the dispersion is slightly more enhanced during 2060-2100 than in 1980-2020 (Fig. 4.6b) (p-values < 0.05). Higher anthropogenic greenhouse gas emissions seem to support clustering, since the climate signal is even more recognizable when comparing 2060-2100 to 1850-1890: here, we find larger and more extended areas of the overdispersion and another small region of preferred clustering at the west coast of the US, approximately between 120-127°W and 39-45°N (not shown). This is most likely the difference of the climate response of 1980-2020 to 1850-1890.

In conclusion, our findings reveal that all statistically significant changes projected for the North Atlantic emerge from a specific region between Newfoundland and Iceland, which is characterized by more regular cyclone occurrences during 2060-2100 compared to 1980-2020. This indicates a smaller potential for cyclones to cluster north of the British Isles. In contrast, along the east coast of the Aleutian Island chain and the west coast states of the US we find that these regions show a significantly enhanced overdispersion during 2060-2100. We assume that the climate signal of 1980-2020 plays a critical role. However, some of these changes are comparably small so that it becomes necessary to investigate the temporal evolution of the dispersion at different grid points.

4.7.3 Trends in Non-Clustered vs. Clustered Events

Since the dispersion might undergo changes over time due to natural variability or anthropogenic warming, it is important to assess the decadal statistics of different grid points of non-clustered (genesis) regions and cluster regions in 1980-2020 and 2060-2100 (see the specific grid points in Fig. 4.5a,c and associated time series in Fig. 4.7-4.8). This can be helpful to identify the regions most affected by clustering. In the current climate, we find that the overdispersion in the Northeast Atlantic cluster region is increasing with time and has become more volatile since the 1990s, but the dispersion in the genesis regions remains stationary in ERA5 (Fig. 4.7a-c, left panel). In the ensemble mean of CESM2-LE, the dispersion of both genesis and cluster regions do not reveal any trends (Fig. 4.7g-i, right panel). Indeed, the

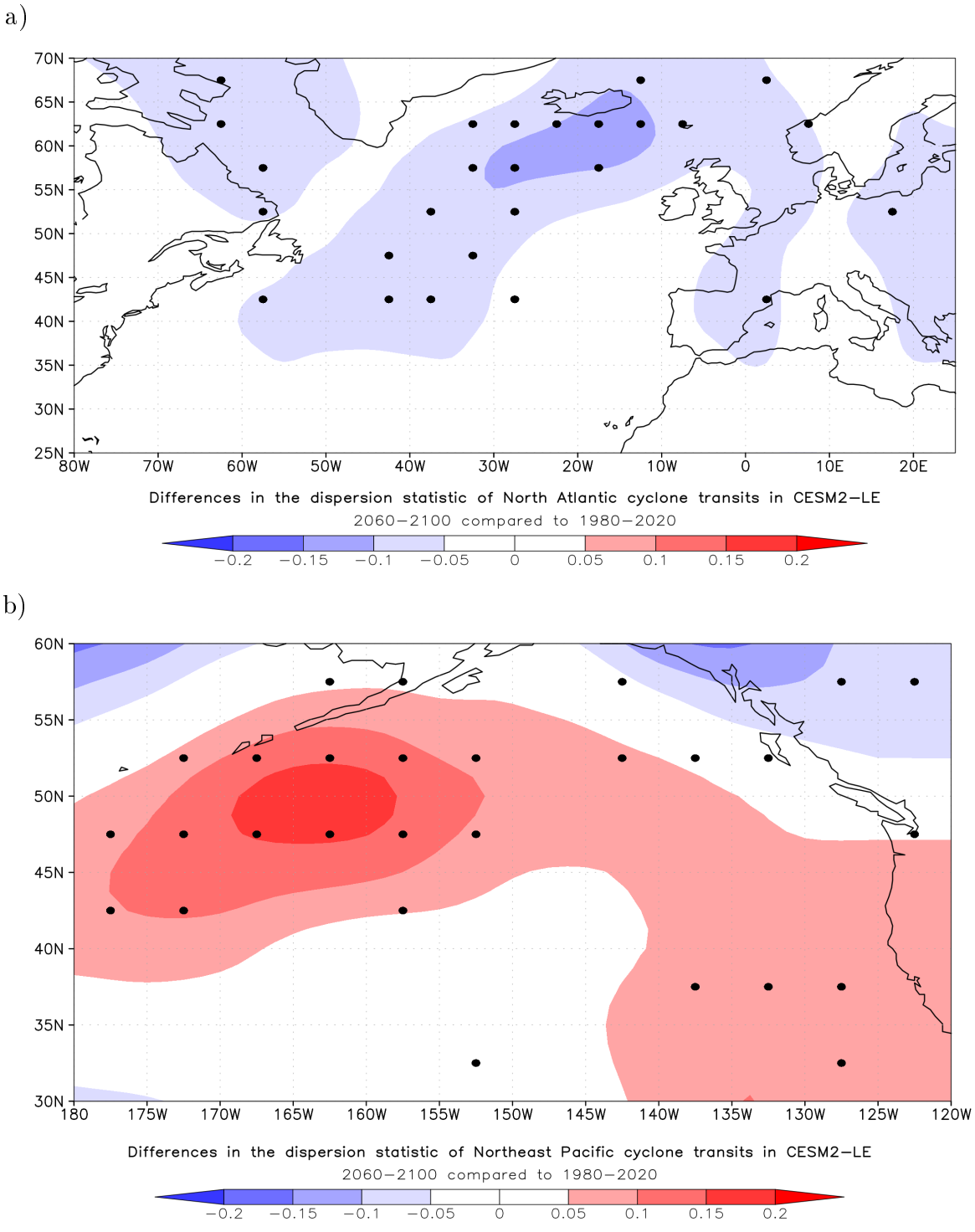

FIGURE 4.6: Differences in the dispersion statistic of a) North Atlantic and of b) Northeast Pacific cyclone transits during 2060-2100 compared to 1980-2020 using CESM2-LE. The black dots mark grid points where differences are significant at the 95% confidence level.

dispersion in the genesis regions is partly more random than regular (Fig. 4.7g-i, right panel). Similar distributions of the dispersion are seen at other grid points (not shown).

In genesis regions of the Northeast Pacific, however, the overdispersion in cluster regions is decreasing, while the dispersion in genesis regions is stationary in 1980-2020 in ERA5 (Fig. 4.7d-f, left panel). Neither genesis nor cluster regions of the Northeast Pacific exhibit any trends at the selected grid points in the large ensemble (Fig. 4.7j-l, right panel). In particular, the distribution of over- and underdispersion are reversed at one grid point (Fig. 4.7l, right panel). Other grid points show similar tendencies (not shown).

To summarize, there are no changes in the dispersion of non-clustered (genesis) regions between 1980-2020 in neither ERA5 nor in CESM2-LE. The overdispersion in both Northern Hemispheric cluster regions, on the other hand, suggests high variability in the current climate in ERA5. For the European region this may imply more clustering over time; while for the Pacific Northwest less clustering is observed. When considering the large ensemble, the dispersion did not change in the period 1980-2020.

Future projections of the dispersion show a different pattern: in the Northeast Atlantic, the dispersion of former genesis regions is less regular and more random by 2060-2100, while the overdispersion in cluster regions remains constant in CESM2-LE (Fig. 4.8a-c, left panel). The trends in the Northeast Pacific are rather similar (Fig. 4.8d-f, right panel), except for two grid points where regular cyclone occurrences of the past are more clustered in the future winter climate (Fig. 4.8e-f, right panel). This suggests that a warmer atmosphere might contribute to the enhanced clustering. As the storm track shifts poleward on zonal and annual average (e.g., Bengtsson et al. (2006), Harvey et al. (2020), and Karwat et al. (2022)), it could also have an impact on the locations where we see alterations in the dispersion. Furthermore, clustering might be uncertain in future decades (larger spread). As the large ensemble does not reflect the variability in the dispersion of clustered cyclones that we have seen for both Northern Hemisphere storm tracks in ERA5, we will next investigate the different cyclone cluster types directly to determine whether the large ensemble supports the indicated trends by ERA5.

4.8 Clustering Analysis based on storm numbers

4.8.1 ERA5 and CESM2-LE in recent climate conditions

Now we examine clustered events from the cyclone tracking data directly. First we compare how many cluster type events were identified by ERA5 and CESM2-LE during 1980-2020, respectively. For 3 cyclones within 7 days, ERA5 identifies 17 clustered events on average; 14 in CESM2-LE (Fig. 4.9a). There have only been up to 5 clustered events in the most extreme 5th and 10th percentiles over Europe in the past, since these are very rare events. Along the west coast of the US and Canada we find that the intensity of clustered cyclones is clearly lower, indeed, there has been only one occurrence in the 20th percentile, while the median is characterized by approximately 10 clustered events during 1980-2020 (Fig. 4.9b). In contrast, cyclones in the Gulf of Alaska cluster on average almost 10 times more often than along the

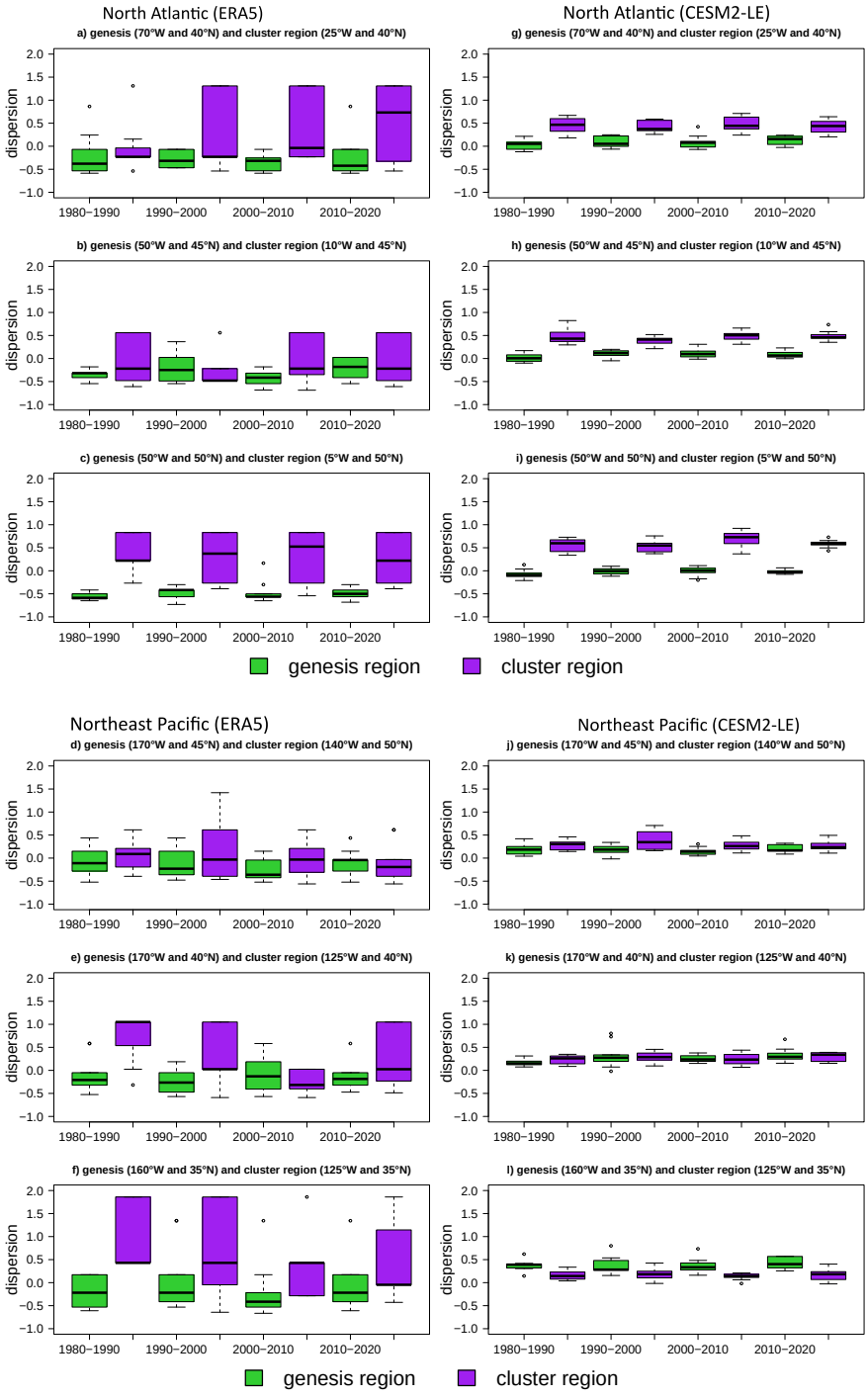

FIGURE 4.7: Dispersion statistics in the indicated periods of North Atlantic cyclone transits at specific grid points in cyclogenesis (green boxes) and cluster (purple boxes) regions (a-f); similar for Northeast Pacific cyclone transits (g-l). The dispersion statistics were computed from ERA5 (left panel) and CESM2-LE (right panel) for 1980-2020. The decadal uncertainty of the dispersion is given by the range of the box plots.

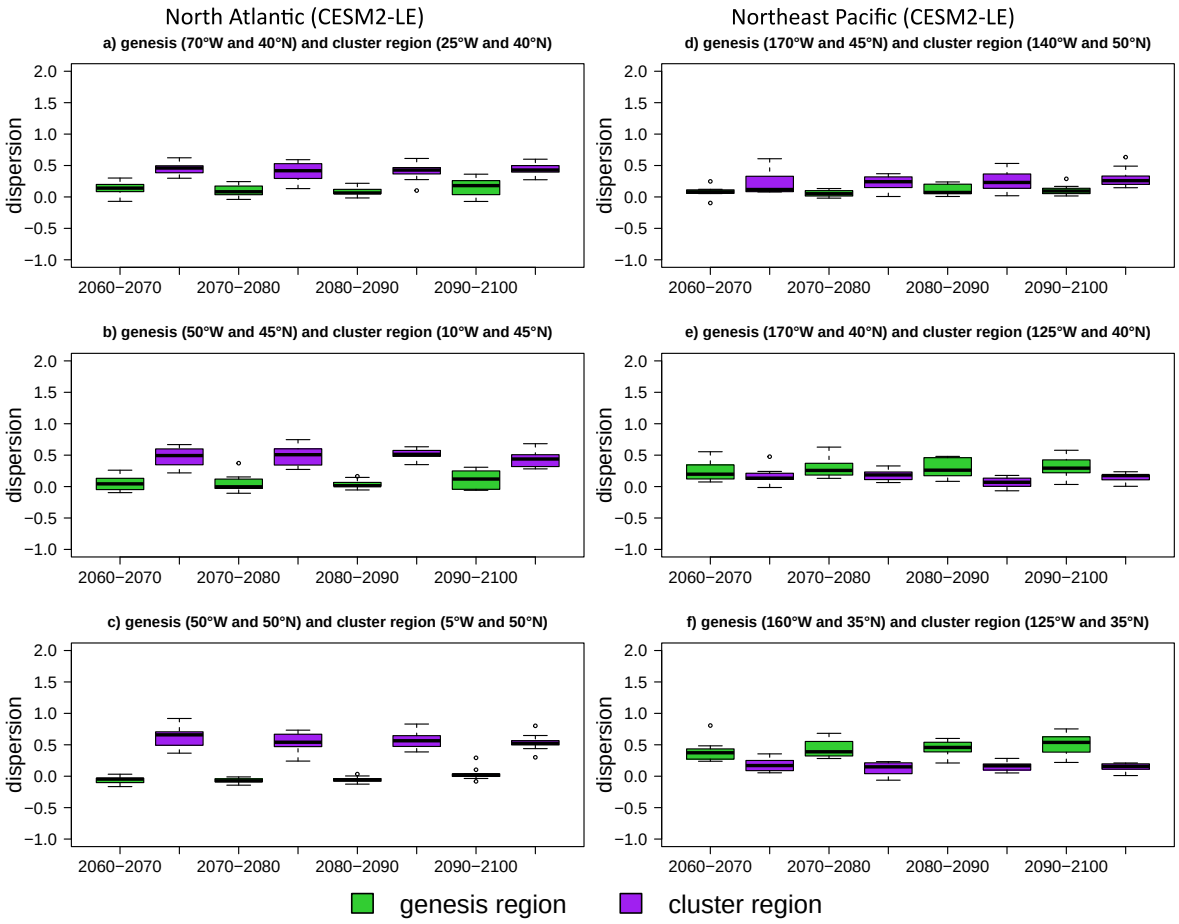

FIGURE 4.8: Dispersion statistics in the indicated periods of North Atlantic cyclone transits at specific grid points in cyclogenesis (green boxes) and cluster (purple boxes) regions (a-c); similar for Northeast Pacific cyclone transits (d-f). The dispersion statistics were computed from CESM2-LE for 2060-2100. The decadal uncertainty of the dispersion is given by the range of the box plots.

west coast of the US and Canada and 5-6 times more often than over Europe: the deviation between CESM2-LE and ERA5 is less than 6% (Fig. 4.9c). Extremely intense cyclone clusters, e.g., 5th percentile, occur about every 5-6 years in this region.

To summarize, ERA5 and CESM2-LE are highly comparable over different percentiles in 1980-2020. Thus, the large ensemble shows reasonable skill compared to ERA5 in identifying clustered events with different cyclone intensities.

4.8.2 Future projections of different cyclone cluster events in CESM2-LE

We now look at possible trends (positive, negative, or none) in the different type of cyclone cluster events between 1980-2020 and 2060-2100. To quantify clustering we look at 3, 4, 5 and 6 cyclones within 7 days as the cumulative percentage of ensemble members. These high numbers are necessary because of the already high number in weekly cyclone occurrences (see *Appendix* B).

For 3 cyclones within 7 days, the ensemble members agree by 72% in the median that there will be more clustering over Europe (Fig. 4.10a). Furthermore, the large ensemble finds no changes in extreme cyclone quadruples concerning the 5th percentile of mslp in 7 days (up to 90% agreement, Fig. 4.10b). However, the ensemble shows medium confidence in an increase of 4 cyclones within 7 days in the future (62% agreement, Fig. 4.10b). In terms of 5 or 6 cyclones within 7 days, values that rarely occur in this area, there is very high ensemble confidence across almost all percentiles that there are no changes expected by 2060-2100 (Fig. 4.10c-d). Comparing 1850-1890 with 2060-2100, we find similar projections (not shown). In conclusion, the large ensemble predicts more clustering over Europe for cyclone triples and quadruples within 7 days, but no changes in the most extreme percentile and concerning 5 or 6 cyclones.

For the west coast states of the US and Canada, 74% of the ensemble members agree on a decrease in the median of mslp for 3 cyclones within 7 days (Fig. 4.11a). For cyclone quadruples we find no changes across different percentiles except for an overall decrease in clustering indicated by the median for 7 days (58% ensemble agreement, Fig. 4.11b). The trends we have seen in the median are more confident between 1850-1890 and 2060-2100, and agree with the current climate (not shown). Considering 5 or 6 cyclones, which also rarely occur in this area, the large ensemble shows overall no trend across different percentiles between 2060-2100 and 1980-2020 (Fig. 4.11a-d). This is an important finding, since it suggests that extreme cyclone clusters might not necessarily become more common in the Pacific Northwest.

In the Gulf of Alaska, the clustering of cyclone triples within 7 days decreases in the 20th percentile according to 98% of all ensemble members (Fig. 4.12a). Cyclone quadruples are also shown to be decreasing overall in the future (up to 72% agreement, Fig. 4.12b). In addition no trend is identified in the 5th percentile of mslp concerning 5 cyclones in 7 days (Fig. 4.12c). However, there seems to be a clear cut when comparing 6 cyclones in 7 days: here, we detect high ensemble confidence for less clustered cyclones in the 20th percentile and especially in the median (Fig. 4.12d). We find that the ensemble members are even more confident in the decrease of clustering across all percentiles when comparing these projections to 1850-1890

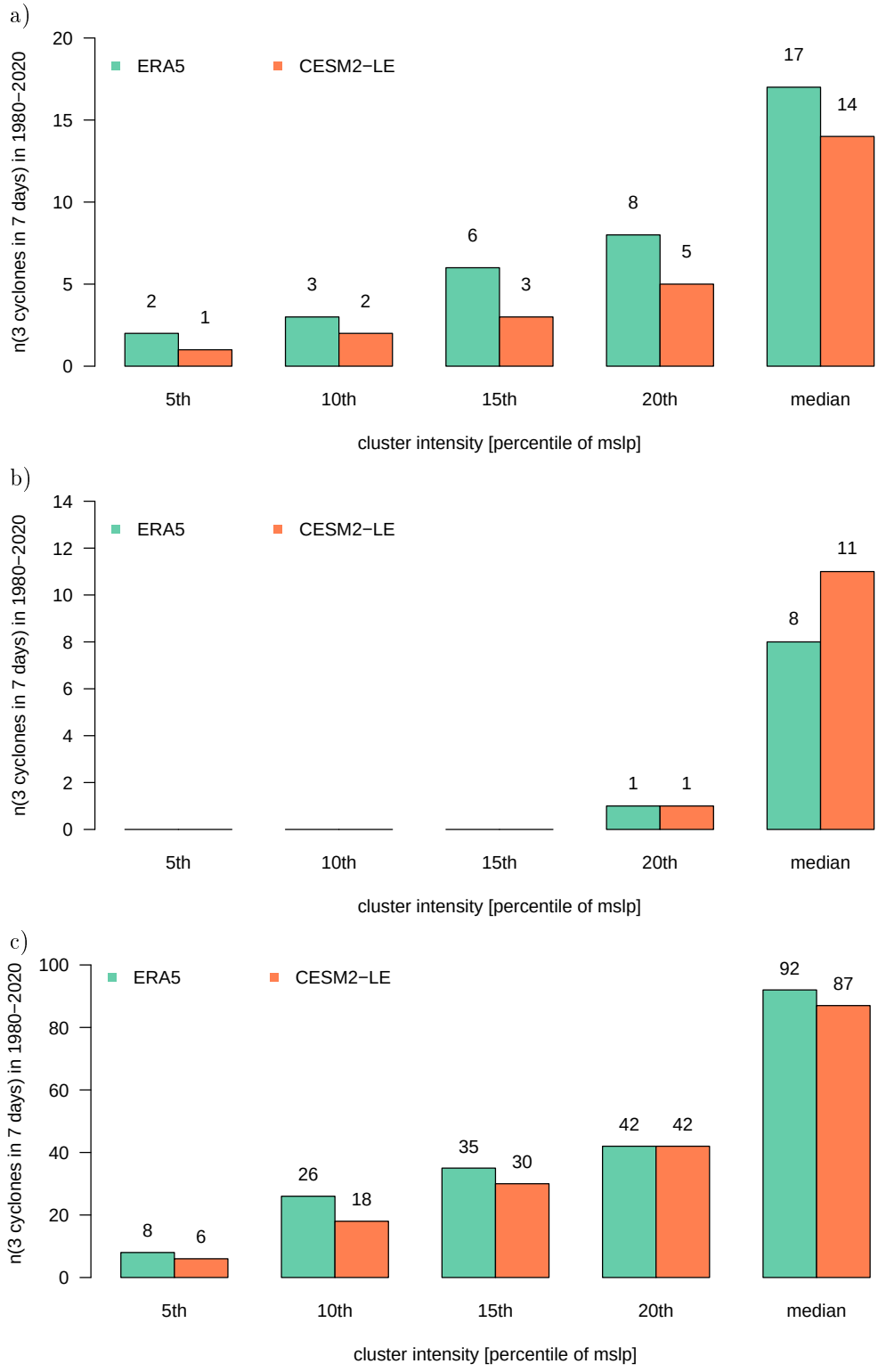

FIGURE 4.9: Total number n of the '3 cyclones in 7 days' cluster type event over a) Europe, b) along the west coast of the US and Canada, and c) in the Gulf of Alaska as identified by ERA5 and CESM2-LE during 1980-2020.

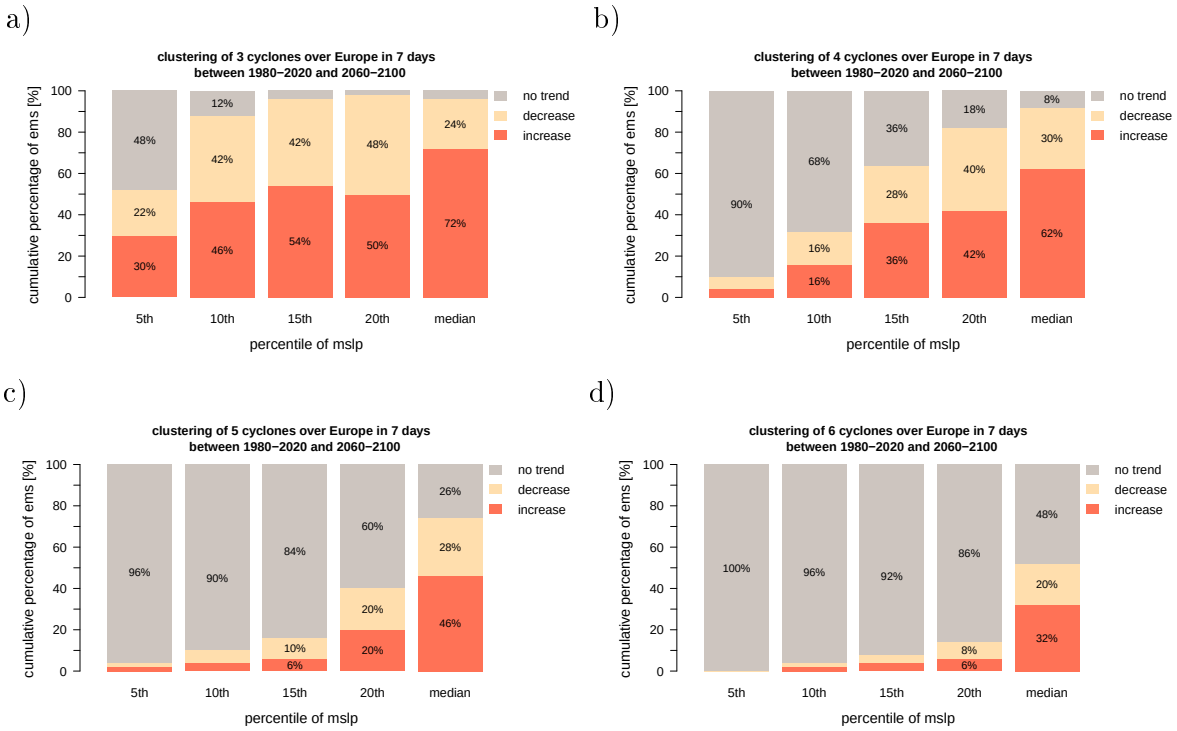

FIGURE 4.10: Ensemble agreement for trends in cyclone clustering over Europe for a) 3 cyclones, b) 4 cyclones, c) 5 cyclones, and d) 6 cyclones in 7 days, respectively. The ensemble agreement is defined as the cumulative percentage of all 50 ensemble members (ems) of CESM2-LE that either predict an increase (orange bars), decrease (beige bars) or no trend (grey bars) between 2060-2100 and 1980-2020.

and 2060-2100 (not shown). This could be due to the climate signal more noticeable between pre-industrial times and the SSP3-7.0 scenario in the future.

To summarize, the majority of ensemble members agree that enhanced cyclone clustering will occur over Europe in the future, but only on average rather than in the most extreme percentile. Clustering along the west coast of the US and Canada is seen to generally decline or remain steady in lower percentiles; the ensemble agreement on clustering to decrease in the Gulf of Alaska in a future winter climate is similarly confident.

4.8.3 Ensemble Agreement on Projections in CESM2-LE

For different types of clustering we can now compare the mean cyclone clustered activity to the significance derived from our ensemble agreement (Tab. 4.3). Concerning Europe, we find an increase of 21.5% for 3 cyclones within 7 days by 2060-2100 compared to 1980-2020 (high confidence) (Tab. 4.3). Similarly, cyclone quadruples are increasing over Europe within 7 days by 25% during 2060-2100 compared to 1980-2020 (medium confidence). Along the west coast of the US and Canada cyclone triples within 7 days decrease by 24.3% during 2060-2100 compared to 1980-2020 (medium ensemble confidence, Tab. 4.3). However, the actual numbers here are small, since these are very rare events. Over the Gulf of Alaska, clustering is

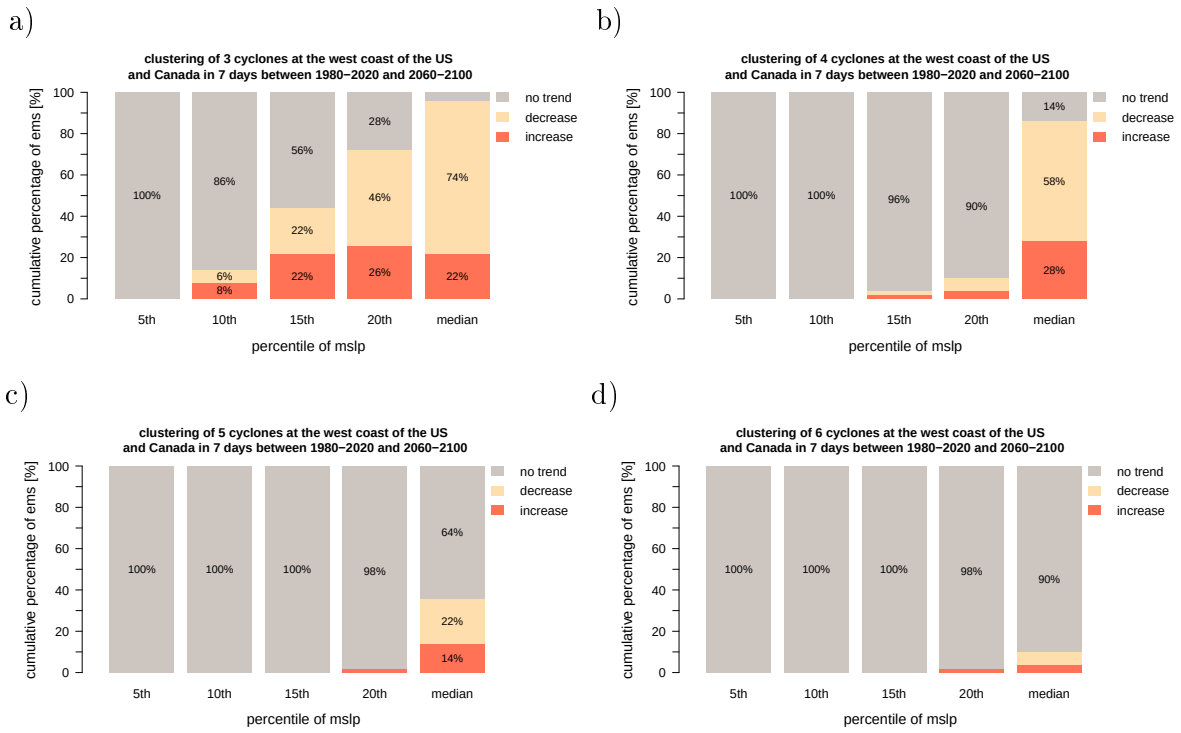

FIGURE 4.11: Ensemble agreement for trends in cyclone clustering at the west coast of the US and Canada for a) 3 cyclones, b) 4 cyclones, c) 5 cyclones, and d) 6 cyclones in 7 days, respectively. The ensemble agreement is defined as the cumulative percentage of all 50 ensemble members (ems) of CESM2-LE that either predict an increase (orange bars), decrease (beige bars) or no trend (grey bars) between 2060-2100 and 1980-2020.

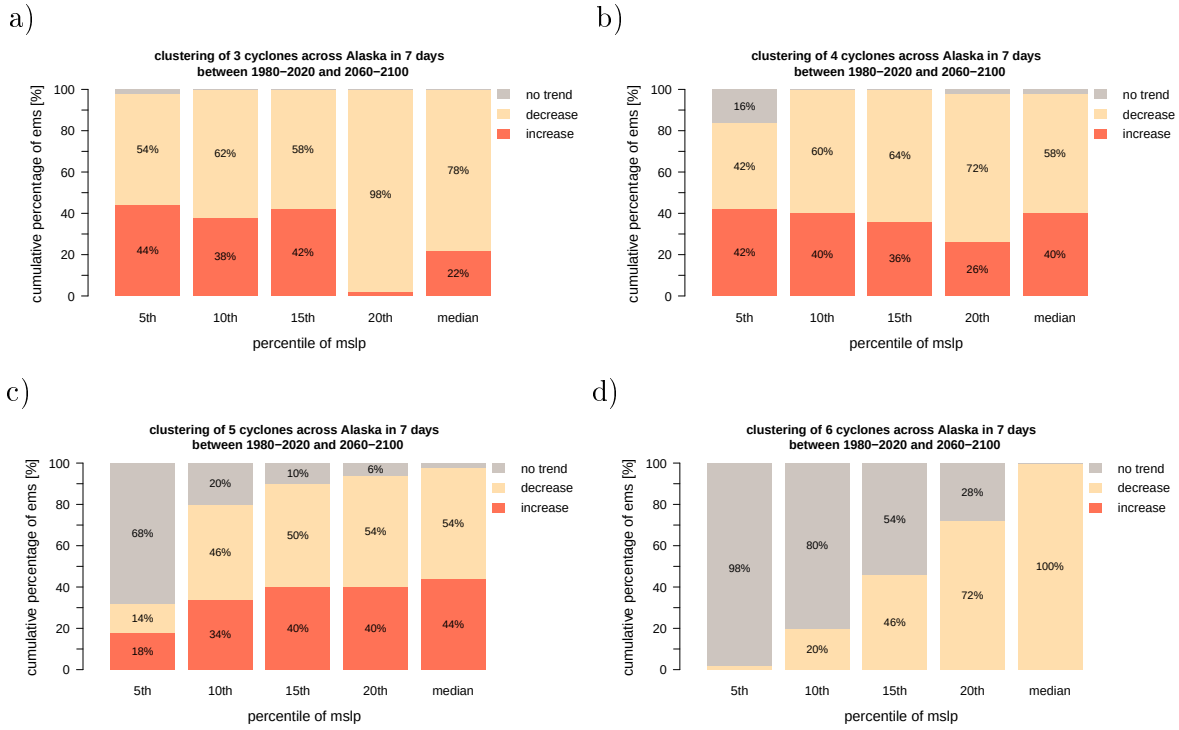

FIGURE 4.12: Ensemble agreement for trends in cyclone clustering in the Gulf of Alaska for a) 3 cyclones, b) 4 cyclones, c) 5 cyclones, and d) 6 cyclones in 7 days, respectively. The ensemble agreement is defined as the cumulative percentage of all 50 ensemble members (ems) of CESM2-LE that either predict an increase (orange bars), decrease (beige bars) or no trend (grey bars) between 2060-2100 and 1980-2020.

TABLE 4.3: Trends in cyclone clustering of 3 or 4 clustered cyclones in 7 days as mean numbers per winter and as mean percentage change for Europe, the west coast regions of the US and Canada, and the Gulf of Alaska during 2060-2100 compared to 1980-2020 and 1850-1890 in CESM2-LE. Ensemble confidence is defined as the agreement of the same trend that is identified by at least 60% (medium), 70% (high), and 80% (very high) of all individual ensemble members in 2060-2100 compared to the reference period 1980-2020.

Clustering Type	no. in 1980-2020	no. in 2060-2100	% change in 2060-1980	% change in 2060-1850	ensemble confidence
Europe					
3 cyclones in 7 days	1	1.2	21.5	13	high
4 cyclones in 7 days	0.3	0.4	25	26.2	medium
US and Canadian West Coast					
3 cyclones in 7 days	0.5	0.4	-24.3	-27.9	medium
4 cyclones in 7 days	0.15	0.1	-23.5	-19.1	< medium
Gulf of Alaska					
3 cyclones in 7 days	6	5.4	-10.1	-15.2	high
4 cyclones in 7 days	3.4	3.1	-8.3	-17.2	medium

more common and decreases by 10.1% in the same period (high confidence, Tab. 4.3).

To conclude, there is high confidence in the ensemble for more cyclone clustering over Europe and for less clustering in the Pacific Northwest regions based on this metric. Overall, this direct approach of comparing cyclone triples and quadruples and the other cyclone cluster types appears to be more suitable when determining actual changes in future cyclone clustering compared to the theoretical approach (dispersion statistic). The dispersion was less helpful since changes were either small or insignificant. In addition the ensemble was not able to capture any variability. Therefore, relating different types of cyclone cluster events to the ensemble confidence provides robust results.

4.9 Large-scale features of clustered cyclones

4.9.1 Possible links between clustering and large-scale patterns in CESM2-LE

There are considerable knowledge gaps in the physical mechanisms that underlie possible changes in cyclone clustering, which is thus quite uncertain (Dacre and Pinto, 2020). Changes in baroclinicity brought on by global warming and substantial variations in large-scale conditions are often considered as the main two factors to influence (clustered) cyclone occurrences (Walz et al., 2018). Pinto et al. (2009) showed that a positive North Atlantic Oscillation (NAO) phase is more favourable

for the growth conditions of extreme cyclones than a negative NAO phase. Additionally, the impact of the NAO on cyclone clustering is largely independent from the cyclone tracking algorithm used (Pinto et al., 2016). For the positive phase of the Pacific-North American (PNA) pattern, Mailier et al. (2006) found a decrease in cyclone counts across the Canadian west coast but an overall increase of cyclones in the North Pacific.

Here, we examine the large-scale patterns that have been caused by cyclone clustering in 2060-2100 and compare them to patterns from 1980-2020 (Fig. 4.13). We focus on the 5th percentile of the 3 cyclones within 7 days scenario to capture the most severe cluster events in CESM2-LE. A minimum in mslp over Northern Ireland was shown during cyclone clustering in 1980-2020 (Fig. 4.13a). By 2060-2100, the minimum has moved further east towards Scotland (Fig. 4.13b).

In 1980-2020, cyclones cluster along the west coast of the US and Canada when a minimum in mslp is located near Vancouver Island (Fig. 4.13c). There may also be a second low pressure system present north of the Aleutian Islands (Fig. 4.13c). In the future, however, these two low pressure systems have merged into one overall system (Fig. 4.13d). This suggests that the energy from the clustered cyclones may become more concentrated.

Cyclones in the Gulf of Alaska cluster during the occurrence of a mslp minimum south of the Aleutian Islands (see 970 hPa isobar in Fig. 4.13e). We find that this minimum shifts further east and slightly expands by 2060-2100 (Fig. 4.13f). However, there is little change to the impact regions.

Thus, the large-scale patterns might not project onto the NAO, PNA or other teleconnections. When considering different intensities (other percentiles) or types of cyclone clusters, similar patterns are found (not shown). This confirms that the overall large-scale conditions are rather persistent during times of cyclone clustering (Hauser et al., 2023), which could be useful not only for weather predictions but also for future projections.

4.9.2 Trends in Cyclone Characteristics in CESM2-LE

Finally, we investigate possible changes in cyclone characteristics in a warming climate, considering both non-clustered and clustered cyclones. For the North Atlantic, we find evidence that cyclones are decreasing in mslp, life time, radius, and depth during 2060-2100 compared to 1980-2020 (p-values ≤ 0.05, Tab. 4.4). Regularly occurring cyclones also travel longer distances in the future (p-value ≤ 0.05, Tab. 4.4). These trends are in line with a previous study where cyclones have been shown to be more intense in recent decades and traveling longer distances (Karwat et al., 2022). Next we focus on clustered cyclones in the North Atlantic, but specifically on "3 cyclones in 7 days" as this seems to be the most representative scenario compared to what is used by insurance companies to evaluate the socio-economic losses of clustered storms (Alert Air Worldwide, 2022c; Alert Air Worldwide, 2022b). We find that clustered cyclones in the North Atlantic are more intense than regularly occurring storms, have larger radii and travel longer distances during 2060-2100 compared to 1980-2020 (median, p-values ≤ 0.05, Tab. 4.5). When considering the most extreme clustered cyclones, the 5th percentile of mslp, we find that mslp is decreasing during 2060-2100 (p-values ≤ 0.05, Tab. 4.5). At the same

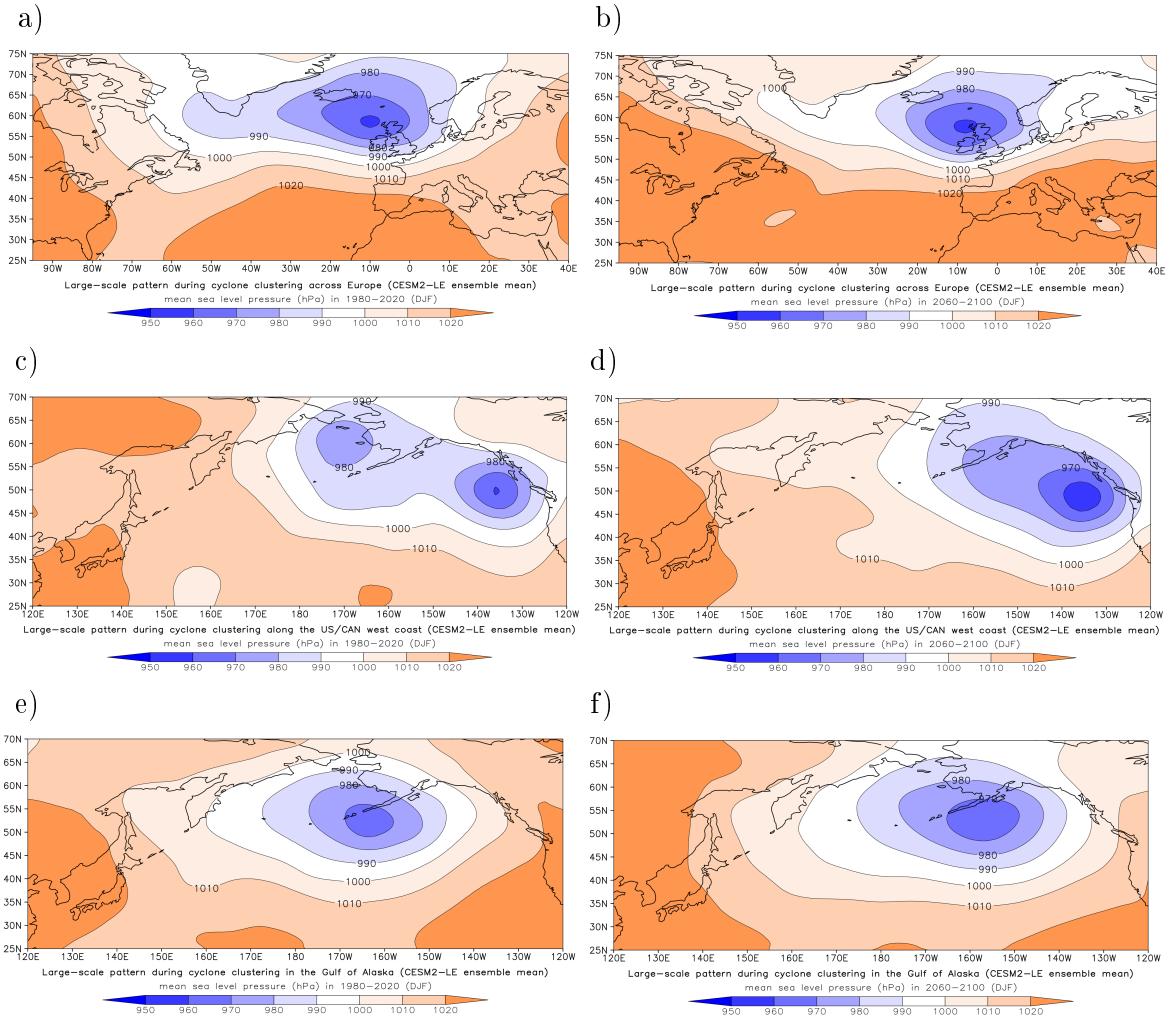

FIGURE 4.13: Ensemble mean of the large-scale patterns during historical clustering of cyclone triples within 7 days over a) Europe, c) along the west coast of Canada and the US, and e) in the Gulf of Alaska in 1980-2020; b), d), f) analogously but for 2060-2100. Here, only the strongest cyclones are considered, e.g., the 5th percentile of mslp of 3 cyclones within 7 days. We find similar patterns for other intensities of clustered cyclones using CESM2-LE (not shown).

TABLE 4.4: Trends in North Atlantic (NA) and North Pacific (NP) cyclone characteristics of non-clustered cyclones using the ensemble mean of CESM2-LE. We compare the cyclone characteristics of intensity (mslp), life time, radius, depth, and distance traveled during 2060-2100 to the reference period 1980-2020.

	1980-2020		**2060-2100**		**NA**	**NP**
	NA	**NP**	**NA**	**NP**	**p-value**	**p-value**
mslp [hPa]	990.5	990.5	989.8	990	$3.8{\cdot}10^{-11}$	$1.6{\cdot}10^{-7}$
life time [hours]	85.5	87.7	85.1	88.5	0.003	$3.5{\cdot}10^{-8}$
radius [km]	403.7	404	401.1	405.1	$8.5{\cdot}10^{-11}$	0.007
depth [m]	712.5	730.4	702	719	$1{\cdot}10^{-13}$	$2{\cdot}10^{-17}$
distance [km]	3330	3039	3440	3105	$5.6{\cdot}10^{-23}$	$9.3{\cdot}10^{-17}$

time the most extreme cyclone clusters have larger radii and depths in the future, while they also travel longer distances than during 1980-2020 (p-values ≤ 0.05, Tab. 4.5). As a result, trends in the 5th percentile of mslp are similar to the median. Thus, especially North Atlantic clustered cyclones of different intensities will intensify in the future. This implies increases in socio-economic losses for Europe.

Non-clustered North Pacific cyclones, like North Atlantic cyclones, are decreasing in mslp and depth, but are showing longer life times, radii and distances traveled during 2060-2100 compared to 1980-2020 (p-values ≤ 0.05, Tab. 4.4). This intensification can also be seen in clustered cyclones, which have larger radii during 2060-2100 in comparison with 1980-2020 (median, p-values ≤ 0.05, Tab. 4.5). The most extreme cyclones show similar trends in radius and depth, however, the trends are not statistically significant (Tab. 4.5). Hence, North Pacific clustered cyclones reveal the same trends as North Atlantic clustered cyclones, but are significant in only a few variables.

In conclusion, all Northern Hemispheric cyclones are intensifying, but especially clustered cyclones reveal larger radii and depths in future decades. While it is not clear what may cause the enhanced growth rates in clustered cyclones, there are several factors that could play a role. These include the fact that clustered cyclones might have lower static stability and higher moisture content available than non-clustered cyclones due to the previous storms. Therefore, they may develop better in a warmer and wetter climate. This might explain why certain cyclones are intensifying more rapidly than others under the SSP3-7.0 scenario.

TABLE 4.5: Trends in North Atlantic (NA) and North Pacific (NP) cyclone characteristics of clustered cyclones using the ensemble mean of CESM2-LE. We compare the cyclone characteristics of intensity (mslp), radius, depth, and distance traveled during 2060-2100 to the reference period 1980-2020. Here, the "3 cyclones in 7 days" scenario is considered for the median and the 5th percentile of mslp.

3 cyclones in 7 days: median						
	1980-2020		**2060-2100**		**NA**	**NP**
	NA	**NP**	**NA**	**NP**	**p-value**	**p-value**
mslp [hPa]	979	980	978	978	$4.6{\cdot}10^{-7}$	$6.8{\cdot}10^{-21}$
radius [km]	514	489	518	496	0.006	$2.07{\cdot}10^{-6}$
depth [m]	1065	983	1071	1003	0.2	$8.2{\cdot}10^{-6}$
distance [km]	5190	4373	5455	4369	$2.3{\cdot}10^{-15}$	0.9
3 cyclones in 7 days: 5th percentile						
mslp [hPa]	959	960	957	958	$1.6{\cdot}10^{-8}$	$1.9{\cdot}10^{-15}$
radius [km]	653	597	668	606	0.001	0.16
depth [m]	1497	1313	1542	1340	0.0007	0.2
distance [km]	5299	4150	5802	4100	$1.4{\cdot}10^{-6}$	0.61

4.10 Conclusions

Using the ERA5 and CESM2-LE data, we analyzed the representation of Northern Hemisphere extra-tropical cyclone characteristics and specifically of cyclone clustering under recent and future climate conditions for boreal winter. With this aim, we have considered two different metrics for clustering, a dispersion statistic and an absolute measure based on storm numbers. The main conclusions are as follows:

1. During 1980-2020, we find that clustered cyclones often form close to the Iberian Peninsula and over the British Isles. For the Northeast Pacific, most of the clustered cyclones occur in the Gulf of Alaska and along the US and Canadian west coast. Compared to ERA5, CESM2-LE provides an accurate estimate on the storm tracks and characteristics, but some uncertainties on the precise location of the identified cluster regions remain. The identified cluster regions are in line with the studies that have examined cyclone clustering in the Northern Hemisphere (e.g., Mailier et al. (2006), Blender et al. (2015), and Dacre and Pinto (2020)).

2. Using a relative metric (dispersion statistic), CESM2-LE is not able to capture any of the decadal variability as shown in ERA5 and thus cannot predict any trends. The dispersion statistic is also limited to only distinguish between regular and clustered cyclones, excluding different cyclone intensities. Using an absolute metric (clustering based on storm numbers) on the CESM2-LE, however, we find robust results across different percentiles and thus can identify significant trends in cyclone clusters with varying intensities: during 2060-2100, clustering increases by up to 25% on average for 3 and 4 cyclones within

7 days over Europe, but decreases by 24.3% along the west coast states of the US and Canada and by 10.1% in the Gulf of Alaska compared to 1980-2020.

3. In the SSP3-7.0 scenario, the large-scale patterns do not change under cyclone clustering in 2060-2100 in comparison with 1980-2020, which may be useful for predicting future cluster events. At the same time cyclones are intensifying by having lower mslp minima but especially clustered cyclones may develop even better in a warmer winter climate, since they have much larger radii and depths than non-clustered cyclones in the future. This highlights the need for new studies addressing the changes in the dynamics behind clustering.

Projected changes in the spatial distribution of the dispersion statistic could be related to a poleward shift of the storm tracks on zonal average (e.g., Bengtsson et al. (2006), Harvey et al. (2020), and Karwat et al. (2022)). It is likely that clustering is also affected by cyclone tracks shifting northward and therefore affecting the dispersion. Despite the CESM2-LE being less successful than ERA5 in reproducing the dispersion statistic, its signal on trends in clustering is overly confident and robust as shown by a strong ensemble agreement across different intensities of cyclone triples, quadruples and even higher numbers of cyclones in the future. Moreover, this direct approach appears to be more suitable when comparing socio-economic losses and quantifying future changes in cyclone clustering. Thus, the new insights presented here may facilitate a better probability on future cyclone clustering in different regions.

Our study has only considered the SSP3-7.0 scenario where higher greenhouse gas emissions lead to more clustering over Europe, and to less clustering and shifts in the dispersion statistic on part of the Pacific Northwest. Thus, the obtained probabilities may be different for other scenarios.

To conclude, our study provides evidence that cyclone clustering over the Northern Hemisphere may change in a warmer climate, with implications also for the associated hazards, primarily strong wind gusts, heavy rainfall, and storm surges. Studies that combine clustering of storms and impacts are strongly needed. It has already been shown that clustering of precipitation extremes alone increases under global warming (Franzke, 2022). Thus, an adequate quantification of clustering and its impacts in a warming climate is very important. Finally, the uncertainties can be reduced when utilizing large ensembles of data, like in the present study, which ideally would be CMIP6 type multi-model ensembles.

4.11 Acknowledgments

The simulations were conducted on the IBS/ICCP supercomputer "Aleph," 1.43 peta flops high-performance Cray XC50-LC Skylake computing system with 18,720 processor cores, 9.59 PB storage, and 43 PB tape archive space. We also acknowledge the support of KREONET.

AK, JGP and RB were supported by the Federal Ministry of Education and Research (BMBF) consortium ClimXtreme, projects B3.6 and A6 (01LP1902F, 01LP1901A). CF and SSL were supported by the Institute for Basic Science (IBS), Republic of Korea, under IBS-R028-D1 and CF by the National Research Fund of Korea (NRF-2022M3K3A1097082). JGP thanks the AXA Research Fund for support.

4.12 Data Availability Statement

The ERA5 reanalysis is openly available in the Climate Data Store of the ECMWF at https://cds.climate.copernicus.eu/cdsapp#!/search?type=dataset. The CESM2-LE ensemble members are available in the Climate Data Gateway at NCAR https://www.earthsystemgrid.org/dataset/ucar.cgd.cesm2le.atm.proc.6hourly_ave.PSL.html and at request at the IBS/ICCP in Busan, South Korea: https://ibsclimate.org/research/cesm2-large-ensemble-community-project/.

Chapter 5

Discussion and Conclusions

5.1 Overview of the Thesis

Extra-tropical cyclones are one of the largest disturbances of the atmospheric circulation in the Northern Hemisphere. These storms, whether they form alone or appear as clusters, represent a direct threat to both nature and human life in the mid-latitudes. In order to be able to quantify any storm changes in a warmer future winter climate, a deeper statistical understanding of the long-term behaviour of cyclone characteristics and of the storms' potential to cluster are required.

This thesis has investigated long-term trends of Northern Hemispheric winter cyclones and related impacts such as wind gusts and heavy precipitation in the extended ERA5 reanalysis during 1950-2021. Furthermore, clustered cyclone activity was assessed in historical ERA5 data and quantified for a warmer winter climate using large ensemble simulations from CESM2-LE, following the SSP3-7.0 scenario. The specific aims of this thesis were summarized by 6 research questions presented in Section 1.8 and answered throughout this study. These questions are:

RQ1: Are the different ERA5-BE and ERA5 data sets compatible to perform a long-term trend analysis on storms and impacts in the full period 1950-2021?

RQ2: To what limit does a Lagrangian-based analysis allow for a comprehensive assessment of cyclone characteristics, for example, frequency, size, and intensity in the extended ERA5 reanalysis?

RQ3: Are there significant trends in the Northern Hemisphere storm tracks that provide us with new data on the atmospheric circulation response to global warming?

RQ4: How is clustered cyclone activity in the Northern Hemisphere mid-latitudes characterized in the ERA5 reanalysis and CESM2-LE in 1980-2020?

RQ5: How is extra-tropical cyclone clustering projected to change by 2060-2100 compared to 1980-2020 based on two metrics?

RQ6: What are possible reasons in terms of large-scale dynamics and cyclone characteristics for these projected changes?

Section 5.2 is dedicated to addressing these questions based on the results presented in Chapters 3 and 4. In Section 5.3, the implications and limitations of the results are discussed, with the concluding remarks of this thesis presented in Section 5.4. Finally, suggestions for potential future work are outlined in Section 5.5.

5.2 Key Findings

In this section, the key findings of this thesis based on the results of Chapters 3 and 4 are discussed. Each of the 6 research questions posed in Section 1.8 are addressed individually.

5.2.1 RQ1

Are the different ERA5-BE and ERA5 data sets compatible to perform a long-term trend analysis on storms and impacts in the full period 1950-2021?

Using a systematic change-point analysis, we showed that the pre-satellite ERA5 data of the Backward Extension (covering 1950-1978) is highly compatible with the standard ERA5 (1979-2021) data set. The joint ERA5 data from 1950 to 2021 is consistent in all storm-related quantities, including the tracking measure (the 1000 hPa geopotential) and impact measures (e.g., 10m wind gust and total precipitation). However, when testing a different tracking measure such as relative vorticity at 850 hPa for change-points, we found very few change-points in the transition phase of 1978/79 in the North Atlantic. However, these change-points are found in only 1.41% of the bootstrap samples and are therefore outside the 95th percentile (not significant). Since our tracking does not depend on relative vorticity, the combined ERA5 data set is compatible to perform a long-term trend analysis on storms and impacts in the full period 1950-2021.

5.2.2 RQ2

To what limit does a Lagrangian-based analysis allow for a comprehensive assessment of cyclone characteristics, for example, frequency, size, and intensity in the extended ERA5 reanalysis?

The Lagrangian-based approach is the only perspective that allows for the tracking of cyclonic features, for example, storm speed and intensity, at any point in space and time. Using the extended ERA5 reanalysis, we were able to detect significant long-term trends of the cyclone characteristics such as the frequency, radius, and intensity in 1950-2021. Moreover, impacts like wind gusts and heavy precipitation could be directly linked to individual storms – in an Eulerian approach this would not be feasible. Thus, there is no limit to a Lagrangian-based analysis when assessing cyclone characteristics in long-term studies.

5.2.3 RQ3

Are there significant trends in the Northern Hemisphere storm tracks that provide us with new data on the atmospheric circulation response to global warming?

Overall, our findings suggest that extra-tropical cyclones have intensified in both Northern Hemispheric storm track regions from 1950 to 2021. We also find a significant decrease in cyclone speed in both study areas. Long-term trends derived from the extended ERA5 reanalysis show a significant northward (poleward) shift of the North Atlantic cyclone track from 1950 to the present. In addition, we were able to identify more recent significant increases in wind gusts (North Atlantic) and in cyclone-related precipitation (North Pacific) from 1979 to 2021. Our trend analysis also revealed that the number of North Pacific cyclones is significantly increasing; these storms show longer life cycles and travel longer distances, while they grow more slowly in 1950-2021. Thus, there are several significant trends in the Northern Hemisphere storm tracks emerging off the long-term study of cyclone characteristics in the extended ERA5 reanalysis.

5.2.4 RQ4

How is clustered cyclone activity in the Northern Hemisphere mid-latitudes characterized in the ERA5 reanalysis and CESM2-LE in 1980-2020?

We used a dispersion statistic to identify the preferred locations of clustered cyclones in the Northern Hemisphere mid-latitudes using the ERA5 reanalysis and CESM2-LE in 1980-2020. In Europe, clustered cyclones primarily form over or close to the British Isles and the Iberian Peninsula. Thus, clustered cyclones typically form in the eastern ocean basin of the North Atlantic. This tendency is also evident in clustered North Pacific cyclones, notably in the Gulf of Alaska and over the Aleutian Islands – hence in the North Pacific's eastern ocean basin. In addition, clustered cyclones are also identified along the west coasts of the US and Canada. Notwithstanding some uncertainty about the exact locations of the indicated cluster regions, CESM2-LE adequately replicates the storm tracks and characteristics when compared to ERA5.

5.2.5 RQ5

How is extra-tropical cyclone clustering projected to change by 2060-2100 compared to 1980-2020 based on two metrics?

We employed two metrics to assess possible changes in Northern Hemisphere cyclone clustering during 2060-2100 compared to 1980-2020: a relative metric (dispersion statistic) and an absolute metric (cyclone clustering based on storm numbers). This led to crucial differences in the projections. Using a dispersion statistic, CESM2-LE was unable to detect any variability in the dispersion over time in both

Northern Hemisphere storm tracks. This was initially evident when comparing the dispersion at different grid points of cyclogenesis and cluster regions under present climate conditions (1980-2020), as CESM2-LE could not reproduce the high variability that was seen in ERA5. Under future climate conditions, CESM2-LE also showed no changes in the overdispersion. In contrast to the relative metric, by defining different cyclone cluster types, such as 3-6 cyclones in 7 days with different intensities (5th, 10th, 15th, 20th percentiles and median), we found significant trends and some shifts in the preferred cyclone cluster regions. For Europe, clustering increases by up to 25% on average for cyclone triples and quadruples within 7 days during 2060-2100 compared to the reference period 1980-2020. In contrast, the Pacific Northwest appears to be less affected: cyclone clustering decreases on average by 24.3% along the west coast states of the US and Canada and by 10.1% in the Gulf of Alaska for the same periods. Overall, there is high ensemble confidence across different percentiles. Thus, CESM2-LE cannot represent the climate variability over time when depending on the dispersion statistic, but it is more successful when quantifying trends in absolute numbers of diverse cluster types as indicated by high agreement among the different ensemble members.

5.2.6 RQ6

What are possible reasons in terms of large-scale dynamics and cyclone characteristics for these projected changes?

In the SSP3-7.0 scenario, we found that the large-scale patterns are rather persistent under cyclone clustering with only minor changes to the impact regions reported for 2060-2100. Significant trends in future cyclone characteristics, on the other hand, might explain and account for the projected changes in cyclone clustering: Northern Hemisphere mid-latitude cyclones are generally intensifying by having lower mslp minima but especially clustered cyclones may develop even better in a warmer winter climate, since they have much larger radii and depths than non-clustered cyclones in the future.

5.3 Implications and Limitations of the Thesis

5.3.1 Implications

This thesis has investigated long-term trends of extra-tropical cyclones in the extended ERA5 reanalysis and cyclone clustering in a warmer future winter climate. The key findings discussed above have several implications.

First of all, we provided evidence that the joint ERA5 data of the Backward Extension (ERA5-BE; 1950-1978) and ERA5 (1979-2021) is consistent in all storm-related quantities and impact measures, and thus allows for a comprehensive statistical assessment of cyclone characteristics. Multiple significant trends were detected in both regions of the Northern Hemisphere storm tracks as shown in Chapter 3.

For example, North Atlantic cyclones intensify significantly in higher percentiles in 1950-2021. This implies possible changes for lysis regions where more socio-economic damage can be expected in the future. Storms also move more northward. This is in line with studies by, e.g., Bengtsson et al. (2006) and Harvey et al. (2014), but here we provide further information in terms of where such shifts are observed: in the mean and in the 40th/60th percentiles, but not in the extreme upper or lower percentiles. Numerous locations are affected, e.g., Northern England, Scotland, islands in Northern Germany and Southern Denmark, as well as cities along the Polish Baltic coast side.

In the North Pacific, we find a northward shift of the strongest North Pacific cyclones in the 95th percentile – approximately at the level of Anchorage, Alaska's biggest city. The increasing latitudinal shift of storms could be due to the accelerated land warming and Arctic sea ice loss. Cyclones may also move poleward as a result of the increase in anthropogenic greenhouse gas emissions (Studholme et al., 2022).

There are significant long-term trends concerning the traveled distance and the slower speed of Northern Hemisphere winter cyclones between 1950 and 2021. The significant trends in cyclone track lengths affect both storms of medium strength and those with higher intensity. This seems to be in accordance with the decrease in the cyclonic deepening and the longer life cycles, especially in the North Pacific. As the atmospheric circulation weakens due to global warming, a slower speed is expected. This is a noteworthy trend that is also seen in tropical cyclones, hurricanes, and typhoons (Kossin, 2018; Lai et al., 2020; Zhang et al., 2020).

As a result of the warming atmosphere, a potential change in the intensity and position of the Icelandic Low and the Azores High might explain such trends, since a reduced baroclinic instability might also determine how storms develop in the future. This is a critical knowledge gap that needs to be addressed in further research. Alterations in the cyclonic growth rates and development processes, e.g., latent heating, could be another potential explanation for the observed changes in cyclone characteristics (e.g., Besson et al. (2021) and Pinto et al. (2009)).

The increase in Northern Hemisphere storminess and more recent increases in heavy precipitation and wind gusts from winter storms indicate that storms have significantly intensified in the last decades. Previous research has not been able to quantify trends in storminess over longer time periods (Storch and Weisse, 2008; Feser et al., 2015). This further illustrates the importance of re-evaluating key variables. Moreover, in terms of impacts, it is crucial to comprehend the regional-to-local component in order to project future impact areas. Thus, our findings call for more efforts from policymakers to prepare socio-economies against intense cyclones in the most vulnerable environments.

Our study on clustered cyclones yielded important results about their significance and thus has implifications for different regions of the Northern Hemisphere storm tracks. Using the ERA5 and CESM2-LE data, we found that clustered cyclones in the Northern Hemisphere mainly form i) over the British Isles and near the Iberian Peninsula, ii) in the Gulf of Alaska and iii) along the west coast of the US and Canada during 1980-2020. While the main focus of previous studies has been on North Atlantic cluster regions, less light is shed onto cluster regions in the Northeast Pacific. Here, we have added to the current understanding by taking into account these underrepresented regions.

By 2060-2100, we found significant trends and some shifts in the preferred cyclone cluster regions compared to 1980-2020 and 1850-1890, respectively. The shifts in the spatial distribution of the dispersion could be related to a poleward shift of cyclones (e.g., Bengtsson et al. (2006), Harvey et al. (2020), and Karwat et al. (2022)). Since cyclone tracks migrate northward, which affects the dispersion, this is likely to have an impact on clustering. As cyclone clustering increases over Europe in 2060-2100, there will be more triples and quadruples within 7 days (up to 25%) on average in the future. This implies that clustering will occur more often over Europe, increasing the likelihood of socio-economic losses.

In contrast, the Pacific Northwest appears to be less affected by clustering in the future: the large ensemble showed that clustering decreases on average along the west coast of the US and Canada (up to 24.3%) and in the Gulf of Alaska (up to 10.1%) in 2060-2100 in comparison with 1980-2020. This has important implications for, i.e., coast cities at the west coast of the US, where less socio-economic damage from clustered cyclones is expected. The results presented in Chapter 4 show high ensemble agreement using the '3-6 cyclones in 7 days' metric. This demonstrates that using a large ensemble with 50 ensemble members is a feasible and alternative approach to individual climate models.

Under the SSP3-7.0 scenario, not only are Northern Hemisphere winter storms intensifying, but only clustered cyclones have larger radii and depths by 2060-2100. This highlights the need for new studies addressing the changes in the dynamics behind clustering in different future scenarios.

Large-scale drivers, such as the NAO, PNA or other sea-surface temperature anomalies from different teleconnection indices, may also modify the direction and intensity of the storm tracks. This has implifications for the occurrence and frequency of clustered cyclones. Here, we have shown that the large-scale patterns caused by cyclone clustering do not change much by 2060-2100. This may be useful for predicting future cluster events.

Finally, we have seen that the climate signal between 2060-2100 and historical winter climates implies some (amplified) alterations in the clustering of cyclones due to anthropogenic warming. This emphasizes that the quantification of clustering will become more important in the decades to come.

5.3.2 Limitations

There are several limitations to the analysis and results presented in this study. Studying the long-term behaviour of cyclonic features is often limited by short data sets, making trend quantification difficult. As a result, any trends must adhere to a certain confidence level in order to demonstrate that the results are significant. Here, we have shown that it is indeed possible to detect significant trends in cyclones, however, some of these trends are rather small (see Chapter 3). This is not unexpected: cyclones might undergo changes only slowly and over an even longer period. Thus, detecting trends might be limited by uncertainty in the historical data and by natural bias. Since our study is the first to analyze long-term trends of cyclone characteristics in the extended ERA5 reanalysis, any of these uncertainties cannot be compared to other studies.

Quantifying clustered cyclones in warmer future winter climates also presents a challenge: while the dynamics behind cyclone clustering are somewhat well known, especially for the North Atlantic, there is a substantial gap in the statistical assessment of cyclone clusters. Firstly, there are some differences in the dispersion statistic of clustered cyclones between ERA5 and CESM2-LE during 1980-2020 (see Chapter 4). The key characteristics of clustered North Atlantic cyclones in the current climate are well reproduced by the large ensemble, although the overdispersion in ERA5 is more dipole in north-south direction, but more zonal and west-east oriented in CESM2-LE. However, both data sets agree on the main locations of clustered cyclones (e.g., British Isles and close to the Iberian Peninsula). Clustering in the Northeast Pacific, on the other hand, slightly differs from the results we have seen in ERA5. In ERA5, the main area of clustered cyclones is located along the west coast, whereas the origin of the cyclone clusters is shifted more toward the central Northeast Pacific in CESM2-LE. Furthermore, CESM2-LE was less certain on the dispersion statistic, in particular, it was unable to represent the climate variability of the dispersion over time that was observed in ERA5. In addition the dispersion statistic is also limited to only distinguish between regular and clustered cyclones, excluding different cyclone intensities.

This study has only considered the SSP3-7.0 scenario where higher greenhouse gas emissions lead to more clustering over Europe, and to less clustering and shifts in the dispersion statistic in the Pacific Northwest. As a result, the obtained probabilities may be different for other scenarios.

5.4 Key Conclusions

Overall, this thesis has provided a thorough statistical assessment of Northern Hemisphere extra-tropical cyclone characteristics and related impacts in the extended ERA5 reanalysis, as well as of clustered cyclones, using data from ERA5 and the CESM2 large ensemble in historical and future winter climates. From the results presented in this thesis, several key conclusions have been found.

- Long-term trends in cyclones show that storms have significantly intensified, travel longer distances, and show longer life cycles, while there have also been more recent increases in storm-related precipitation and wind gusts of more extreme storms. Both storm tracks and lysis regions are affected. This new knowledge calls for stronger efforts from policymakers and stakeholders to adapt socio-economies to future damage.

- Our findings emphasize the importance of quantifying changes in clustered cyclones due to their potential to cause large destruction of both human-made structures and natural environments. Here, we have shown that cyclone clustering is a complex phenomenon whose quantification depends on the metric. From the relative metric (dispersion statistic), it transpires that CESM2-LE was unable to capture any variability, while an absolute metric, such as using one of the respective '3-6 cyclones within 7 days' scenarios, produced robust results.

- Significant trends in future cyclone clustering were identified: over Europe we found increases in 3 and 4 cyclones within 7 days (up to 25% on average) in 2060-2100 in comparison with 1980-2020. In contrast, clustering decreases on average along the west coast of the US and Canada (up to 24.3%) and in the Gulf of Alaska (up to 10.1%) for the same periods. An overall high ensemble agreement across different percentiles showed that large ensemble simulations are an important alternative to individual climate models, since they can reduce uncertainties in future projections. By defining categories of different cyclone intensities, it was further demonstrated that this is a feasible method to capture the variability of each of these clusters and to provide robust estimates on future cyclone clustering.

In conclusion, this thesis has shown that Northern Hemisphere extra-tropical cyclones are multi-dimensional natural hazards with many different characteristics. Therefore, statistical quantification is important in order to predict future impacts on nature and human socio-economics. Finally, additional warming should be avoided regardless of the scenario to minimize all socio-economic impacts, as it has been demonstrated by devastating storm events in the past and those that may occur in the future.

5.5 Potential Future Work

The work completed in this thesis has opened up a number of interesting new directions for further research. These directions are presented below.

- A recent study reported that the Southern Hemisphere is even stormier than the Northern Hemisphere due to topography and ocean circulation (Shaw et al., 2022). Thus, an in-depth analysis of extra-tropical cyclone characteristics in the Southern Hemisphere would be of interest. For example, insights into the long-term behaviour of storms over Southern America, Southern Africa, Southern Australia and New Zealand might extend our knowledge on extra-tropical cyclones in different hemispheres (Jones and Simmonds, 1993; Mendes et al., 2010; Marrafon et al., 2021; Pepler and Dowdy, 2022).

- With more than 83 years of data, the most recent expansion of the ERA5 reanalysis back to 1940 might present an excellent opportunity to extend this study by examining historical storm events during the decade of war.

- This study has taken advantage of using large ensemble simulations with fine resolution from CESM2-LE. However, a caveat of the results presented in Chapter 4 is that these results depend on the SSP3-7.0 scenario. This is because there is a substantial lack of different CMIP6 ensemble simulations and climate models that are available for a consistently longer time frame – and temporally or spatially high enough to perform cyclone tracking. Thus, expanding this cluster analysis by including more future scenarios might be beneficial as new model simulations become available in finer resolution.

- In relation to the previous suggestion, high-resolution data of impact measures, like wind gusts and total precipitation, are in dire need to conduct compound analyses of individual or clustered cyclones in future climate simulations. This would be most helpful for the prediction and preparation against severe cyclone occurrences and their impacts on different environments.

- As it is hypothesized that the intensity of storms may increase due to higher amounts of atmospheric moisture content available in a warmer world (Booth et al., 2013; Priestley and Catto, 2022), it is crucial to comprehend the mechanisms underlying changes in extra-tropical cyclones. It is still not clear how global warming quantitatively affects the moist energy budget of storms. In particular, the dynamic response to extreme storm events is rather uncertain. Machine learning methods might help in answering these questions.

- Extra-tropical cyclone development can be influenced by latent and sensible heat fluxes from the sea surface temperature (SST) (Bui and Spengler, 2021). Air-sea interactions, for example, were determined to be a significant factor in the unusual 2013/14 winter season SST cooling anomaly (Dacre et al., 2020). As the mechanisms by which cyclones contribute to seasonal SST anomalies have not yet been thoroughly understood, more research into quantifying the coupled atmosphere-ocean feedback is highly encouraged.

- Further research that may be able to explain the increase in clustering over Europe and the decrease in clustering in the Northeast Pacific is in dire need. The regional differences in future clustered cyclones highlighted by this study emphasize, for instance, the possibility that atmospheric teleconnections might play a more significant role than previously assumed (McDonald, 2011; Guo et al., 2017; Walz et al., 2018).

- Given its complexity and limitations, identifying the dynamics of cyclone clustering in the Gulf of Alaska, for example, might be of interest and contribute to our understanding of extra-tropical cyclones in the Pacific Northwest.

- In a recent study, a strong connection between the magnitude of mid-latitude storminess and cloud-albedo was detected (Hadas et al., 2023). This implies, e.g., less cyclones when the cloud albedo is lower. It is still unclear how future baroclinic activity affects storminess and the projected storm changes.

- During particularly stormy winters, flooding and coastal erosion can occur, which may even be exacerbated under a higher SSP scenario. A final avenue for further research would thus be to assess whether there is a preceding pattern behind severe storms that would allow for a better estimation of socio-economic damage in future warmer winter climates.

Appendix A

Supplementary Material for Chapter 3

A.1 Long-Term Trends of Northern Hemispheric Winter Cyclones in the Extended ERA5 Reanalysis

A.1.1 Time series histograms

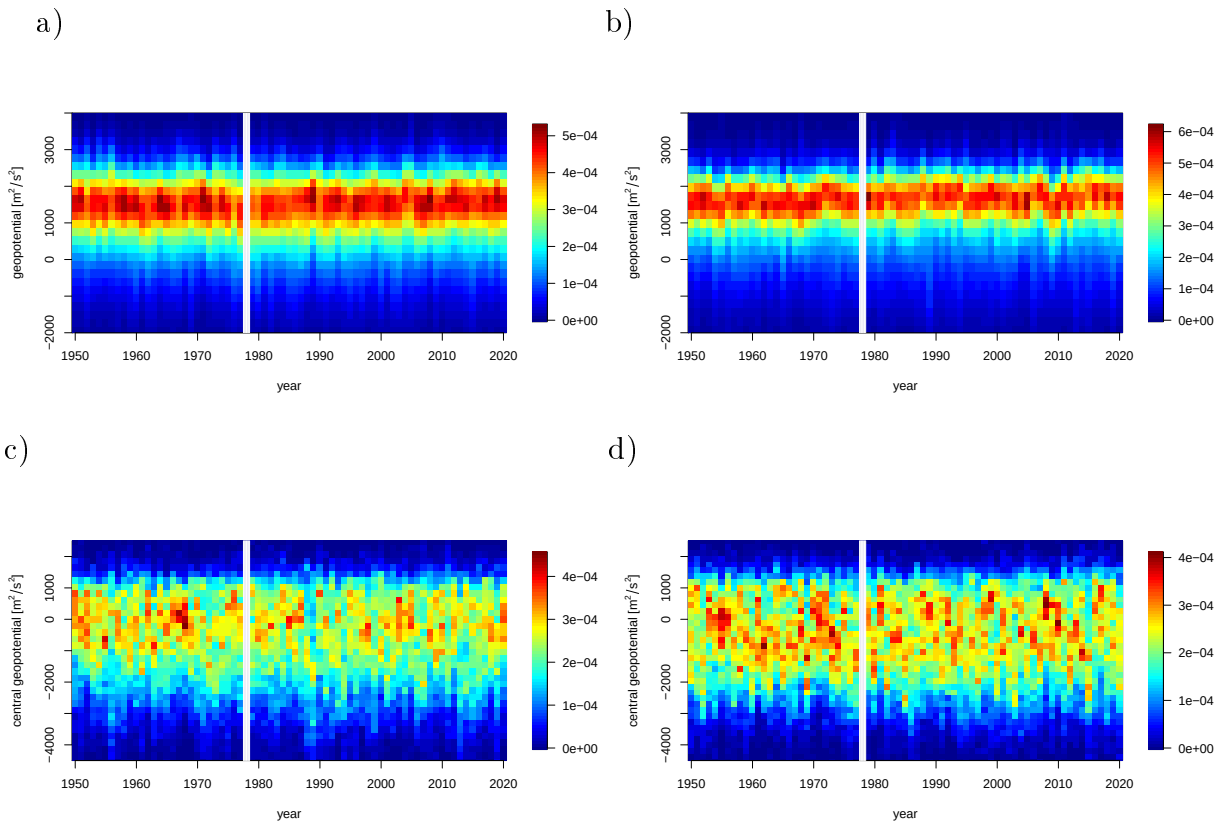

FIGURE A.1: Time series histograms of the geopotential from the extended ERA5 data of the a) North Atlantic and b) North Pacific and time series histograms of the central geopotential from the c) North Atlantic and d) North Pacific cyclone tracks in 1950-2021. The white vertical lines represent the transition between the ERA5-BE and ERA5 data.

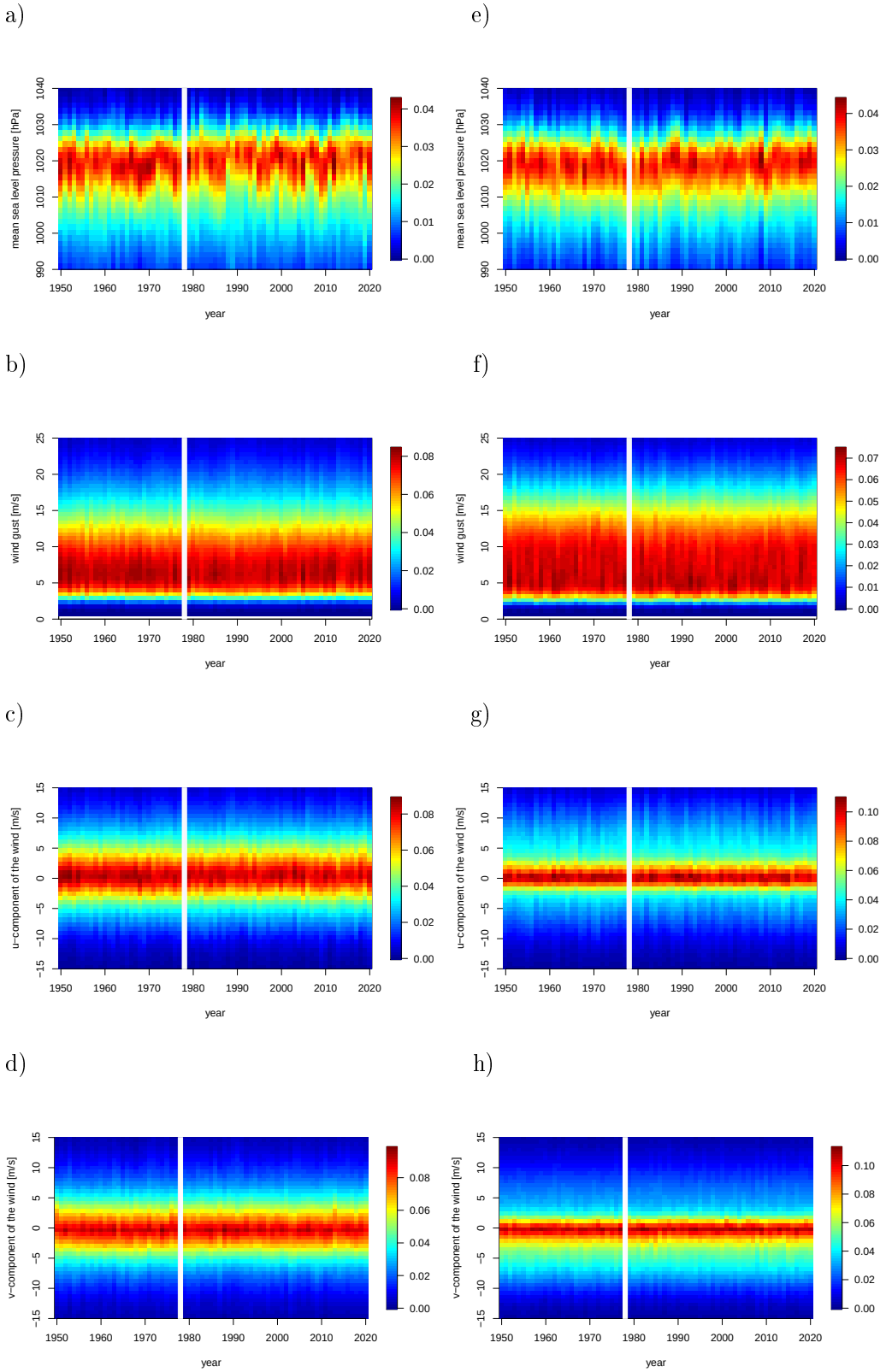

FIGURE A.2: Time series histograms of mean sea level pressure, wind gust, u-component of the wind and v-component of the wind for the North Atlantic (left row, a-d) and North Pacific (right row, e-h) in 1950-2021. The white vertical lines represent the transition between the ERA5-BE and ERA5 data.

A.1.2 Cyclone frequency in the Northern Hemisphere in 1950-2021

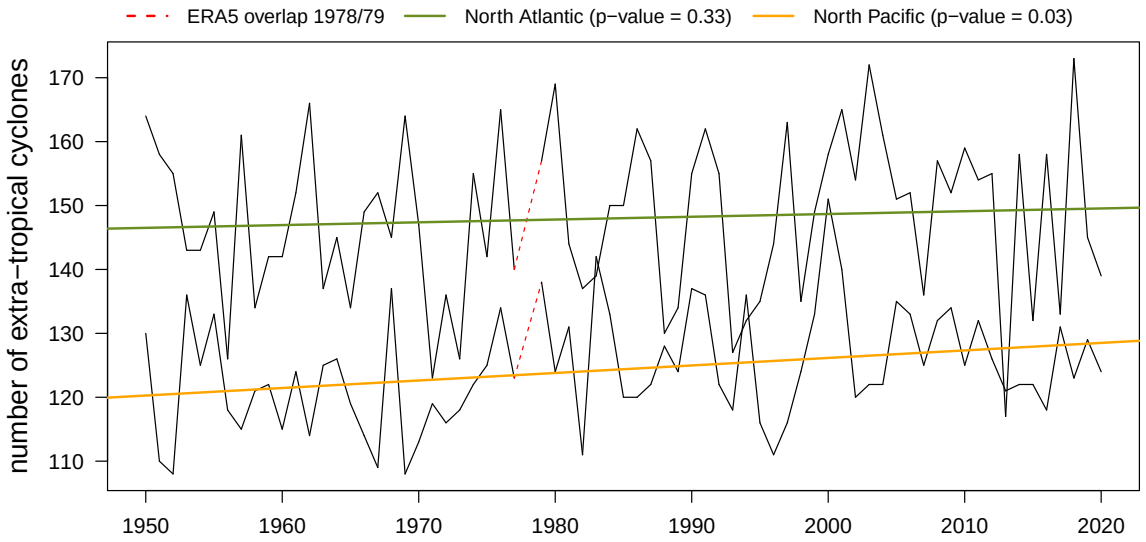

FIGURE A.3: Number of extra-tropical cyclones in the extended ERA5 data set.

A.1.3 Additional significant trend in the North Atlantic in 1950-2021

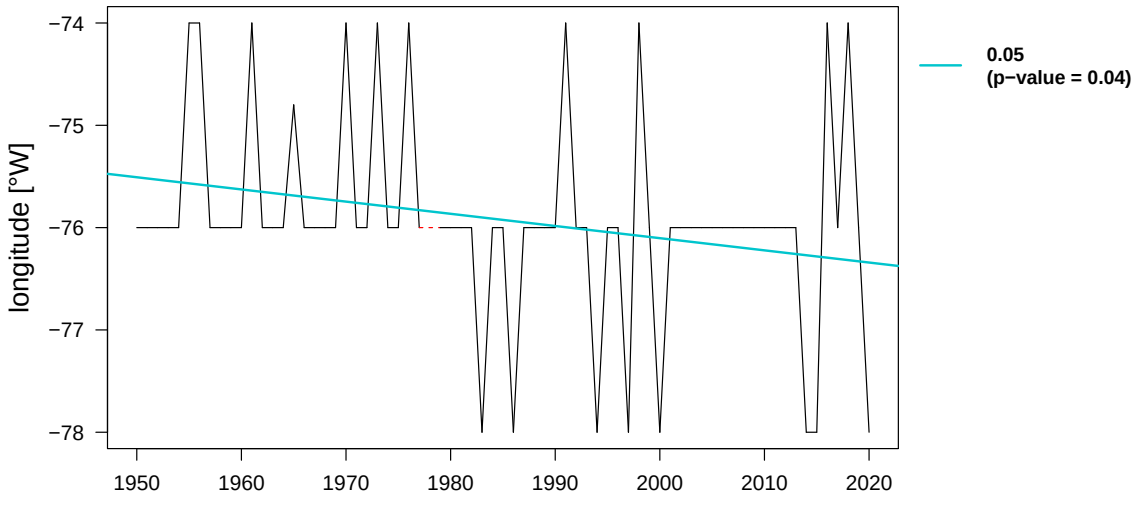

FIGURE A.4: Quantile regression of the 5th percentile of the longitude in the North Atlantic in 1950-2021. The red dashed line shows the transition phase of 1978/79 to 1979/80.

A.1.4 Additional significant trends in the North Pacific in 1950-2021

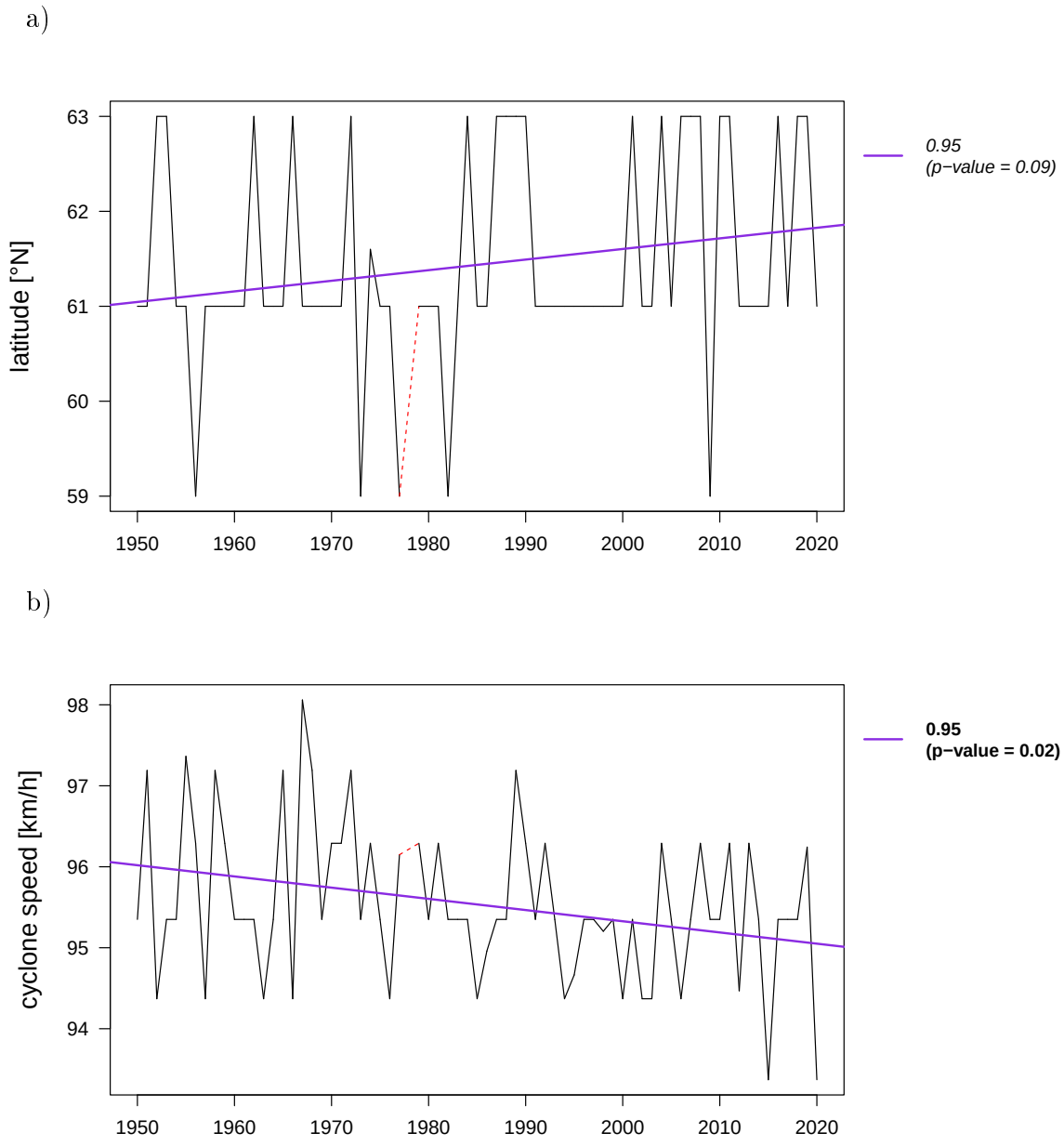

FIGURE A.5: Quantile regression of the 95th percentile of the a) latitude and b) cyclone speed in 1950-2021. The red dashed line shows the transition phase of 1978/79 to 1979/80. p-values ≤ 0.05 are marked in bold and p-values ≤ 0.1 are in italic.

Appendix B

Supplementary Material for Chapter 4

B.1 Northern Hemisphere Extra-Tropical Cyclone Clustering in ERA5 Reanalysis and the CESM2 Large Ensemble

First, we describe cyclone clustering by a dispersion index (deviation of a Poisson process), which is defined by Mailier et al. (2006) as

$$\psi = \text{Fano factor} - 1 = (\sigma^2/\mu) - 1. \tag{B.1}$$

where σ^2 and μ are the variance and mean of the number of cyclone occurrences at each grid point, respectively. Second, we define cyclone clustering using an absolute measure based on storm counts within 7 days (following e.g., Pinto et al. (2014)). To assess the effect of clustered cyclones it is necessary to consider higher numbers of cyclones, e.g. 3-6 storms in 7 days, since the weekly cyclone occurrences are already high in CESM2-LE (see Tab. B.1).

TABLE B.1: Number of weekly cyclone occurrences and standard deviation in the three study regions using CESM2-LE for the different time slices 1850-1890, 1980-2020, and 2060-2100.

	1850-1890	**1980-2020**	**2060-2100**
Europe	2.87 ± 0.22	2.8 ± 0.21	2.85 ± 0.18
US/CAN west coast	3.6 ± 0.22	3.7 ± 0.19	3.6 ± 0.15
Gulf of Alaska	6.3 ± 0.3	6.2 ± 0.32	6.1 ± 0.19

B.1.1 Differences in mslp between ERA5 and CESM2-LE during 1980-2020

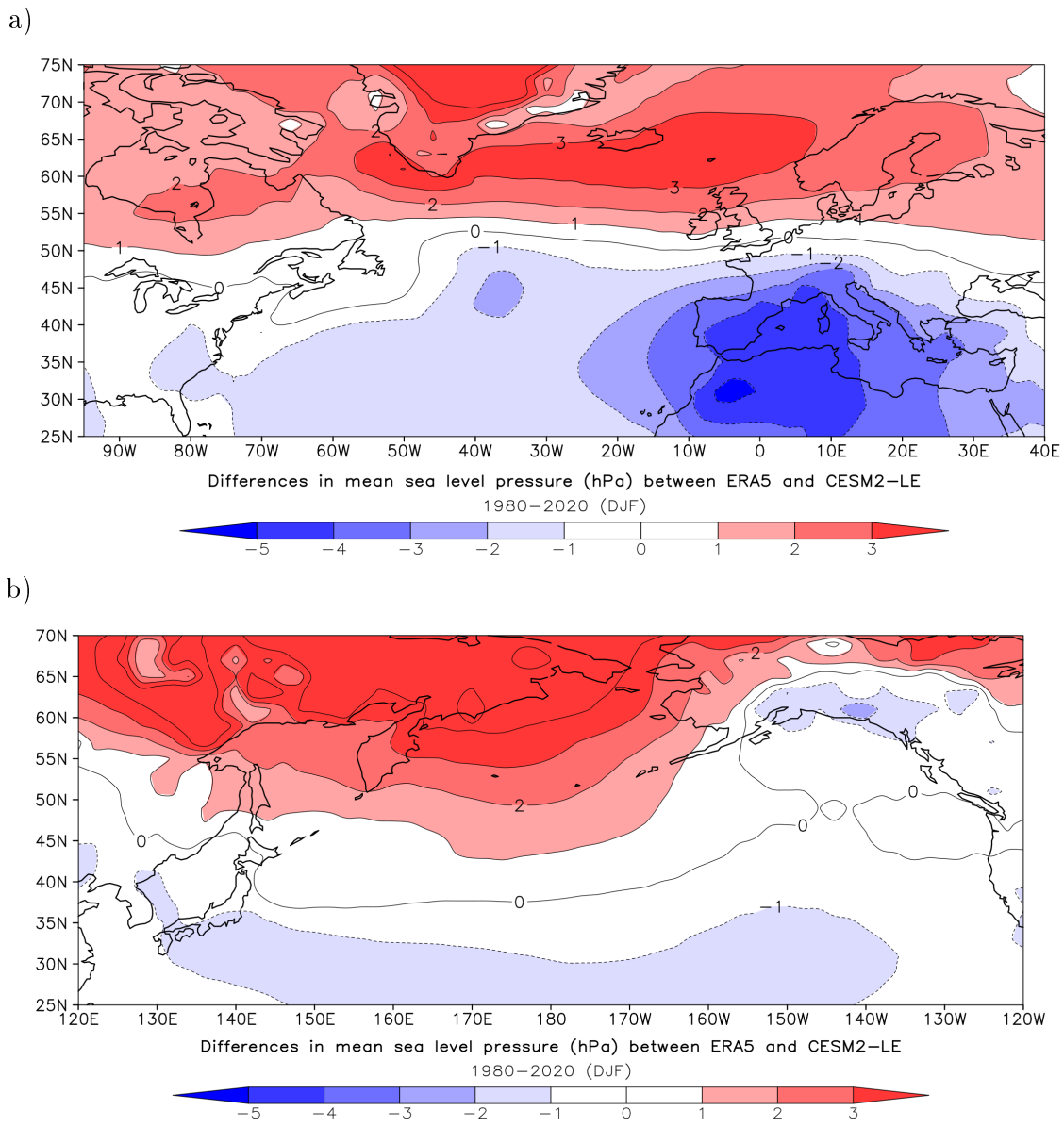

FIGURE B.1: Differences in mean sea level pressure between ERA5 and CESM2-LE in the a) North Atlantic and b) North Pacific storm track regions during 1980-2020.

List of Candidate's Publications

A summary of all the candidate's papers pre-published or in review

[1] **Karwat, A.** and C. L. E. Franzke (2021), "Future Projections of Heat Mortality Risk for Major European Cities", *Weather Clim. Soc.*, vol. 13, no. 4, pp. 913–931, https://doi.org/10.1175/WCAS-D-20-0142.1

[2] **Karwat, A.**, C. L. E. Franzke, and R. Blender (2022), "Long-Term Trends of Northern Hemispheric Winter Cyclones in the Extended ERA5 Reanalysis", *J. Geophys. Res. Atmos.*, vol. 127, no. 22, e2022JD036952, https://doi.org/10.1029/2022JD036952

[3] Caldas-Alvarez, A., M. Augenstein, G. Ayzel, K. Barfus, R. Cherian, L. Dillenardt, F. Fauer, H. Feldmann, M. Heistermann, **A. Karwat**, F. Kaspar, H. Kreibich, E. E. Lucio-Eceiza, E. P. Meredith, S. Mohr, D. Niermann, S. Pfahl, F. Ruff, H. W. Rust, L. Schoppa, T. Schwitalla, S. Steidl, A. H. Thieken, J. S. Tradowsky, V. Wulfmeyer, and J. Quaas (2022), "Meteorological, impact and climate perspectives of the 29 June 2017 heavy precipitation event in the Berlin metropolitan area", *Nat. Hazards Earth Syst. Sci.*, vol. 22, no. 11, pp. 3701–3724, https://doi.org/10.5194/nhess-22-3701-2022

[4] Gliksman, D., P. Averbeck, N. Becker, B. Gardiner, V. Goldberg, J. Grieger, D. Handorf, K. Haustein, **A. Karwat**, F. Knutzen, H. S. Lentink, R. Lorenz, D. Niermann, J. G. Pinto, R. Queck, A. Ziemann, and C. L. E. Franzke (2022), "Review Article: Wind and storm damage: From Meteorology to Impacts", *Nat. Hazards Earth Syst. Sci.*, https://doi.org/10.5194/nhess-2022-159, *in review*.

[5] Flaounas, E., L. Aragão, L. Bernini, S. Dafis, B. Doiteau, H. L. Flocas, S. Gray, **A. Karwat**, J. Kouroutzoglou, P. Lionello, F. Pantillon, C. Pasquero, P. Patlakas, M. A. Picornell, F. Porcù, M. D. K. Priestley, M. Reale, M. Roberts, H. Saaroni, D. Sandler, E. Scoccimarro, M. Sprenger, and B. Ziv (2023), "A composite approach to produce reference datasets for extratropical cyclone tracks: Application to Mediterranean cyclones", *Weather Clim. Dyn.*, https://doi.org/10.5194/wcd-2022-63, *in review*.

[6] **Karwat, A.**, C. L. E. Franzke, J. G. Pinto, S.-S. Lee, and R. Blender (2023), "Northern Hemisphere Extra-Tropical Cyclone Clustering in ERA5 Reanalysis and the CESM2 Large Ensemble", *submitted*.

Bibliography

Alert Air Worldwide (2009), *Looking Back, Looking Forward: Anatol, Lothar and Martin Ten Years Later*, https://www.air-worldwide.com/publications/air-currents/looking-back-looking-forward-anatol-lothar-and-martin-ten-years-later/.

— (2020), *Winter Storm Ciara Sabine 2020*, https://alert.air-worldwide.com/extratropical-cyclone/2020/winter-storm-ciara-sabine-2020/first-posting/.

— (2022a), *Europe Hit by a Storm Triplet within Six Days*, https://www.air-worldwide.com/blog/posts/2022/02/europe-storm-triplet-in-six-days/.

— (2022b), *Modeling Fundamentals: Accounting for the Hours Clause*, https://www.air-worldwide.com/publications/air-currents/2019/Modeling-Fundamentals--Accounting-for-the-Hours-Clause/.

— (2022c), *Storms Dudley and Eunice - Post-Event Analysis | Summary*, https://alert.air-worldwide.com/extratropical-cyclone/2022/storms-dudley-and-eunice/post-event-analysis/.

Alexandersson, H., T. Schmith, K. Iden, and H. Tuomenvirta (1998), "Long-term trend variations of the storm climate over NW Europe", *The Global Atmos. Oc. System*, vol. 6, no. 1, pp. 97–120.

— (2000), "Trends of storms in NW Europe derived from an updated pressure data set", *Clim. Res.*, vol. 14, no. 1, pp. 71–73, doi: https://doi.org/10.3354/cr014071.

Bancroft, G. (2016), "Marine Weather Summary, North Pacific and North Atlantic Areas", *Mariners Weather Log*, vol. 60, no. 3.

Befort, D. J., S. Wild, T. Kruschke, U. Ulbrich, and G. C. Leckebusch (2016), "Different long-term trends of extra-tropical cyclones and windstorms in ERA-20C and NOAA-20CR reanalyses", *Q. J. R. Meteorol. Soc.*, vol. 17, no. 11, pp. 586–595, doi: https://doi.org/10.1002/asl.694.

Bell, B., H. Hersbach, A. Simmons, P. Berrisford, P. Dahlgren, A. Horányi, J. Muñoz-Sabater, J. Nicolas, R. Radu, D. Schepers, C. Soci, S. Villaume, J.-R. Bidlot, L. Haimberger, J. Woollen, C. Buontempo, and J.-N. Thépaut (2021), "The ERA5 Global Reanalysis: Preliminary Extension to 1950", *Q. J. R. Meteorol. Soc.*, vol. 147, no. 741, pp. 4186–4227, doi: https://doi.org/10.1002/qj.4174.

Bengtsson, L., K. I. Hodges, and E. Roeckner (2006), "Storm tracks and climate change", *J. Clim.*, vol. 19, no. 15, pp. 3518–3543, doi: https://doi.org/10.1175/jcli3815.1.

Besson, P., L. J. Fischer, S. Schemm, and M. Sprenger (2021), "A global analysis of the dry-dynamic forcing during cyclone growth and propagation", *Weather Clim. Dyn.*, vol. 2, no. 4, pp. 991–1009, doi: https://doi.org/10.5194/wcd-2-991-2021.

Bjerknes, J. (1922), "Life cycle of cyclones and the polar front theory of atmospheric circulation", *Geophys. Publik.*, vol. 3, no. 1, pp. 1–18, doi: https://doi.org/10.1175/1520-0493(1922)50<468:jbahso>2.0.co;2.

Blackmon, M. L. (1976), "A climatological spectral study of the 500 mb geopotential height of the Northern Hemisphere", *J. Atmos. Sci.*, vol. 33, no. 8, pp. 1607–1623, doi: https://doi.org/10.1175/1520-0469(1976)033<1607:acssot>2.0.co;2.

Blender, R., K. Fraedrich, and F. Lunkeit (1997), "Identification of cyclone-track regimes in the North Atlantic", *Q. J. R. Meteorol. Soc.*, vol. 123, no. 539, pp. 727–741, doi: https://doi.org/10.1002/qj.49712353910.

Blender, R., C. C. Raible, and F. Lunkeit (2015), "Non-exponential return time distributions for vorticity extremes explained by fractional Poisson processes", *Q. J. R. Meteorol. Soc.*, vol. 141, no. 686, pp. 249–257, doi: https://doi.org/10.1002/qj.2354.

Blender, R. and M. Schubert (2000), "Cyclone tracking in different spatial and temporal resolutions", *Mon. Weather Rev.*, vol. 128, no. 2, pp. 377–384, doi: https://doi.org/10.1175/1520-0493(2000)128<0377:ctidsa>2.0.co;2.

Bollmeyer, C., J. D. Keller, C. Ohlwein, S. Wahl, S. Crewell, P. Friederichs, A. Hense, J. Keune, S. Kneifel, I. Pscheidt, et al. (2015), "Towards a high-resolution regional reanalysis for the European CORDEX domain", *Q. J. R. Meteorol. Soc.*, vol. 141, no. 686, pp. 1–15, doi: https://doi.org/10.1002/qj.2486.

Booth, J. F., S. Wang, and L. Polvani (2013), "Midlatitude storms in a moister world: Lessons from idealized baroclinic life cycle experiments", *Clim. Dyn.*, vol. 41, no. 1, pp. 787–802, doi: https://doi.org/10.1007/s00382-012-1472-3.

Bui, H. and T. Spengler (2021), "On the influence of sea surface temperature distributions on the development of extratropical cyclones", *J. Atmos. Sci.*, vol. 78, no. 4, pp. 1173–1188, doi: https://doi.org/10.1175/jas-d-20-0137.1.

Caldas-Alvarez, A., M. Augenstein, G. Ayzel, K. Barfus, R. Cherian, L. Dillenardt, F. Fauer, H. Feldmann, M. Heistermann, A. Karwat, et al. (2022), "Meteorological, impact and climate perspectives of the 29 June 2017 heavy precipitation event in the Berlin metropolitan area", *Nat. Hazards Earth Syst. Sci.*, vol. 22, no. 11, 3701–3724, doi: https://doi.org/10.5194/nhess-22-3701-2022.

Catto, J. L., D. Ackerley, J. F. Booth, A. J. Champion, B. A. Colle, S. Pfahl, J. G. Pinto, J. F. Quinting, and C. Seiler (2019), "The future of midlatitude cyclones", *Curr. Clim. Change Rep.*, vol. 5, no. 1, pp. 407–420, doi: https://doi.org/10.1007/s40641-019-00149-4.

Chatterjee, S. and A. S. Hadi (2000), "Regression Analysis by Example", *New York: Wiley*.

Ciasto, L. M., C. Li, J. J. Wettstein, and N. Gunnar Kvamstø (2016), "North Atlantic Storm-Track Sensitivity to Projected Sea Surface Temperature: Local versus Remote Influences", *J. Clim.*, vol. 29, no. 9, pp. 6973–6991, doi: https://doi.org/10.1175/jcli-d-15-0860.1.

Climate Signals (2021), *Climate Signals, Atmospheric Moisture Increase*, https://www.climatesignals.org/climate-signals/atmospheric-moisture-increase.

Cohen, J., J. A. Screen, J. C. Furtado, M. Barlow, D. Whittleston, D. Coumou, J. Francis, K. Dethloff, D. Entekhabi, J. Overland, et al. (2014), "Recent Arctic amplification and extreme mid-latitude weather", *Nat. Geosci.*, vol. 7, no. 9, pp. 627–637, doi: https://doi.org/10.1038/ngeo2234.

Coles, S. et al. (2001), "An Introduction to Statistical Modeling of Extreme Values", *Springer-Verlag London*, vol. 1, doi: https://doi.org/10.1007/978-1-4471-3675-0.

Cox, D. R. and V. Isham (1980), *Point processes*, vol. 12, CRC Press.

Cusack, S. (2016), "The observed clustering of damaging extratropical cyclones in Europe", *Nat. Hazards Earth Syst. Sci.*, vol. 16, no. 4, pp. 901–913, doi: https://doi.org/10.5194/nhess-16-901-2016.

Dacre, H. F. (2020), "A review of extratropical cyclones: Observations and conceptual models over the past 100 years", *Weather*, vol. 75, no. 1, pp. 4–7, doi: https://doi.org/10.1002/wea.3653.

Dacre, H. F., S. A. Josey, and A. L. M. Grant (2020), "Extratropical-cyclone-induced sea surface temperature anomalies in the 2013–2014 winter", *Weather Clim. Dyn.*, vol. 1, no. 1, pp. 27–44, doi: https://doi.org/10.5194/wcd-1-27-2020.

Dacre, H. F. and J. G. Pinto (2020), "Serial clustering of extratropical cyclones: A review of where, when and why it occurs", *NPJ Clim. Atmos. Sci.*, vol. 3, no. 1, pp. 1–10, doi: https://doi.org/10.1038/s41612-020-00152-9.

Danabasoglu, G., J.-F. Lamarque, J. Bacmeister, D. A. Bailey, A. K. DuVivier, J. Edwards, L. K. Emmons, J. Fasullo, R. Garcia, A. Gettelman, C. Hannay, M. M. Holland, W. G. Large, P. H. Lauritzen, D. M. Lawrence, J. T. M. Lenaerts, K. Lindsay, W. H. Lipscomb, M. J. Mills, R. Neale, K. W. Oleson, B. Otto-Bliesner, A. S. Phillips, W. Sacks, S. Tilmes, L. van Kampenhout, M. Vertenstein, A. Bertini, J. Dennis, C. Deser, C. Fischer, B. Fox-Kemper, J. E. Kay, D. Kinnison, P. J. Kushner, V. E. Larson, M. C. Long, S. Mickelson, J. K. Moore, E. Nienhouse, L. Polvani, P. J. Rasch, and W. G. Strand (2020), "The Community Earth System Model Version 2 (CESM2)", *J. Adv. Model. Earth Syst.*, vol. 12, no. 2, e2019MS001916, doi: https://doi.org/10.1029/2019ms001916.

Daniels, E. E., G. Lenderink, R. W. A. Hutjes, and A. A. M. Holtslag (2014), "Spatial precipitation patterns and trends in The Netherlands during 1951–2009", *Int. J. Climatol.*, vol. 34, no. 6, pp. 1773–1784, doi: https://doi.org/10.1002/joc.3800.

Della-Marta, P. M. and J. G. Pinto (2009), "Statistical uncertainty of changes in winter storms over the North Atlantic and Europe in an ensemble of transient climate simulations", *Geophys. Res. Lett.*, vol. 36, no. 14, p. L14703, doi: https://doi.org/10.1029/2009gl038557.

Derrick, B., D. Toher, and P. White (2016), "Why Welch's test is Type I error robust", *Quant. Meth. Psych.*, vol. 12, no. 1, doi: https://doi.org/10.20982/tqmp.12.1.p030.

Donat, M. G., T. Pardowitz, G. C. Leckebusch, U. Ulbrich, and O. Burghoff (2011), "High-resolution refinement of a storm loss model and estimation of return periods of loss-intensive storms over Germany", *Nat. Hazards Earth Syst. Sci.*, vol. 11, no. 10, pp. 2821–2833, doi: https://doi.org/10.5194/nhess-11-2821-2011.

Donner, R. V., R. Ehrcke, S. M. Barbosa, J. Wagner, J. F. Donges, and J. Kurths (2012), "Spatial patterns of linear and nonparametric long-term trends in Baltic sea-level variability", *Nonlinear Process. Geophys.*, vol. 19, no. 1, pp. 95–111, doi: https://doi.org/10.5194/npg-19-95-2012.

Dullaart, J. C. M., S. Muis, N. Bloemendaal, and J. C. J. H. Aerts (2019), "Advancing global storm surge modelling using the new ERA5 climate reanalysis", *Clim. Dyn.*, vol. 54, no. 1, pp. 1007–1021, doi: https://doi.org/10.1007/s00382-019-05044-0.

Economou, T., D. B. Stephenson, J. G. Pinto, L. C. Shaffrey, and G. Zappa (2015), "Serial clustering of extratropical cyclones in a multi-model ensemble of historical

and future simulations", *Q. J. R. Meteorol. Soc.*, vol. 141, no. 693, pp. 3076–3087, doi: https://doi.org/10.1002/qj.2591.

Edwards, A. W. F. and L. L. Cavalli-Sforza (1965), "A Method for Cluster Analysis", *Biometrics*, vol. 21, no. 1, pp. 362–375.

European Centre for Medium-Range Weather Forecasts (ECMWF) (2020), *European Centre for Medium-Range Weather Forecasts - Datasets*, https://www.ecmwf.int, [online; accessed 20 November 2020].

Fazel-Rastgar, F. (2020), "Seasonal Analysis of Atmospheric Changes in Hudson Bay during 1998-2018", *Am. J. Clim. Cha.*, vol. 9, no. 2, p. 100, doi: https://doi.org/10.4236/ajcc.2020.92008.

Feser, F., M. Barcikowska, O. Krueger, F. Schenk, R. Weisse, and L. Xia (2015), "Storminess over the North Atlantic and northwestern Europe—A review", *Q. J. R. Meteorol. Soc.*, vol. 141, no. 687, pp. 350–382, doi: https://doi.org/10.1002/qj.2364.

Fink, A. H., T. Brücher, V. Ermert, A. Krüger, and J. G. Pinto (2009), "The European storm Kyrill in January 2007: synoptic evolution, meteorological impacts and some considerations with respect to climate change", *Nat. Hazards Earth Syst. Sci.*, vol. 9, no. 2, pp. 405–423, doi: https://doi.org/10.5194/nhess-9-405-2009.

Flaounas, E., L. Aragão, L. Bernini, S. Dafis, B. Doiteau, S. Flocas H. L. Gray, A. Karwat, J. Kouroutzoglou, P. Lionello, et al. (2023), "A composite approach to produce reference datasets for extratropical cyclone tracks: Application to Mediterranean cyclones", *Weather Clim. Dyn.*, pp. 1–32, doi: https://doi.org/10.5194/wcd-2022-63.

Franzke, C. L. E. (2012), "Nonlinear trends, long-range dependence, and climate noise properties of surface temperature", *J. Clim.*, vol. 25, no. 12, pp. 4172–4183, doi: https://doi.org/10.1175/jcli-d-11-00293.1.

— (2015), "Local trend disparities of European minimum and maximum temperature extremes", *Geophys. Res. Lett.*, vol. 42, no. 15, pp. 6479–6484, doi: https://doi.org/10.1002/2015gl065011.

— (2017), "Impacts of a changing climate on economic damages and insurance", *Econ. Disaster Clim. Chang.*, vol. 1, no. 1, pp. 95–110, doi: https://doi.org/10.1007/s41885-017-0004-3.

— (2021), "Towards the development of economic damage functions for weather and climate extremes", *Ecol. Econ.*, vol. 189, p. 107172, doi: https://doi.org/10.1016/j.ecolecon.2021.107172.

— (2022), "Changing temporal volatility of precipitation extremes due to global warming", *Int. J. Climatol.*, vol. 42, no. 16, pp. 8971–8983, doi: https://doi.org/10.1002/joc.7789.

Franzke, C. L. E., A. Ciullo, E. A. Gilmore, D. M. Matias, N. Nagabhatla, A. Orlov, S. K. Paterson, J. Scheffran, and J. Sillmann (2022), "Perspectives on tipping points in integrated models of the natural and human Earth system: cascading effects and telecoupling", *Environ. Res. Lett.*, vol. 17, no. 1, p. 015004, doi: https://doi.org/10.1088/1748-9326/ac42fd.

Franzke, C. L. E. and M. Czupryna (2019), "Probabilistic assessment and projections of US weather and climate risks and economic damages", *Clim. Change*, vol. 158, no. 1, pp. 503–515, doi: https://doi.org/10.1007/s10584-019-02558-8.

Gao, M. and C. L. E. Franzke (2017), "Quantile Regression-Based Spatiotemporal Analysis of Extreme Temperature Change in China", *J. Clim.*, vol. 30, no. 24, pp. 897–9914, doi: https://doi.org/10.1175/jcli-d-17-0356.1.

Gardiner, B., K. Blennow, J.-M. Carnus, P. Fleischer, F. Ingemarsson, G. Landmann, M. Lindner, M. Marzano, B. Nicoll, C. Orazio, et al. (2010), "Destructive storms in European forests: past and forthcoming impacts", *European Forest Institute*.

Gavrilov, M. B., I. Tošić, S. B. Marković, M. Unkašević, and P. Petrović (2016), "Analysis of annual and seasonal temperature trends using the Mann-Kendall test in Vojvodina, Serbia", *Q. J. H. Meteorol. Serv.*, vol. 120, no. 2, pp. 183–198.

German Weather Service (DWD) (2020), *"VICTORIA" rekordverdächtig? - Thema des Tages*, https://www.dwd.de/DE/wetter/thema_des_tages/2020/2/17.html.

Gliksman, D., P. Averbeck, N. Becker, B. Gardiner, V. Goldberg, J. Grieger, D. Handorf, K. Haustein, A. Karwat, F. Knutzen, et al. (2022), "Wind and storm damage: From Meteorology to Impacts", *Nat. Hazards Earth Syst. Sci.*, pp. 1–47, doi: https://doi.org/10.5194/nhess-2022-159.

Guo, Y., T. Shinoda, J. Lin, and E. K. M. Chang (2017), "Variations of Northern Hemisphere storm track and extratropical cyclone activity associated with the Madden–Julian oscillation", *J. Clim.*, vol. 30, no. 13, pp. 4799–4818, doi: https://doi.org/10.1175/jcli-d-16-0513.1.

Hadas, O., G. Datseris, J. Blanco, S. Bony, R. Caballero, B. Stevens, and Y. Kaspi (2023), "The role of baroclinic activity in controlling Earth's albedo in the present and future climates", *Proc. Natl. Acad. Sci. U.S.A.*, vol. 120, no. 5, e2208778120, doi: https://doi.org/10.1073/pnas.220877812.

Hamed, K. H. and A. R. Rao (1998), "A modified Mann-Kendall trend test for autocorrelated data", *J. Hydrol.*, vol. 204, doi: https://doi.org/10.1016/s0022-1694(97)00125-x.

Harvey, B. J., P. Cook, L. C. Shaffrey, and R. Schiemann (2020), "The Response of the Northern Hemisphere Storm Tracks and Jet Streams to Climate Change in the CMIP3, CMIP5, and CMIP6 Climate Models", *J. Geophys. Res. Atmos.*, vol. 125, no. 23, e2020JD032701, doi: https://doi.org/10.1029/2020jd032701.

Harvey, B. J., L. C. Shaffrey, and T. J. Woollings (2014), "Equator-to-pole temperature differences and the extra-tropical storm track responses of the CMIP5 climate models", *Clim. Dyn.*, vol. 43, no. 5, pp. 1171–1182, doi: https://doi.org/10.1007/s00382-013-1883-9.

Hauser, S., S. Mueller, X. Chen, T.-C. Chen, J. G. Pinto, and C. M. Grams (2023), "The Linkage of Serial Cyclone Clustering in Western Europe and Weather Regimes in the North Atlantic-European Region in Boreal Winter", *Geophys. Res. Lett.*, vol. 50, no. 2, e2022GL101900, doi: https://doi.org/10.1029/2022gl101900.

Hawcroft, M. K., L. C. Shaffrey, K. I. Hodges, and H. F. Dacre (2012), "How much Northern Hemisphere precipitation is associated with extratropical cyclones?", *Geophys. Res. Lett.*, vol. 39, no. 24, doi: https://doi.org/10.1029/2012gl053866.

Hersbach, H., B. Bell, P. Berrisford, S. Hirahara, A. Horányi, J. Muñoz-Sabater, J. Nicolas, C. Peubey, R. Radu, D. Schepers, et al. (2020), "The ERA5 global reanalysis", *Q. J. R. Meteorol. Soc.*, vol. 146, no. 730, pp. 1999–2049, doi: https://doi.org/10.1002/qj.3803.

Hodges, K. I. (1995), "Feature tracking on the unit sphere", *Mon. Weather Rev.*, vol. 123, no. 12, pp. 3458–3465, doi: https://doi.org/10.1175/1520-0493(1995)123<3458:ftotus>2.0.co;2.

— (1996), "Spherical nonparametric estimators applied to the UGAMP model integration for AMIP", *Mon. Weather Rev.*, vol. 124, no. 12, pp. 2914–2932, doi: https://doi.org/10.1175/1520-0493(1996)124<2914:sneatt>2.0.co;2.

— (1999), "Adaptive constraints for feature tracking", *Mon. Weather Rev.*, vol. 127, no. 6, pp. 1362–1373, doi: https://doi.org/10.1175/1520-0493(1999)127<1362:acfft>2.0.co;2.

Hoskins, B. J. and K. I. Hodges (2002), "New perspectives on the Northern Hemisphere winter storm tracks", *J. Atmos. Sci.*, vol. 59, no. 6, pp. 1041–1061, doi: https://doi.org/10.1175/1520-0469(2002)059<1041:npotnh>2.0.co;2.

Hu, G. and C. L. E. Franzke (2020), "Evaluation of daily precipitation extremes in reanalysis and gridded observation-based data sets over Germany", *Geophys. Res. Lett.*, vol. 47, no. 18, e2020GL089624, doi: https://doi.org/10.1029/2020gl089624.

Huang, L., A. Timmermann, S.-S. Lee, K. B. Rodgers, R. Yamaguchi, and E.-S. Chung (2022), "Emerging unprecedented lake ice loss in climate change projections", *Nat. Commun.*, vol. 13, no. 1, pp. 1–12, doi: https://doi.org/10.1038/s41467-022-33495-3.

Jeong, H., H.-S. Park, M. F. Stuecker, and S.-W. Yeh (2022), "Record low Arctic sea ice extent in 2012 linked to two-year La Niña-driven sea surface temperature pattern", *Geo. Res. Lett.*, vol. 49, no. 9, e2022GL098385, doi: https://doi.org/10.1029/2022gl098385.

Jiang, J. and W. Perrie (2007), "The impacts of climate change on autumn North Atlantic midlatitude cyclones", *J. Clim.*, vol. 20, no. 7, pp. 1174–1187, doi: https://doi.org/10.1175/jcli4058.1.

Jones, D. A. and I. Simmonds (1993), "A climatology of Southern Hemisphere extratropical cyclones", *Clim. Dyn.*, vol. 9, no. 1, pp. 131–145, doi: https://doi.org/10.1007/bf00209750.

Karremann, M. K., J. G. Pinto, M. Reyers, and M. Klawa (2014a), "Return periods of losses associated with European windstorm series in a changing climate", *Environ. Res. Lett.*, vol. 9, no. 12, p. 124016, doi: https://doi.org/10.1088/1748-9326/9/12/124016.

Karremann, M. K., J. G. Pinto, P. J. Von Bomhard, and M. Klawa (2014b), "On the clustering of winter storm loss events over Germany", *Nat. Hazards Earth Syst. Sci.*, vol. 14, no. 8, pp. 2041–2052, doi: https://doi.org/10.5194/nhess-14-2041-2014.

Karwat, A. and C. L. E. Franzke (2021), "Future Projections of Heat Mortality Risk for Major European Cities", *Weather Clim. Soc.*, vol. 13, no. 4, pp. 913–931, doi: https://doi.org/10.1175/wcas-d-20-0142.1.

Karwat, A., C. L. E. Franzke, and R. Blender (2022), "Long-Term Trends of Northern Hemispheric Winter Cyclones in the Extended ERA5 Reanalysis", *J. Geophys. Res. Atmos.*, vol. 127, no. 22, e2022JD036952, doi: https://doi.org/10.1029/2022jd036952.

Kendall, M. G. (1975), "Rank Correlation Methods", *4th ed. London. Charles Griffin*, vol. 4, no. 202.

Kendon, M. and M. McCarthy (2015), "The UK's wet and stormy winter of 2013/2014", *Weather*, vol. 70, no. 2, pp. 40–47, doi: https://doi.org/10.1002/wea.2465.

Kettle, A. J. (2020), "Storm Xaver over Europe in December 2013: Overview of energy impacts and North Sea events", *Adv. Geosci.*, vol. 54, no. 1, pp. 137–147, doi: https://doi.org/10.5194/adgeo-54-137-2020.

— (2021), "Storm Anatol over Europe in December 1999: impacts on societal and energy infrastructure", *Adv. Geosci.*, vol. 56, no. 1, pp. 141–153, doi: https://doi.org/10.5194/adgeo-56-141-2021.

Killick, R. and I. A. Eckley (2014), "changepoint: An R Package for Changepoint Analysis", *J. Stat. Softw.*, vol. 58, no. 3, pp. 1–19, doi: https://doi.org/10.18637/jss.v058.i03.

Klawa, M. and U. Ulbrich (2003), "A model for the estimation of storm losses and the identification of severe winter storms in Germany", *Nat. Hazards Earth Syst. Sci.*, vol. 3, no. 6, pp. 725–732, doi: https://doi.org/10.5194/nhess-3-725-2003.

Koenker, R. and K. F. Hallock (2001), "Quantile Regression", *J. Econ. Perspect.*, vol. 15, no. 4, doi: https://doi.org/10.1257/jep.15.4.143.

Koks, E. E. and T. Haer (2020), "A high-resolution wind damage model for Europe", *Sci. Rep.*, vol. 10, no. 1, p. 6866, doi: https://doi.org/10.1038/s41598-020-63580-w.

Koks, E. E., D. Le Bars, A. H. Essenfelder, S. Nirandjan, and P. Sayers (2022), "The impacts of coastal flooding and sea level rise on critical infrastructure: a novel storyline approach", *Sustain. Resilient Infrastruct.*, vol. 8, no. S1, pp. 1–25, doi: https://doi.org/10.1080/23789689.2022.2142741.

Kossin, J. P. (2018), "A global slowdown of tropical-cyclone translation speed", *Nature*, vol. 558, no. 7708, pp. 104–107, doi: https://doi.org/10.1038/s41586-018-0158-3.

Krueger, O., F. Feser, L. Bärring, E. Kaas, T. Schmith, H. Tuomenvirta, and H. von Storch (2013), "Comment on "Trends and low frequency variability of extratropical cyclone activity in the ensemble of twentieth century reanalysis"", *Clim. Dyn.*, vol. 42, no. 3, pp. 1127–1128, doi: https://doi.org/10.1007/s00382-013-1814-9.

Krueger, O., F. Feser, and R. Weisse (2019), "Northeast Atlantic Storm Activity and Its Uncertainty from the Late Nineteenth to the Twenty-First Century", *J. Clim.*, vol. 32, no. 6, pp. 1919–1931, doi: https://doi.org/10.1175/jcli-d-18-0505.1.

Lai, Y., J. Li, X. Gu, Y. D. Chen, D. Kong, T. Y. Gan, M. Liu, Q. Li, and G. Wu (2020), "Greater flood risks in response to slowdown of tropical cyclones over the coast of China", *Proc. Natl. Acad. Sci. U.S.A.*, vol. 117, no. 26, pp. 14751–14755, doi: https://doi.org/10.1073/pnas.191898711.

Lee, M., D.-H. Cha, J. Moon, J. Park, C.-S. Jin, and J. C. L. Chan (2019), "Long-term trends in tropical cyclone tracks around Korea and Japan in late summer and early fall", *Atmospheric Sci. Lett.*, vol. 20, no. 11, e939, doi: https://doi.org/10.1002/asl.939.

Mailier, P. J., D. B. Stephenson, C. A. T. Ferro, and K. I. Hodges (2006), "Serial clustering of extratropical cyclones", *Mon. Weather Rev.*, vol. 134, no. 8, pp. 2224–2240, doi: https://doi.org/10.1175/mwr3160.1.

Mann, H. B. (1945), "Nonparametric tests against trend", *Econometrica*, vol. 13, no. 3, doi: https://doi.org/10.2307/1907187.

Marrafon, V. H., M. S. Reboita, R. P. da Rocha, and N. M. Crespo (2021), "Extratropical Cyclones in the Southern Hemisphere: comparison among different Reanalyses", *Rev. Bras. Climatol*, vol. 28, no. 1, pp. 48–73, doi: http://dx.doi.org/10.5380/rbclima.v28i0.74460.

Mass, C. (2008), "The Weather of the Pacific Northwest", *University of Washington Press*.

Masson-Delmotte, V., P. Zhai, A. Pirani, S. L. Connors, C. Péan, S. Berger, N. Caud, Y. Chen, L. Goldfarb, M.I. Gomis, M. Huang, K. Leitzell, E. Lonnoy, J.B.R. Matthews, T.K. Maycock, T. Waterfield, O. Yelekçi, R. Yu, and B. Zhou (2021), "IPCC, 2021: Climate Change 2021: The Physical Science Basis. Contribution of Working Group I to the Sixth Assessment Report of the Intergovernmental Panel on Climate Change", in: Cambridge, United Kingdom and New York, NY, USA: Cambridge University Press.

Matthews, T., C. Murphy, R. L. Wilby, and S. Harrigan (2014), "Stormiest winter on record for Ireland and UK", *Nat. Clim. Change*, vol. 4, no. 9, pp. 738–740, doi: https://doi.org/10.1038/nclimate2336.

Matulla, C., W. Schöner, H. Alexandersson, H. von Storch, and X. L. Wang (2008), "European storminess: late nineteenth century to present", *Clim. Dyn.*, vol. 32, no. 2, pp. 125–130, doi: https://doi.org/10.1007/s00382-007-0333-y.

Mbengue, C. and T. Schneider (2016), "Storm-Track Shifts under Climate Change: Toward a Mechanistic Understanding Using Baroclinic Mean Available Potential Energy", *J. Atmos. Sci.*, vol. 74, no. 1, pp. 93–110, doi: https://doi.org/10.1175/jas-d-15-0267.1.

McCallum, E. (1990), "The Burns' Day Storm, 25 January 1990", *Weather*, vol. 45, no. 5, pp. 166–173.

McDonald, J. H. (2009), *Handbook of biological statistics*, vol. 2.

McDonald, R. E. (2011), "Understanding the impact of climate change on Northern Hemisphere extra-tropical cyclones", *Clim. Dyn.*, vol. 37, no. 1, pp. 1399–1425, doi: https://doi.org/10.1007/s00382-010-0916-x.

Meleshko, V. P., O. M. Johannessen, A. V. Baidin, T. V. Pavlova, and V. A. Govorkova (2016), "Arctic amplification: does it impact the polar jet stream?", *Tellus A: Dyn. Meteorol. Oceanogr.*, vol. 68, no. 1, p. 32330, doi: https://doi.org/10.3402/tellusa.v68.32330.

Mendes, D., E. P. Souza, J. A. Marengo, and M. C. D. Mendes (2010), "Climatology of extratropical cyclones over the South American–southern oceans sector", *Theor. Appl. Climatol.*, vol. 100, pp. 239–250, doi: https://doi.org/10.1007/s00704-009-0161-6.

Messmer, M. and I. Simmonds (2021), "Global analysis of cyclone-induced compound precipitation and wind extreme events", *Weather Clim. Extremes*, vol. 32, no. 5, p. 100324, doi: https://doi.org/10.1016/j.wace.2021.100324.

Montoya Duque, E., F. Lunkeit, and R. Blender (2021), "North Atlantic midwinter storm track suppression and the European weather response in ERA5 reanalysis", *Theor. Appl. Climatol.*, vol. 144, no. 3, pp. 839–845, doi: https://doi.org/10.1007/s00704-021-03517-z.

Mühr, B., L. Eisenstein, J. G. Pinto, P. Knippertz, S. Mohr, and M. Kunz (2022), "CEDIM Forensic Disaster Analysis Group (FDA): Winter storm series: Ylenia,

Zeynep, Antonia (int: Dudley, Eunice, Franklin)-February 2022 (NW & Central Europe)", doi: https://doi.org/10.5445/ir/1000143470.

Munich Re (2002), *Winterstorms in Europe (II) — Analysis of 1999 losses and loss potentials*, Munich Re Group, Munich.

Murray, R. J. and I. Simmonds (1991), "A numerical scheme for tracking cyclone centres from digital data", *Aust. Meteorol. Mag.*, vol. 39, no. 3, pp. 155–166.

National Environmental Satellite Data and Information Service (2021), *Record-Setting Storm "Explodes" While Approaching Alaska - Home*, https://www.nesdis.noaa.gov/content/record-setting-storm-%E2%80%9Cexplodes%E2%80%9D-while-approaching-alaska, [online; accessed 16 August 2021].

Neu, U., M. G. Akperov, N. Bellenbaum, R. Benestad, R. Blender, R. Caballero, A. Cocozza, H. F. Dacre, Y. Feng, K. Fraedrich, et al. (2013), "IMILAST: A community effort to intercompare extratropical cyclone detection and tracking algorithms", *Bull. Am. Meteorol. Soc.*, vol. 94, no. 4, pp. 529–547, doi: https://doi.org/10.1175/bams-d-11-00154.1.

O'Neill, B. C., C. Tebaldi, D. P. Van Vuuren, V. Eyring, P. Friedlingstein, G. Hurtt, R. Knutti, E. Kriegler, J.-F. Lamarque, J. Lowe, et al. (2016), "The scenario model intercomparison project (ScenarioMIP) for CMIP6", *Geosci. Model Dev.*, vol. 9, no. 9, pp. 3461–3482, doi: https://doi.org/10.5194/gmd-9-3461-2016.

Owen, L. E., J. L. Catto, D. B. Stephenson, and N. J. Dunstone (2021), "Compound precipitation and wind extremes over Europe and their relationship to extratropical cyclones", *Weather Clim. Extremes*, vol. 33, no. 1, p. 100324, doi: https://doi.org/10.1016/j.wace.2021.100342.

Patt, A., S. Pfenninger, and J. Lilliestam (2013), "Vulnerability of solar energy infrastructure and output to climate change", *Clim. Change*, vol. 121, no. 1, pp. 93–102, doi: https://doi.org/10.1007/s10584-013-0887-0.

Pepler, A. S. and A. J. Dowdy (2022), "Australia's Future Extratropical Cyclones", *J. Clim.*, vol. 35, no. 23, pp. 4195–4210, doi: https://doi.org/10.1175/jcli-d-22-0312.1.

Pinto, J. G., N. Bellenbaum, M. K. Karremann, and P. M. Della-Marta (2013), "Serial clustering of extratropical cyclones over the North Atlantic and Europe under recent and future climate conditions", *J. Geophys. Res. Atmos.*, vol. 118, no. 22, pp. 12–476, doi: https://doi.org/10.1002/2013jd020564.

Pinto, J. G, I. Gómara, G. Masato, H. F. Dacre, T. Woollings, and R. Caballero (2014), "Large-scale dynamics associated with clustering of extratropical cyclones affecting Western Europe", *J. Geophys. Res. Atmos.*, vol. 119, no. 24, pp. 13–704, doi: https://doi.org/10.1002/2014jd022305.

Pinto, J. G., M. K. Karremann, K. Born, P. M. Della-Marta, and M. Klawa (2012), "Loss potentials associated with European windstorms under future climate conditions", *Clim. Res.*, vol. 54, no. 1, pp. 1–20, doi: https://doi.org/10.3354/cr01111.

Pinto, J. G., T. Spangehl, U. Ulbrich, and P. Speth (2005), "Sensitivities of a cyclone detection and tracking algorithm: individual tracks and climatology", *Meteorol. Zeitschrift*, vol. 14, no. 6, pp. 823–838, doi: https://doi.org/10.1127/0941-2948/2005/0068.

Pinto, J. G., S. Ulbrich, T. Economou, D. B. Stephenson, M. K. Karremann, and L. C. Shaffrey (2016), "Robustness of serial clustering of extratropical cyclones to the

choice of tracking method", *Tellus A: Dyn.*, vol. 68, no. 1, p. 32204, doi: https://doi.org/10.3402/tellusa.v68.32204.

Pinto, J. G., S. Zacharias, A. H. Fink, G. C. Leckebusch, and U. Ulbrich (2009), "Factors contributing to the development of extreme North Atlantic cyclones and their relationship with the NAO", *Clim. Dyn.*, vol. 32, no. 1, pp. 711–737, doi: https://doi.org/10.1007/s00382-008-0396-4.

Potter, G. L., G. J. Huffman, D. T. Bolvin, M. G. Bosilovich, J. Hertz, and L. E. Carriere (2020), "Histogram Anomaly Time Series: A Compact Graphical Representation of Spatial Time Series Data Sets", *Bull. Am. Meteorol. Soc.*, vol. 101, no. 12, pp. 1–17, doi: https://doi.org/10.1175/bams-d-20-0130.1.

Priestley, M. D. K. and J. L. Catto (2022), "Future changes in the extratropical storm tracks and cyclone intensity, wind speed, and structure", *Weather Clim. Dyn.*, vol. 3, no. 1, pp. 337–360, doi: https://doi.org/10.5194/wcd-3-337-2022.

Priestley, M. D. K., H. F. Dacre, L. C. Shaffrey, K. I. Hodges, and J. G. Pinto (2018), "The role of serial European windstorm clustering for extreme seasonal losses as determined from multi-centennial simulations of high-resolution global climate model data", *Nat. Hazards Earth Syst. Sci.*, vol. 18, no. 11, pp. 2991–3006, doi: https://doi.org/10.5194/nhess-18-2991-2018.

Priestley, M. D. K., H. F. Dacre, L. C. Shaffrey, S. Schemm, and J. G. Pinto (2020), "The role of secondary cyclones and cyclone families for the North Atlantic storm track and clustering over western Europe", *Q. J. R. Meteorol. Soc.*, vol. 146, no. 728, pp. 1184–1205, doi: https://doi.org/10.1002/qj.3733.

Priestley, M. D. K., J. G. Pinto, H. F. Dacre, and L. C. Shaffrey (2017), "The role of cyclone clustering during the stormy winter of 2013/2014", *Weather*, vol. 72, no. 7, pp. 187–192, doi: https://doi.org/10.1002/wea.3025.

Raible, C. C., P. M. Della-Marta, C. Schwierz, H. Wernli, and R. Blender (2008), "Northern Hemisphere extratropical cyclones: A comparison of detection and tracking methods and different reanalyses", *Mon. Weather Rev.*, vol. 136, no. 3, pp. 880–897, doi: https://doi.org/10.1175/2007mwr2143.1.

Raible, C. C., M. Messmer, F. Lehner, T. F. Stocker, and R. Blender (2018), "Extratropical cyclone statistics during the last millennium and the 21st century", *Clim. Past*, vol. 14, no. 10, pp. 1499–1514, doi: https://doi.org/10.5194/cp-14-1499-2018.

Ranson, M., C. Kousky, M. Ruth, L. Jantarasami, A. Crimmins, and L. Tarquinio (2014), "Tropical and extratropical cyclone damages under climate change", *Clim. Change*, vol. 127, no. 1, pp. 227–241, doi: https://doi.org/10.1007/s10584-014-1255-4.

Reale, M., W. D. Cabos Narvaez, L. Cavicchia, D. Conte, E. Coppola, E. Flaounas, F. Giorgi, S. Gualdi, A. Hochman, L. Li, et al. (2022), "Future projections of Mediterranean cyclone characteristics using the Med-CORDEX ensemble of coupled regional climate system models", *Clim. Dyn.*, vol. 58, no. 9, pp. 2501–2524, doi: https://doi.org/10.1007/s00382-021-06018-x.

Riahi, K., D. P. Van Vuuren, E. Kriegler, J. Edmonds, B. C. O'neill, S. Fujimori, N. Bauer, K. Calvin, R. Dellink, O. Fricko, et al. (2017), "The Shared Socioeconomic Pathways and their energy, land use, and greenhouse gas emissions implications: An overview", *Glob. Environ. Change*, vol. 42, no. 1, pp. 153–168, doi: https://doi.org/10.1016/j.gloenvcha.2016.05.009.

Rivière, G., P. Arbogast, and A. Joly (2014), "Eddy kinetic energy redistribution within windstorms Klaus and Friedhelm", *Q. J. R. Meteorol. Soc.*, vol. 141, no. 688, pp. 925–938, doi: https://doi.org/10.1002/qj.2412.

Roberts, J. F., A. J. Champion, L. C. Dawkins, K. I. Hodges, L. C. Shaffrey, D. B. Stephenson, M. A. Stringer, H. E. Thornton, and B. D. Youngman (2014), "The XWS open access catalogue of extreme European windstorms from 1979 to 2012", *Nat. Hazards Earth Syst. Sci.*, vol. 14, no. 9, pp. 2487–2501, doi: https://doi.org/10.5194/nhess-14-2487-2014.

Rodgers, K. B., S.-S. Lee, N. Rosenbloom, A. Timmermann, G. Danabasoglu, C. Deser, J. Edwards, J.-E. Kim, I. R. Simpson, K. Stein, et al. (2021), "Ubiquity of human-induced changes in climate variability", *Earth Syst. Dyn.*, vol. 12, no. 4, pp. 1393–1411, doi: https://doi.org/10.5194/esd-12-1393-2021.

Ross, S. M. (2020), *Introduction to probability and statistics for engineers and scientists*, Academic press.

Russell, P. E. (1993), "Mechanisms for beach erosion during storms", *Cont. Shelf Res.*, vol. 13, no. 11, pp. 1243–1265, doi: https://doi.org/10.1016/0278-4343(93)90051-x.

Salathé Jr, E. P. (2006), "Influences of a shift in North Pacific storm tracks on western North American precipitation under global warming", *Geophys. Res. Lett.*, vol. 33, no. 19, doi: https://doi.org/10.1029/2006gl026882.

Santer, B. D., C. Mears, F. G. Wentz, K. E. Taylor, P. J. Gleckler, T. M. L. Wigley, T. P. Barnett, J. S. Boyle, W. Brüggemann, N. P. Gillett, S. A. Klein, G. A. Meehl, T. Nozawa, D. W. Pierce, P. A. Stott, W. M. Washington, and M. F. Wehner (2007), "Identification of human-induced changes in atmospheric moisture content", *Proc. Natl. Acad. Sci. USA.*, vol. 104, no. 39, pp. 15248–15253, doi: https://doi.org/10.1073/pnas.070287210.

Santos Mesquita, M. dos, D. E. Atkinson, and K. I. Hodges (2010), "Characteristics and Variability of Storm Tracks in the North Pacific, Bering Sea, and Alaska*", *J. Clim.*, vol. 23, no. 2, pp. 294–311, doi: https://doi.org/10.1175/2009jcli3019.1.

Schaller, N., A. L. Kay, R. Lamb, N. R. Massey, G. J. Van Oldenborgh, F. E. L. Otto, S. N. Sparrow, R. Vautard, P. Yiou, I. Ashpole, et al. (2016), "Human influence on climate in the 2014 southern England winter floods and their impacts", *Nat. Clim. Change*, vol. 6, no. 6, pp. 627–634, doi: https://doi.org/10.1038/nclimate2927.

Schenker, N. and J. F. Gentleman (2001), "On judging the significance of differences by examining the overlap between confidence intervals", *Am. Stat.*, vol. 55, no. 3, pp. 182–186.

Schüepp, M., H. H. Schiesser, H. Huntrieser, H. U. Scherrer, and H. Schmidtke (1994), "The winterstorm "Vivian" of 27 February 1990: About the meteorological development, wind forces and damage situation in the forests of Switzerland", *Theor. Appl. Climatol.*, vol. 49, no. 1, pp. 183–200, doi: https://doi.org/10.1007/bf00865533.

Schneidereit, A., R. Blender, and K. Fraedrich (2010), "A radius–depth model for midlatitude cyclones in reanalysis data and simulations", *Q. J. R. Meteorol. Soc.*, vol. 136, no. 646, pp. 50–60, doi: https://doi.org/10.1002/qj.523.

Schultz, D. M., L. F. Bosart, B. A. Colle, H. C. Davies, C. Dearden, D. Keyser, O. Martius, P. J. Roebber, W. J. Steenburgh, H. Volkert, et al. (2019), "Extratropical cyclones: A century of research on meteorology's centerpiece", *Meteorol. Monogr.*,

vol. 59, no. 1, 16.1–16.56, doi: https://doi.org/10.1175/amsmonographs-d-18-0015.1.

Schwierz, C., P. Köllner-Heck, E. Zenklusen Mutter, D. N. Bresch, P.-L. Vidale, M. Wild, and C. Schär (2010), "Modelling European winter wind storm losses in current and future climate", *Clim. Change*, vol. 101, no. 3, pp. 485–514, doi: https://doi.org/10.1007/s10584-009-9712-1.

Serreze, M. C., B. Raup, C. Braun, D. R. Hardy, and R. S. Bradley (2017), "Rapid wastage of the Hazen Plateau ice caps, northeastern Ellesmere Island, Nunavut, Canada", *The Cryo.*, vol. 11, no. 1, pp. 169–177, doi: https://doi.org/10.5194/tc-11-169-2017.

Shapiro, M. A. and D. Keyser (1990), "Fronts, jet streams and the tropopause", in: *Extratropical cyclones*, pp. 167–191, doi: https://doi.org/10.1007/978-1-944970-33-8_10.

Shapiro, S. S. and M. B. Wilk (1965), "An analysis of variance test for normality (complete samples)", *Biometrika*, vol. 52, no. 3/4, pp. 591–611.

Shaw, T. A., M. Baldwin, E. A. Barnes, R. Caballero, C. I. Garfinkel, Y.-T. Hwang, C. Li, P. A. O'gorman, G. Rivière, I. R. Simpson, et al. (2016), "Storm track processes and the opposing influences of climate change", *Nat. Geosci.*, vol. 9, no. 9, pp. 656–664, doi: https://doi.org/10.1038/ngeo2783.

Shaw, T. A., O. Miyawaki, and A. Donohoe (2022), "Stormier Southern Hemisphere induced by topography and ocean circulation", *Proc. Natl. Acad. Sci. U.S.A.*, vol. 119, no. 50, e2123512119, doi: https://doi.org/10.1073/pnas.2123512119.

Sickmöller, M., R. Blender, and K. Fraedrich (2000), "Observed winter cyclone tracks in the Northern Hemisphere in re-analysed ECMWF data", *Q. J. R. Meteorol. Soc.*, vol. 126, no. 563, pp. 591–620, doi: https://doi.org/10.1002/qj.49712656311.

Sillmann, J., T. G. Shepherd, B. van den Hurk, W. Hazeleger, O. Martius, J. Slingo, and J. Zscheischler (2021), "Event-based storylines to address climate risk", *Earth's Future*, vol. 9, no. 2, e2020EF001783, doi: https://doi.org/10.1029/2020ef001783.

Sinclair, M. R. (1994), "An objective cyclone climatology for the Southern Hemisphere", *Mon. Weather Rev.*, vol. 122, no. 10, pp. 2239–2256, doi: https://doi.org/10.1175/1520-0493(1994)122<2239:aoccft>2.0.co;2.

Stocker, T. F., D. Qin, G. K. Plattner, M. Tignor, S. K. Allen, J. Boschung, A. Nauels, Y. Xia, V. Bex, and P. M. Midgley (eds.) (2013), *IPCC, 2013: Climate Change 2013: The Physical Science Basis. Contribution of Working Group I to the Fifth Assessment Report of the Intergovernmental Panel on Climate Change*, tech. rep., United Nations.

Storch, H. von and R. Weisse (2008), "Regional storm climate and related marine hazards in the Northeast Atlantic", *Weather. Clim. Extremes*, vol. 54, no. 1, p. 73, doi: https://doi.org/10.1017/cbo9780511535840.007.

Stoyan, D., W. S. Kendall, S. N. Chiu, and J. Mecke (2013), *Stochastic Geometry and Its Applications*, Wiley Series in Probability and Statistics, Wiley.

Studholme, J., A. V. Fedorov, S. K. Gulev, K. Emanuel, and K. Hodges (2022), "Poleward expansion of tropical cyclone latitudes in warming climates", *Nat. Geosci.*, vol. 15, no. 1, pp. 14–28, doi: https://doi.org/10.1038/s41561-021-00859-1.

Tamarin, T. and Y. Kaspi (2017), "The poleward shift of storm tracks under global warming: A Lagrangian perspective", *Geophys. Res. Lett.*, vol. 44, no. 20, pp. 10,666–10,674, doi: https://doi.org/10.1002/2017gl073633.

Trenberth, K. E. and J. W. Hurrell (1994), "Decadal atmosphere-ocean variations in the Pacific", *Clim. Dyn.*, vol. 9, no. 6, pp. 303–319, doi: https://doi.org/10.1007/bf00204745.

Ulbrich, U., A. H. Fink, M. Klawa, and J. G. Pinto (2001), "Three extreme storms over Europe in December 1999", *Weather*, vol. 56, no. 3, pp. 70–80, doi: https://doi.org/10.1002/j.1477-8696.2001.tb06540.x.

Ulbrich, U., G. C. Leckebusch, and J. G. Pinto (2009), "Extra-tropical cyclones in the present and future climate: a review", *Theor. Appl. Climatol.*, vol. 96, no. 1, pp. 117–131, doi: https://doi.org/10.1007/s00704-008-0083-8.

Upton, G. J. G. (1992), "Fisher's exact test", *J. R. Stat. Soc. Ser. A. Stat. Soc.*, vol. 155, no. 3, pp. 395–402.

Vitolo, R., D. B. Stephenson, I. M. Cook, and K. Mitchell-Wallace (2009), "Serial clustering of intense European storms", *Meteorol. Zeitschrift*, vol. 18, no. 4, pp. 411–424, doi: https://doi.org/10.1127/0941-2948/2009/0393.

Walker, E., D. Mitchell, and W. Seviour (2020), "The numerous approaches to tracking extratropical cyclones and the challenges they present", *Weather*, vol. 75, no. 11, pp. 336–341, doi: https://doi.org/10.1002/wea.3861.

Wallace, J. M., G.-H. Lim, and M. L. Blackmon (1988), "Relationship between cyclone tracks, anticyclone tracks and baroclinic waveguides", *J. Atmos. Sci.*, vol. 45, no. 3, pp. 439–462, doi: https://doi.org/10.1175/1520-0469(1988)045<0439:rbctat>2.0.co;2.

Walz, M. A., D. J. Befort, N. O. Kirchner-Bossi, U. Ulbrich, and G. C. Leckebusch (2018), "Modelling serial clustering and inter-annual variability of European winter windstorms based on large-scale drivers", *Int. J. Clim.*, vol. 38, no. 7, pp. 3044–3057, doi: https://doi.org/10.1002/joc.5481.

Wang, J., H. M. Kim, and E. K. M. Chang (2017), "Changes in Northern Hemisphere Winter Storm Tracks under the Background of Arctic Amplification", *J. Clim.*, vol. 30, no. 10, pp. 3705–3724, doi: https://doi.org/10.1175/jcli-d-16-0650.1.

Wang, X. L., Y. Feng, G. P. Compo, V. R. Swail, F. W. Zwiers, R. J. Allan, and P. D. Sardeshmukh (2012), "Trends and low frequency variability of extra-tropical cyclone activity in the ensemble of twentieth century reanalysis", *Clim. Dyn.*, vol. 40, no. 11, 2775–2800, doi: https://doi.org/10.1007/s00382-012-1450-9.

Wernli, H. and C. Schwierz (2006), "Surface cyclones in the ERA-40 dataset (1958–2001). Part I: Novel identification method and global climatology", *J. Atmos. Sci.*, vol. 63, no. 10, pp. 2486–2507, doi: https://doi.org/10.1175/jas3766.1.

Wettstein, J. J. and J. M. Wallace (2010), "Observed patterns of month-to-month storm-track variability and their relationship to the background flow", *J. Atmos. Sci.*, vol. 67, no. 5, pp. 1420–1437, doi: https://doi.org/10.1175/2009jas3194.1.

Wilks, D. S. (2011), *Statistical Methods in the Atmospheric Sciences*, Academic Press.

Woollings, T., J. M. Gregory, J. G. Pinto, M. Reyers, and D. J. Brayshaw (2012), "Response of the North Atlantic storm track to climate change shaped by ocean–atmosphere coupling", *Nat. Geosci*, vol. 5, no. 1, 313–317, doi: https://doi.org/10.1038/ngeo1438.

Xie, A., J. Zhu, S. Kang, X. Qin, B. Xu, and Y. Wang (2022), "Polar amplification comparison among Earth's three poles under different socioeconomic scenarios from CMIP6 surface air temperature", *Nat. Sci. rep.*, vol. 12, no. 1, pp. 1–15, doi: https://doi.org/10.1038/s41598-022-21060-3.

Yang, M., D. Luo, C. Li, Y. Yao, X. Li, and X. Chen (2021), "Influence of atmospheric blocking on storm track activity over the North Pacific during boreal winter", *Geophys. Res. Lett.*, vol. 48, no. 17, e2021GL093863, doi: https://doi.org/10.1029/2021gl093863.

Zappa, G., L. C. Shaffrey, and K. I. Hodges (2013a), "The ability of CMIP5 models to simulate North Atlantic extratropical cyclones", *J. Clim.*, vol. 26, no. 15, pp. 5379–5396, doi: https://doi.org/10.1175/jcli-d-12-00501.1.

Zappa, G., L. C. Shaffrey, K. I. Hodges, P. G. Sansom, and D. B. Stephenson (2013b), "A multimodel assessment of future projections of North Atlantic and European extratropical cyclones in the CMIP5 climate models", *J. Clim.*, vol. 26, no. 16, pp. 5846–5862, doi: https://doi.org/10.1175/jcli-d-12-00573.1.

Zhang, G., H. Murakami, T. R. Knutson, R. Mizuta, and K. Yoshida (2020), "Tropical cyclone motion in a changing climate", *Sci. Adv.*, vol. 6, no. 17, eaaz7610, doi: https://doi.org/10.1126/sciadv.aaz7610.

Zhang, R., G. Li, J. Fan, D. L. Wu, and M. J. Molina (2007), "Intensification of Pacific storm track linked to Asian pollution", *Proc. Natl. Acad. Sci. U.S.A.*, vol. 104, no. 13, pp. 5295–5299, doi: https://doi.org/10.1073/pnas.0700618104.

Zheng, L., X. Cheng, X. Shang, Z. Chen, Q. Liang, and K. Wang (2022), "Greenland Ice Sheet daily surface melt flux observed from space", *Geo. Res. Lett.*, vol. 49, no. 6, e2021GL096690, doi: https://doi.org/10.1029/2021gl096690.

Ziv, B., T. Harpaz, H. Saaroni, and R. Blender (2015), "A new methodology for identifying daughter cyclogenesis: application for the Mediterranean Basin", *Int. J. Climatol.*, vol. 35, no. 13, pp. 3847–3861, doi: https://doi.org/10.1002/joc.4250.

Declaration

Eidesstattliche Erklärung
Declaration upon oath

Hiermit erkläre ich an Eides statt, dass ich die vorliegende Dissertationsschrift selbst verfasst und keine anderen als die angegebenen Quellen und Hilfsmittel benutzt habe.

I hereby declare upon oath that I have written the present dissertation independently and have not used further resources and aids than those stated.

Hamburg, 30 March 2023

Alexia Karwat